People's Democratic Republic of Algeria

Ministry of Higher Education and Scientific Research

University M'Hamed BOUGARA- Boumerdes

Institute of Electrical and Electronic Engineering

Department of Power and Control Engineering

Project Report Presented in Partial Fulfilment of

the Requirements of the Degree of

'MASTER'

In Electrical and Electronic engineering

Option: Power Engineering

Title:

Implementation and Analysis of Speed Control of an Induction Motor using Variable Frequency Drive.

Presented By:

HAMRAOUI Oussama

Supervisors:

Pr. KHELDOUN. A

Co-Supervisor:

Dr. BELMADANI. H

June 2024

Abstract

This work examines the implementation and analysis of speed control of an induction motor using a Variable Frequency Drive (VFD). The study focuses on optimizing motor performance through an open loop configuration within an automation system. The implementation was carried out using the Siemens G120 VFD, which receives commands from an S1200 Siemens PLC. The primary goal is to achieve precise speed control of the induction motor, enhancing efficiency and stability in industrial applications. The results provide valuable guidance on the practical usage of VFDs in industrial automation and recommendations for optimizing motor performance based on unique operational needs.

Acknowledgements

I am profoundly thankful to my supervisor Pr. Aissa KHELDOUN, whose invaluable guidance and support have been crucial throughout this endeavor. My heartfelt appreciation also extends to my co-supervisor Dr. Hamza BELMADANI, whose exceptional assistance and insightful feedback have been instrumental in the success of this project. Additionally, I am grateful to my internship training supervisor MAALLEMI Mohamed (Cadre d'études technique maint) for the practical experience and mentorship they have provided, which have been integral to the completion of this thesis. The collective expertise, encouragement, and unwavering dedication of these individuals have been pivotal in helping me achieve this milestone. I extend my sincere gratitude to all of you for your steadfast support and motivation.

Dedication

I dedicate this work to my beloved mother and father, whose unwavering support and encouragement have been my foundation.

To my sisters and cousins, who have always been there with love and companionship.

To my friends, for their constant motivation and understanding.

And to my dear nephews and nieces, who inspire me with their innocence and joy.

This achievement is as much yours as it is mine.

List of Figures

List of Tables

Contents

Table of abbreviation

AC	Alternating Current
DC	Direct Current
VDF	Variable Frequency Drive
RMF	Rotating Magnetic Field
EMF	Electromotive Force
PID	Proportional Integrator Derivative
IGBT	Insulated Gate Bipolar Transistor
RFO	Rotor Flux Orientation
DRFOC	Rotor Direct Rotor Flux Oriented
RFOOC	Indirect Rotor Flux Oriented Control
PWM	Pulse Width Modulation
SPWM	Sinusoidal Pulse Width Modulation
SVPWM	Space Vector Pulse Width Modulation
TIA Portal	Totally Integrated Automation Portal

General Introduction

Optimal speed control for induction motors is a crucial aspect of modern industrial automation, influencing both productivity and energy usage. This study examines the implementation and analysis of speed regulation for an induction motor using a Variable Frequency Drive (VFD). The research emphasizes the optimization of motor performance through an open loop configuration, a fundamental technique for achieving precise and stable motor control.

The investigation involves the use of a Siemens VFD, which receives commands from an S1200 Siemens PLC. Additionally, simulation experiments were conducted using Simulink in both open loop and closed loop configurations, comparing these results to those achieved by the VFD.

The primary goal is to achieve precise speed control, which is essential for maintaining consistent industrial processes and improving overall system performance. Through a comparative analysis of the open loop and closed loop simulation results, this study provides valuable insights into their respective benefits and limitations, guiding the practical application of VFDs in industrial settings. Furthermore, the findings offer recommendations for optimizing motor performance based on unique operational needs.

Advancements in control technology have enabled the creation of systems that operate with greater precision and dependability. Engineers are continuously refining these control mechanisms to enhance their performance and consistency, meeting the evolving needs of various industries.

This thesis explores the study and control of three-phase induction motors, divided into four chapters.

Chapter 1 covers the construction, operation, and performance characteristics of these motors.

Chapter 2 delves into scalar and vector control techniques, including the use of VFDs and SVPWM.

Chapter 3 introduces Programmable Logic Controllers (PLCs), emphasizing their role in industrial automation and integration with VFDs.

Chapter 4 presents simulation models and practical implementations using Siemens G120 VFD and S7-1200 PLC, comparing simulated and practical results to demonstrate the effectiveness of the control methods.

Chapter 1 Three Phase Induction Motors

1.1 Introduction:

AC induction motors have earned their status as the most prevalent choice for industrial motion control systems and main powered home appliances. Their widespread adoption can be attributed to their straightforward and robust design, cost-effectiveness, minimal maintenance requirements, and the ability to directly connect to AC power sources. These inherent advantages make AC induction motors the go-to solution for a multitude of applications.

In this chapter, we aim to provide a comprehensive overview of their construction and principle of operation, performance characteristics, and mathematical modeling. For optimize performance, control and drive innovation in diverse industrial applications.

1.2 Construction of Induction Motors:

The construction of induction motors as shown in Figure 1 is a crucial aspect that defines their efficiency, reliability, and adaptability for various applications. In general, the architecture of an induction motor comprises two main components: the stator and the rotor.

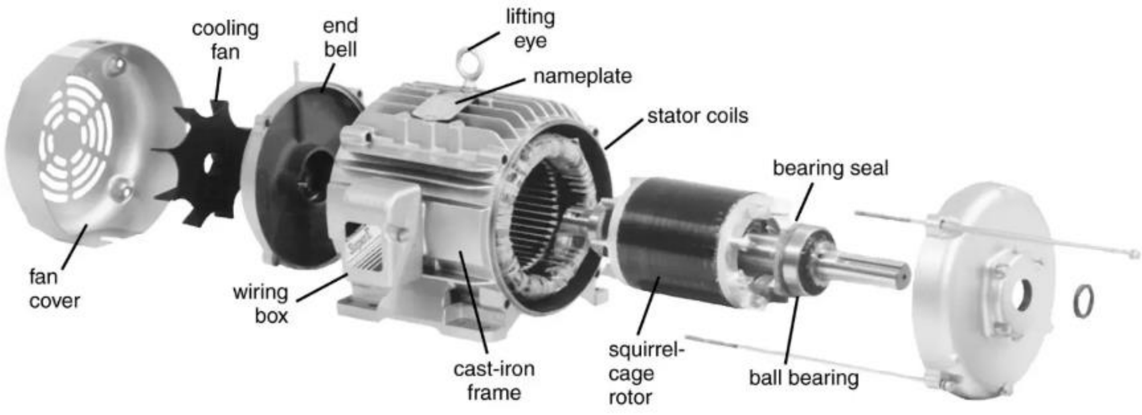

Figure 1: Exploded view of a three-phase induction motor.

1.2.1 Stator Construction:

The stator serves as the stationary component of the motor and plays a fundamental role in generating the rotating magnetic field necessary for motor operation. Typically, the stator is constructed using laminated iron cores with slots to house the stator windings. These windings are often made of copper or aluminum and are configured in a specific pattern to achieve the desired magnetic field when supplied with three-phase alternating current (AC) Figure 2. The number of poles in the stator winding determines the motor's synchronous speed.

Figure 2: Stator construction.

1.2.2 Rotor Construction:

The rotor construction in induction motors varies based on the specific type: wound-rotor or squirrel-cage Figure 3. In the case of a wound-rotor induction motor, the rotor iron is also laminated and slotted to accommodate insulated windings. These windings, similar to those in the stator, are wound for the same number of poles and are typically connected to slip rings mounted on the rotor shaft. This configuration allows for external resistors to be connected via carbon brushes, enabling speed control.

On the other hand, squirrel-cage rotors are characterized by a solid, short-circuited conductor arrangement. The rotor core is made of laminated iron, and the conductors, typically aluminum or copper bars, are placed in the rotor slots. This simplified design enhances durability, reliability, and requires minimal maintenance.

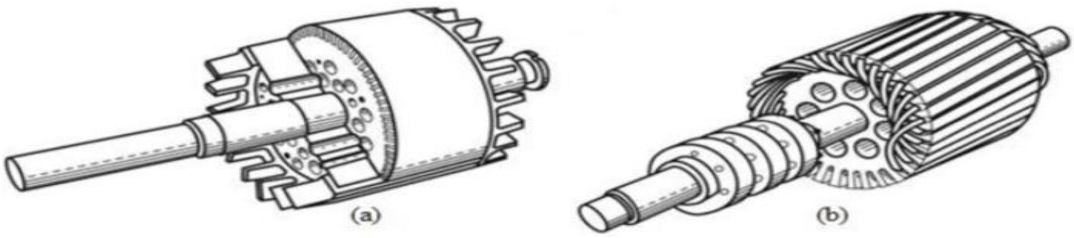

Figure 3: Rotor construction, (a) Cage rotor and (b) Wound rotor induction motor rotor types.

The careful design and construction of both stator and rotor components contribute to the overall performance and efficiency of induction motors. These construction details, combined with advancements in materials and manufacturing techniques, ensure the continued success and widespread use of induction motors across various industrial and domestic applications. In subsequent sections, we will delve deeper into the characteristics, modeling, and control techniques associated with induction motors.

1.3 Principle of Operation:

The operation of three-phase induction machines is grounded in the principles of electromagnetic induction, as described by Faraday's law $E = BVL$.

When connected to a three-phase AC power source, the stator windings generate a rotating magnetic field, which revolves around the periphery of the rotor. This phenomenon is succinctly summarized by Faraday's law, where a changing magnetic field induces a voltage in the rotor conductors [1].

This induced voltage drives current flow within the rotor circuit, leading to the production of a magnetic field that interacts with the rotating stator magnetic field. The resultant force, governed by the Lorentz force law, generates torque, enabling the motor to perform mechanical work.

In a three-phase induction motor, each of the three-phase currents (Ia, Ib, and Ic) has equal magnitude but differs in phase by 120°. When these balanced three-phase currents flow through the windings, they generate magnetic flux **Φ**. This magnetic flux produced by the balanced currents in the three-phase windings results in a rotating magnetic flux (RMF). The RMF rotates at a constant speed known as the synchronous speed **Ns** [2].

As the RMF rotates, it generates a magnetic field in the air gap between the stator and rotor. This changing magnetic field induces a voltage in the short-circuited bars of the rotor. Consequently, current flows through these rotor bars. The interaction between the rotating magnetic flux and the rotor current produces a force, resulting in the development of torque that drives the motor.

In summary, the balanced three-phase currents create a rotating magnetic field in the motor, which induces voltage in the rotor, leading to the flow of current and the generation of torque, ultimately driving the motor's operation.

1.3.1 Slip:

The synchronism between the rotating magnetic field speed and the rotor speed is characterized by slip, denoting the relative difference in speed. While the synchronous speed of the rotating magnetic field can be calculated using the formula (1-1) :

$$\boldsymbol{Ns} = \frac{\mathbf{120} \times \boldsymbol{f}}{\boldsymbol{P}} \tag{1-1}$$

Ns: the synchronous speed in revolutions per minute (rpm).

f: the frequency of the current in hertz (Hz).

P: the number of poles.

The slip **s** describes this relative motion in per unit or in percent. Thus, the slip in per unit (1-2):

$$s = \frac{Ns-Nr}{Ns} \qquad (1\text{-}2)$$

s: slip.

Nr: rotor speed.

The mechanical speed of the rotor, in terms of slip and synchronous speed is given by (1-3):

$$Nm = (1-s)Ns \qquad (1\text{-}3)$$

The slip speed **Nsl** is defined as the difference between synchronous speed and rotor speed and indicates how much the rotor slips behind the synchronous speed [2]. Hence (1-4):

$$Nsl = Ns - Nm = s \times Ns \qquad (1\text{-}4)$$

Nsl: slip speed.

1.3.2 Equivalent circuit:

An induction motor, often referred to as a **rotating transformer**, operates based on electromagnetic induction principles. When an EMF is supplied to its stator, a voltage is induced in its rotor due to electromagnetic induction. Essentially, an induction motor can be thought of as a transformer with a rotating secondary.

- Stator model : The stator winding of the induction motor has two key components:
  - Winding Resistance (R_1): Represents the copper losses occurring in the stator windings.
  - Winding Inductance (X_1): Causes a voltage drop due to inductive reactance.
  - Additionally, there’s a core loss component (**Rc**) and a magnetizing reactance (**Xm**).
- Rotor model : The rotor winding also contributes to the equivalent circuit:
  - Rotor Winding Resistance (R_2’): This resistance is referred to the stator winding.
  - Rotor Winding Inductance (X_2’): Similar to X_1, it’s the inductance of the rotor winding referred to the stator.
  - Rotor Power (R_2/s): Represents the mechanical power output and includes the rotor’s copper losses.

Exact Equivalent Circuit: the exact equivalent circuit accounts for all parameters.

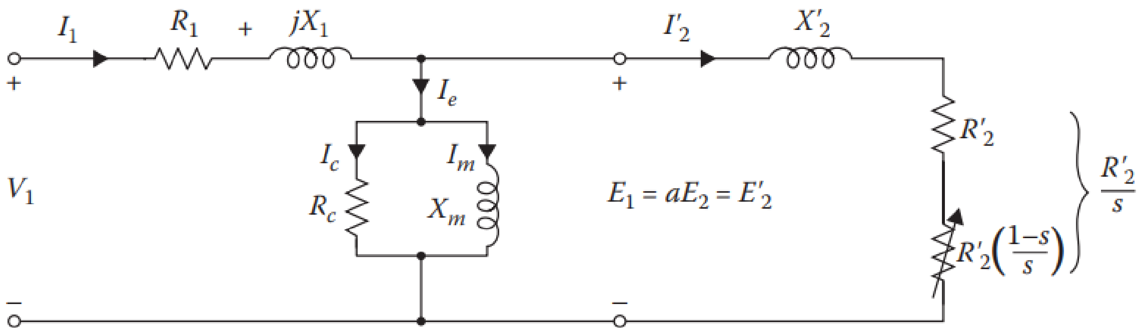

Figure 4: Exact Equivalent Circuit.

Approximate Equivalent Circuit: the approximate circuit simplifies calculations by shifting the shunt branch toward the primary side.

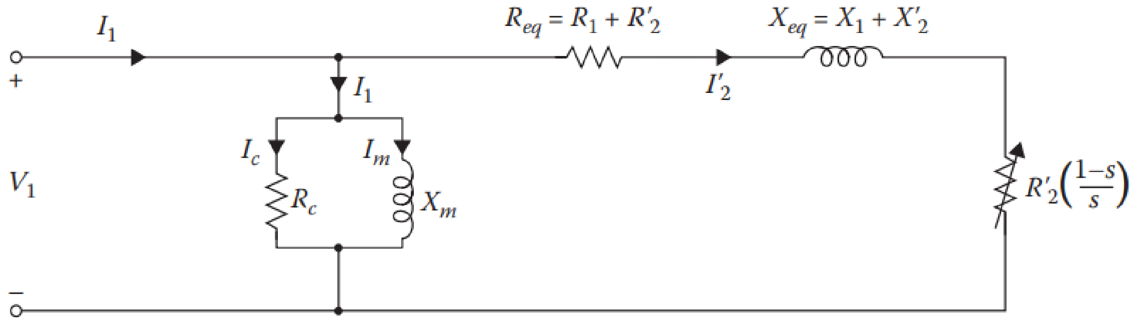

Figure 5: Approximate Equivalent Circuit.

1.4 Performance Characteristics:

From equivalent circuit we can predict performance characteristics:

1.4.1 Power flow and Efficiency:

The power flow of Induction Motor explains the input given to the motor, the losses occurring, and the output of the motor. The input power given to an induction motor is in the form of three-phase voltage and currents [3] [1] [4].

Input power : $$\boldsymbol{P_{in} = 3 \times V_s \times I_s \times \cos \emptyset} \quad (1\text{-}5)$$

Stator copper loss: $$\boldsymbol{P_{ls} = 3 \times Is^2 \times R_s} \quad (1\text{-}6)$$

Rotor copper loss : $$\boldsymbol{P_{lr} = 3 \times Ir^2 \times R_r} \quad (1\text{-}7)$$

Core loss : $$\boldsymbol{P_{lc} = 3 \times E_1{}^2 \times R_c} \quad (1\text{-}8)$$

Power across air gap: $$P_{ag} = 3 \times Ir^2 \times \frac{R_r}{s} \quad (1\text{-}9)$$

Developed Mechanical Power: $$P_d = P_{ag} - P_{lr} = 3 \times Ir^2 \times R_r \times \frac{(1-s)}{s} \quad (1\text{-}10)$$

Shaft Power or Output Power: $$P_{sh} = P_d - P_{fw} \quad (1\text{-}11)$$

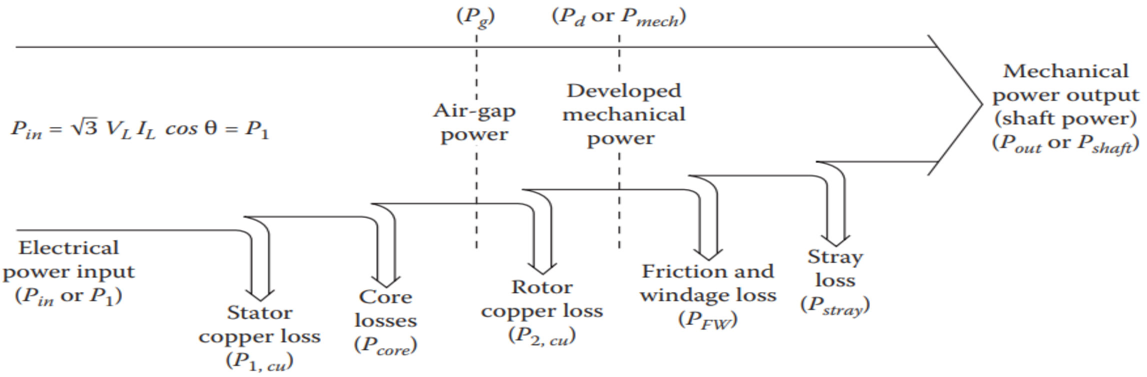

Figure 6: Power flow of induction motor.

The rotor current: $$I_s = \frac{V_s}{(R_s + \frac{R_r}{s})^2 + (X_s + X_r)^2} \quad (1\text{-}12)$$

The efficiency of the induction motor can be determined from (1-13):

$$\eta = \frac{P_{sh}}{P_{in}} = \frac{P_d - P_{fw}}{P_{ls} + P_{lc} + P_{ag}} \quad (1\text{-}13)$$

The efficiency is highly dependent on slip if all losses are neglected except those in the resistance of the rotor circuit (1-14):

$$P_{sh} = P_{ag} \times (1 - s) \quad (1\text{-}14)$$

1.4.2 Torque-Speed Relationship:

Electromagnetic torque developed by motor is (1-15):

$$\tau = \frac{P_d}{\omega_m} = \frac{P_{ag}}{\omega_s} = \frac{3}{\omega_s} \times I_r^{\,2} \times \frac{R_r}{s} = \frac{3V_s}{(R_s + \frac{R_r}{s})^2 + (X_s + X_r)^2} \times \frac{R_r}{s\omega_s} \quad (1\text{-}15)$$

Torque produced due to interaction between induced rotor currents and stator field [3]. The induced torque of the motor is zero at synchronous speed, the torque- speed curve is nearly linear between no load and full load. In this range, the rotor resistance is much larger than the rotor reactance, so the rotor current, the rotor magnetic field, and the induced torque increase linearly with increasing slip.

There is a maximum possible torque that cannot be exceeded. This torque, called the pullout torque or breakdown torque, is 2 to 3 times the rated full load torque of the motor.

The starting torque on the motor is slightly larger than its full-load torque, so this motor will start carrying any load that it can supply at full power.

If the rotor of the induction motor is driven faster than synchronous speed, then the direction of the induced torque in the machine reverses and the machine becomes a generator, converting mechanical power to electric power.

If the motor is turning backward relative to the direction of the magnetic fields, the induced torque in the machine will stop the machine very rapidly and will try to rotate it in the other direction [4].

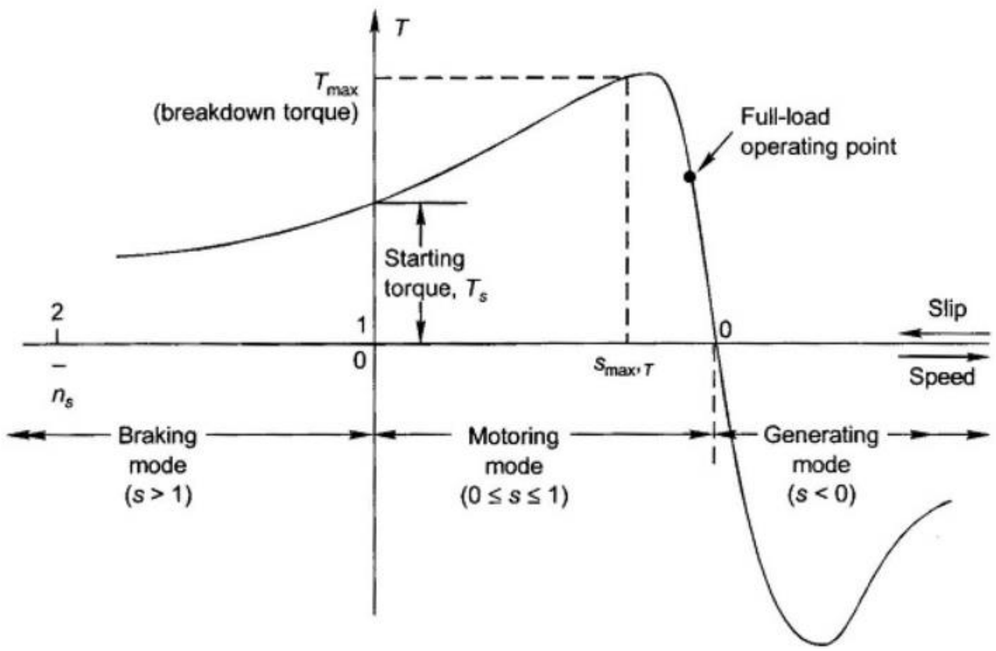

Figure 7: Induction motor torque- speed characteristic curve.

1.4.3 Effect of rotor resistance:

The rotor circuit resistance has significant impact on starting torque, the speed at which the breakdown torque occurs, and the slip during the normal running operation.

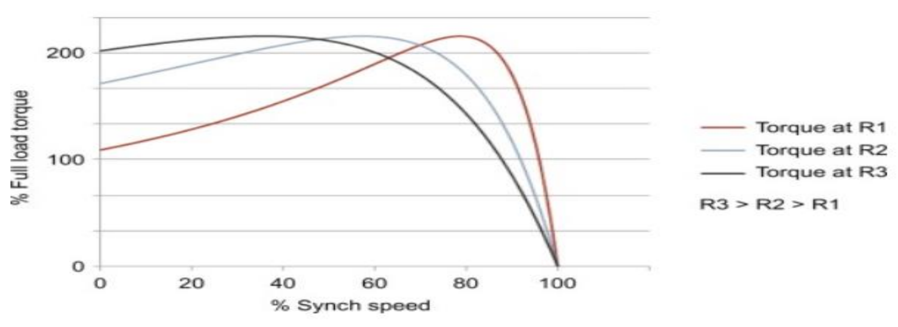

Figure 8: The effect of varying rotor resistance on the torque-speed characteristic

Low rotor resistance results in high full load speed (low slip), high efficiency (low rotor losses), and slightly higher starting current.

High rotor resistance results in high starting torque for line current drawn and slightly lower current during starting, but results in lower full load speed and lower efficiency (high rotor losses).

The National Electrical Manufacturers Association (NEMA) has established four different designs for electrical induction motors: designs A, B, C, and D [1].

Class A: Max slip 5%, has high to medium starting current and normal breakdown torque, it is suited for broad variety of applications such as fans and pumps.

Class B: Max slip 5%, it has low starting current and normal breakdown torque, it is suited for broad variety of applications, normal starting applications are common in HVAC with fans, blowers.

Class C: Max slip 5%, it has low starting current and normal bre1akdown torque, it is suited for equipment's with high inertia.

Class D: Max slip 5-13%, Low starting current and normal breakdown torque, it is used for equipment with high inertia such as cranes, hoist etc.

1.5 Equivalent-circuit Parameters:

The equivalent circuit of an induction motor is a very useful tool for determining the motor's response to changes in load. However, if a model is to be used for a real machine, it is necessary to determine the values of (R_s, X_s, R_r, X_r, X_m) [4].

Several tests are conducted to determine the equivalent-circuit parameters of an induction motor accurately. These tests include:

1.5.1 No-Load Test:

This test involves running the motor with no mechanical load attached while maintaining rated voltage and frequency.

The following measurements are available from the no-load test:

V_{nl} - The line-to-neutral voltage [V]

I_{nl} -- The line current [A]

P_{nl} -- The total electrical input power [W]

$$\boldsymbol{X_{nl} = X_s + X_m} \quad (1\text{-}16)$$

$$\boldsymbol{X_{nl} \approx \frac{V_{nl}}{I_{nl}}} \quad (1\text{-}17)$$

1.5.2 Blocked Rotor Test:

In this test, the rotor is mechanically blocked from rotating while rated voltage and frequency are applied to the stator windings.

The following measurements are available from the blocked rotor test:

V_{bl}= The line-to-neutral voltage [V]

I_{bl} = The line current [V]

p_{bl} = The total electrical input power [W]

f_{nl}= The frequency of the blocked-rotor test [Hz]

$$|Z_{bl}| = \frac{V_{bl}}{\sqrt{3} \times V_{bl} \times I_{bl}} \quad (1\text{-}18)$$

$$Z_{bl} = R_{bl} + jX_{bl} \quad (1\text{-}19)$$

$$R_{bl} = R_s + R_r \quad (1\text{-}20)$$

$$X_{bl} = X_s + X_r \quad (1\text{-}21)$$

1.5.3 DC Test:

Stator resistance: $$R_s = \frac{V_{dc}}{2I_{dc}} \quad (1\text{-}22)$$

In conclusion we use equations (1-16)(1-20)(1-21)(1-22) and [2] to identify the value of (R_s, X_s, R_r, X_r, X_m).

Table 1 Stator and rotor reactance's relationship

Rotor Design	X_1 and X_2 as Fractions of X_{br}	
—	X_1	X_2
Wound rotor	$0.5X_{br}$	$0.5Xb_r$
Design A	$0.5X_{br}$	$0.5X_{br}$
Design B	$0.4X_{br}$	$0.6X_{br}$
Design C	$0.3Xb_r$	$0.7Xb_r$
Design D	$0.5X_{br}$	$0.5X_{br}$

1.6 Starting of 3-phase Induction Motors:

The starting of three-phase induction motors is a critical aspect of their operation, there are two important factors to be considered the starting current and the starting torque, Various methods are employed to start induction motors, each tailored to specific applications and operating conditions.

1.6.1 Direct On-Line (D.O.L.) Starting:

By directly connecting the induction motor to a three-phase supply Figure 9, it can be started. Using this approach, the motor starts at a low power factor and a high starting current (roughly four to seven times the rated current). DOL starting is therefore appropriate for relatively small motors (up to 10 kW) [5].

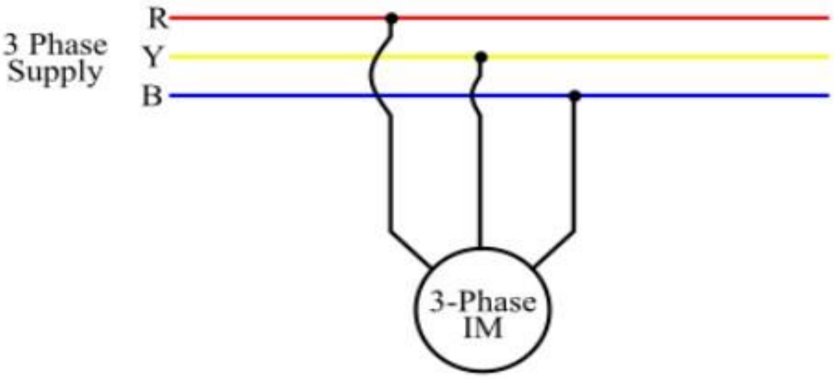

Figure 9: Direct on line starting.

1.6.2 Stator Resistance Starting:

During starting, this method connects the external resistance in series with each phase of the stator winding Figure 10.

There is less voltage available across the motor terminals as a result of the external resistance causing a voltage drop across and the starting current is decreased, after that the starting resistances are totally eliminated once the motor reaches its rated speed.

This method has two drawbacks. Reduced starting torque due to voltage drop and power wastage in the resistances.

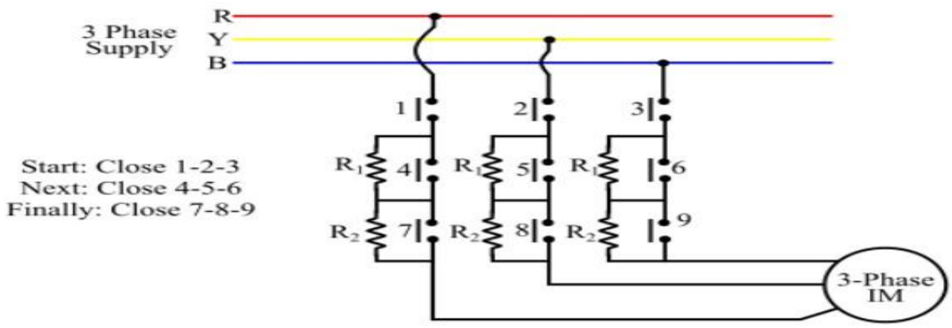

Figure 10: Stator resistance starting diagram

1.6.3 Autotransformer Starting:

This method lowers the induction motor's starting voltage by using an autotransformer Figure 11, when the autotransformer is in the circuit, its tapings are arranged so that the motor receives 60% to 80% of the line voltage when it starts, and it is connected to the full line voltage once it reaches a sufficient speed.

The autotransformer starting has many advantages such as low power loss, low starting current etc. [5].

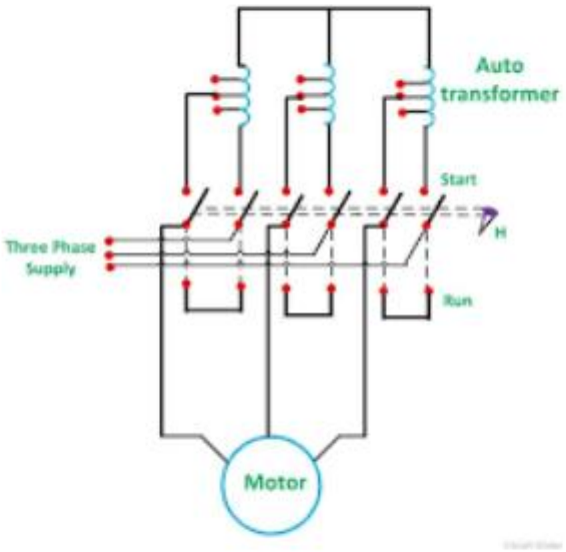

Figure 11: Autotransformer starting diagram.

1.6.4 Star-Delta Starting:

In star-delta starting, the motor is initially connected in a star configuration, reducing the voltage applied to each phase, once the motor reaches a certain speed, it is switched to a delta configuration, applying full voltage across the windings.

This method reduces starting currents by **1/3** compare to original and mechanical stress but requires a star-delta starter or a motor control panel capable of switching between configurations.

The main drawback of this approach is a significant decrease in starting torque because of a voltage drop in the star connection at startup, for medium-sized motors up to 25 horsepower, star-delta starting is utilized [5].

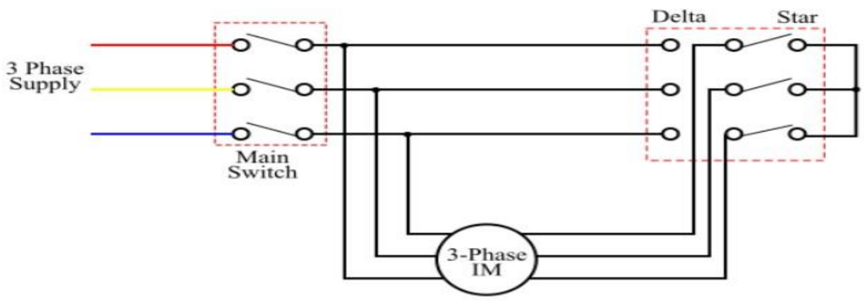

Figure 12: Star delta starting diagram.

1.6.5 Variable frequency drives starting

Variable frequency drives (VFDs) are sophisticated motor control devices that allow for precise control of motor speed by adjusting the frequency of the electrical supply. When used for starting induction motors the VFD ramps up the frequency and voltage gradually, VFDs provide several advantages, including soft-start capabilities, reduced starting current, and improved efficiency [6].

In conclusion each starting method has its advantages and disadvantages, and the choice depends on factors such as the size of the motor, the type of load, and the requirements of the application.

1.7 dq-Model of Induction Motors:

The purpose of this chapter is to mathematically illustrate how to model the induction machine using various state models based on the chosen reference frame. These models are described in a two-phase reference frame, which can either be rotating (dq) or fixed to the stator (αβ). The fixed reference frame is derived from the conventional three-phase reference frame of the induction machine using appropriate mathematical transformations.

The asynchronous machine is a complex system that can be influenced by various physical phenomena, such as magnetic saturation, iron losses, and the skin effect. It is important to consider these factors when setting up the equations for the induction machine, even though the power supply is assumed to be sinusoidal.

1.7.1 The equations of the machine in the abc axis:

The stator is composed of three windings that are spaced out and separated by an electrical angle of 120°. The same principle applies to the rotor, regardless of whether it is a squirrel cage or wound rotor.

Figure 13 depicts the arrangement of the machine's six windings. In the three-phase reference, the three vectors a, b, and c are aligned with the axes of the stator windings. This alignment is also true for the rotor A, B and C.

Typically, the a axis is regarded as a reference point, and the angle θab determines the position of the rotor in relation to the stator.

$$0 = \begin{bmatrix} V_{ra} \\ V_{rb} \\ V_{rc} \end{bmatrix} = \frac{d\phi_r}{dt} + R_r i_r = \frac{d}{dt}\begin{bmatrix} \phi_{ra} \\ \phi_{rb} \\ \phi_{rc} \end{bmatrix} + \begin{bmatrix} R_r & 0 & 0 \\ 0 & R_r & 0 \\ 0 & 0 & R_r \end{bmatrix}\begin{bmatrix} i_{ra} \\ i_{rb} \\ i_{rc} \end{bmatrix} \tag{1-23}$$

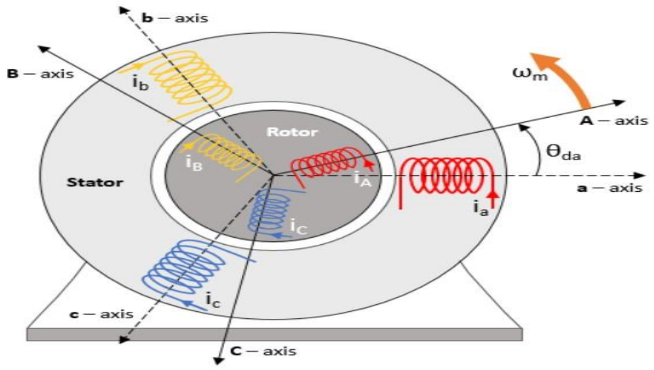

Figure 13: Three-Phase Sinusoidal Model Electrical System.

$$\phi_s = ł_{ss} i_s + m_{sr} i_r \tag{1-24}$$

$$\phi_r = ł_{rr} i_r + m_{rs} i_s \tag{1-25}$$

$$m_{sr} = M \begin{bmatrix} \cos\theta_r & \cos(\theta_r - 4\pi/3) & \cos(\theta_r - 2pi/3) \\ \cos(\theta_r - 2\pi/3) & \cos(\theta_r) & \cos(\theta_r - 4\pi/3) \\ \cos(\theta_r - 4\pi/3) & \cos(\theta_r - 2\pi/3) & \cos\theta_r \end{bmatrix} \tag{1-26}$$

$$l_{ss} \begin{bmatrix} l_s & M_s & M_s \\ M_s & l_s & M_s \\ M_s & M_s & l_s \end{bmatrix}; l_{rr} \begin{bmatrix} l_r & M_r & M_r \\ M_r & l_r & M_r \\ M_r & M_r & l_r \end{bmatrix} \tag{1-27}$$

By rearranging the matrix that represents the mutual inductances of the stator, we can obtain the matrix that represents the mutual inductances of the rotor (1-28).

$$m_{rs} = (m_{sr})^T \tag{1-28}$$

The abc model provides a complete comprehension of the dynamic behavior of the IM. The interconnection of the differential equations is due to the mutual inductance that exists between the windings.

The complexity arises because the connections between the stator and rotor vary with time, depending on the position of the rotor.

To simplify the calculation of the dynamic solution, mathematical transformations like "dq" or "αβ" have been used in the abc model. This leads to relationships that do not rely on the angle θ and makes it easier to reduce the machine's equations [3].

1.7.2 Clark transformation:

The Clark transform is used to convert time-based signals (like voltage, current, and flux) from a three-phase coordinate system (abc) to a fixed two-phase reference frame called αβ Figure 14. This is achieved through a space vector transformation (1-29).

$$\begin{bmatrix} x_0 \\ x_\alpha \\ x_\beta \end{bmatrix} = \frac{2}{3}\begin{bmatrix} 1 & 2 & 1 \\ 2 & -1 & -1 \\ 0 & \frac{\sqrt{3}}{2} & -\frac{\sqrt{3}}{2} \end{bmatrix}\begin{bmatrix} x_a \\ x_b \\ x_c \end{bmatrix} \tag{1-29}$$

The process of converting a fixed reference frame αβ into a three-phase coordinate system abc is achieved by employing the Inverse Clarke transformation. This transformation is specifically defined as

(1-30):

$$\begin{bmatrix} x_a \\ x_b \\ x_c \end{bmatrix} = \frac{2}{3}\begin{bmatrix} \frac{1}{2} & 1 & 0 \\ \frac{1}{2} & -\frac{1}{2} & \frac{\sqrt{3}}{2} \\ \frac{1}{2} & -\frac{1}{2} & -\frac{\sqrt{3}}{2} \end{bmatrix}\begin{bmatrix} x_0 \\ x_\alpha \\ x_\beta \end{bmatrix} \tag{1-30}$$

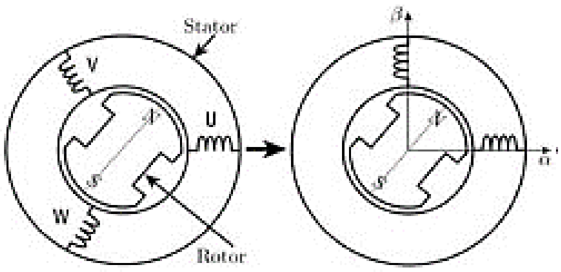

Figure 14: Clark transformation.

The coefficient in the differential equation continues to change over time due to the mutual inductance between the stator and rotor, which is influenced by the rotor's position.

To remove the impact of time, it is essential to perform an additional transformation where all variables related to both the stator and rotor are referenced in a single frame [7].

1.7.3 Park transformation:

Clarck's method simplifies the system by reducing the number of equations from six to four. This is achieved by creating a rotating field in a three phase system using a two phase system with two coils. The relationship between the stator and rotor's mutual induction is still dependent on the speed of rotation. Therefore, it is recommended to utilize the park transformation, which is defined by the transformation matrix provided [3].

$$\mathrm{Te}(\theta_e) = \frac{2}{3}\begin{bmatrix} \frac{1}{2} & \frac{1}{2} & \frac{1}{2} \\ \cos(\theta_e) & \cos\left(\theta_e - \frac{2\pi}{3}\right) & \cos\left(\theta_e - \frac{4\pi}{3}\right) \\ -\sin(\theta_e) & -\sin\left(\theta_e - \frac{2\pi}{3}\right) & -\sin\left(\theta_e - \frac{4\pi}{3}\right) \end{bmatrix} \quad (1\text{-}31)$$

The Park transformation is identified by matrix T_e. Essentially, it entails depicting electric and magnetic properties in a reference frame that rotates at an arbitrary velocity ωe.

$$x_{dq} = T_e(\theta_e)x_{abc} \quad (1\text{-}32)$$

1.7.4 Transformation between αβ and dq reference frames:

The conversion from the αβ reference frame to the dq reference frame is widely utilized in the analysis and control of three-phase AC systems, this can be done using the following transformation (1-33):

$$\begin{bmatrix} x_d \\ x_q \end{bmatrix} = \begin{bmatrix} \cos(\theta_e) & \sin(\theta_e) \\ -\sin(\theta_e) & \cos(\theta_e) \end{bmatrix} \begin{bmatrix} x_\alpha \\ x_\beta \end{bmatrix} \quad (1\text{-}33)$$

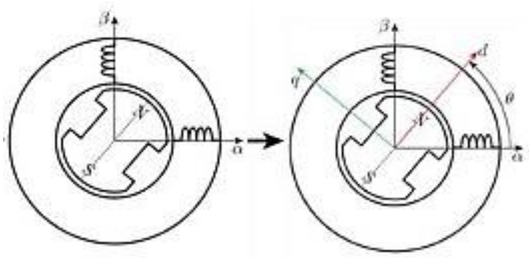

Figure 15: αβ to dq

Using the Clarke and Park transformations in succession streamlines the examination and calculations of a three-phase system by converting the current and voltage waveforms from AC to DC signals. Figure 16 presents a visual representation of the three reference frames previously mentioned.

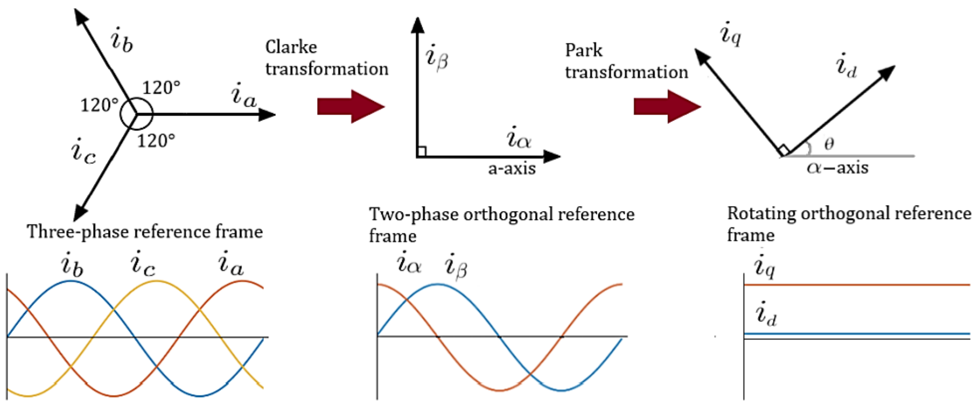

Figure 16: The three different reference frames.

1.7.5 Model of the induction machine in the park referential:

The equation system formulated in the Park reference (dq), rotating at the speed ωe, which defines the functioning of the asynchronous machine in both dynamic and static modes [3] [8], can be written as:

$$\begin{bmatrix} v_{ds} \\ v_{qs} \\ v_{dr} \\ v_{qr} \end{bmatrix} = \begin{bmatrix} R_s + pL_s & -\omega_e L_s & pL_m & -\omega_e L_m \\ \omega_e L_s & R_s + pL_s & \omega_e L_m & pL_m \\ pL_m & -(\omega_e - \omega_r)L_m & R_r + pL_r & -(\omega_e - \omega_r)L_r \\ (\omega_e - \omega_r)L_m & pL_m & (\omega_e - \omega_r)L_r & R_r + pL_r \end{bmatrix} \cdot \begin{bmatrix} i_{ds} \\ i_{qs} \\ i_{dr} \\ i_{qr} \end{bmatrix} \tag{1-34}$$

$$T_e = \frac{2}{3} p \frac{L_m}{L_r} (\psi_{dr} i_{qs} - \psi_{qr} i_{ds}) \tag{1-35}$$

1.7.6 Commonly used reference frames:

The performance of induction motors can be predicted by utilizing the dynamic model based on the reference frames theory.

According to the application purpose, there are three commonly used reference frames derived from the generalized (arbitrary) reference frame model of induction motor:

1.7.6.1 Stationary (Stator) Reference Frame Model:

The reference frame speed is zero i.e. it is equivalent to the stator (stationary) speed$\omega_e = 0$.

$$\begin{bmatrix} v_{ds} \\ v_{qs} \\ v_{dr} \\ v_{qr} \end{bmatrix} = \begin{bmatrix} R_s + pL_s & 0 & pL_m & 0 \\ 0 & R_s + pL_s & 0 & pL_m \\ pL_m & \omega_r L_m & R_r + pL_r & \omega_r L_r \\ -\omega_r L_m & pL_m & -\omega_r L_r & R_r + pL_r \end{bmatrix} \cdot \begin{bmatrix} i_{ds} \\ i_{qs} \\ i_{dr} \\ i_{qr} \end{bmatrix} \tag{1-36}$$

Usually, it is adopted by the stator (scalar) controlled induction motor drives [9].

1.7.6.2 Rotor Reference Frame Model:

This is typically utilized in induction motors where the rotor side is responsible for speed control. The speed of this model is equal to that of the rotor in the reference frame. $\omega_e = \omega_r$

$$\begin{bmatrix} v_{ds}^r \\ v_{qs}^r \\ v_{dr}^r \\ v_{qr}^r \end{bmatrix} = \begin{bmatrix} R_s + pL_s & -\omega_r L_s & pL_m & -\omega_r L_m \\ \omega_r L_s & R_s + pL_s & \omega_r L_m & pL_m \\ pL_m & 0 & R_r + pL_r & 0 \\ 0 & pL_m & 0 & R_r + pL_r \end{bmatrix} \cdot \begin{bmatrix} i_{ds}^r \\ i_{qs}^r \\ i_{dr}^r \\ i_{qr}^r \end{bmatrix} \tag{1-37}$$

Used to simulations of wound-rotor induction motor slip-energy recovery scheme [3].

1.7.6.3 Synchronous Rotating Reference Frame Model:

The reference frame speed of this model is the same as that of the stator supply angular speed of the magnetic flux set-up in the air gap by the stator supply current. $\omega_e = \omega_s = 2\pi f_s$.

$$\begin{bmatrix} v_{ds} \\ v_{qs} \\ v_{dr} \\ v_{qr} \end{bmatrix} = \begin{bmatrix} R_s + pL_s & -\omega_s L_s & pL_m & -\omega_s L_m \\ \omega_s L_s & R_s + pL_s & \omega_s L_m & pL_m \\ pL_m & -(\omega_s - \omega_r)L_m & R_r + pL_r & -(\omega_s - \omega_r)L_r \\ (\omega_s - \omega_r)L_m & pL_m & (\omega_s - \omega_r)L_r & R_r + pL_r \end{bmatrix} \cdot \begin{bmatrix} i_{ds} \\ i_{qs} \\ i_{dr} \\ i_{qr} \end{bmatrix} \tag{1-38}$$

It is used for the machine vector control [8].

These reference frames play a crucial role in the analysis, modeling, and control of induction motors, enabling engineers to design efficient control strategies and improve motor performance in various applications.

1.8 Conclusion:

This chapter provides a comprehensive overview of induction motors, including their construction, principle of operation, performance characteristics, equivalent-circuit parameters, starting methods, and the dq-model. It emphasizes the importance of design features for optimizing efficiency and performance.

The chapter also explores performance characteristics such as efficiency, power factor, and torque-speed curves, which are important for motor selection and optimization, It discusses various starting methods and introduces the dq-model, which is necessary for advanced control strategies.

Overall, this chapter lays the foundation for further discussions on control methods and applications.

Chapter 2 Control Techniques of Induction Motors

2.1 Introduction:

In the past, the induction motor was typically operated at a fixed speed and frequency directly from the electrical grid. However, with the advancements in power electronic converters, it is now possible to use the motor at variable frequencies by incorporating a converter between the motor and the grid. This allows for an adjustable speed motor.

Variable frequency drives (VFDs) offer improved speed adjustment and motor control. Over the years, various AC drives control strategies have been developed to control the speed, torque, and position of the motor. These strategies can be categorized into two main methods: scalar control and vector control. Scalar control is based on the steady state model of the machine, where only the magnitude and frequency of voltage, current, and flux can be controlled.

On the other hand, vector control focuses on the dynamic states and allows for control over not just the magnitudes but also the instantaneous positions of voltage, current, and flux. For the purpose of this project, we will be focusing on scalar control.

2.2 Scalar control:

In systems like fans, pumps, and certain conveyor systems, where exact speed control is not necessary, scalar control is a popular and straightforward solution.

Scalar control is a reliable and effective approach to regulate the speed of induction motors with Variable Frequency Drives (VFDs). It provides a practical solution for achieving variable speed control.

Scalar control is based on the steady-state model of the motor. The control is due to the magnitude variation of the control variables only and disregards the coupling effect in the machine.

There are two main methods of scalar control depending on the type of variable frequency drive (VFD) employed: voltage source inverter and current source inverter.

2.3 Variable Frequency Control from Voltage Source Inverter:

V/f control, also known as variable frequency control from a voltage source, is a popular technique for managing motor speed. It involves adjusting the voltage and frequency supplied to the motor to maintain a consistent ratio between the two. This ensures that the motor operates smoothly and reliably, regardless of the speed or load it is subjected to.

The voltage of a motor can be controlled to control the flux, and frequency or slip can be controlled to control torque [10].

$$\phi_m \propto \frac{V_{ph}}{f} \tag{2-1}$$

The principal of this method is to keep the ratio V/F constant.

Below rated speed the control of speed is done by decreasing the frequency taking on consideration maintaining the flux constant, in this case the torque will be constant.

Above the rated speed the control of speed is done by increasing the frequency and keeping the voltage at rated to avoid instauration breakdown in the stator winding, which result reduction of the torque as shown in the Figure 17.

Above the base speed, the factor governing the torque become complex [11].

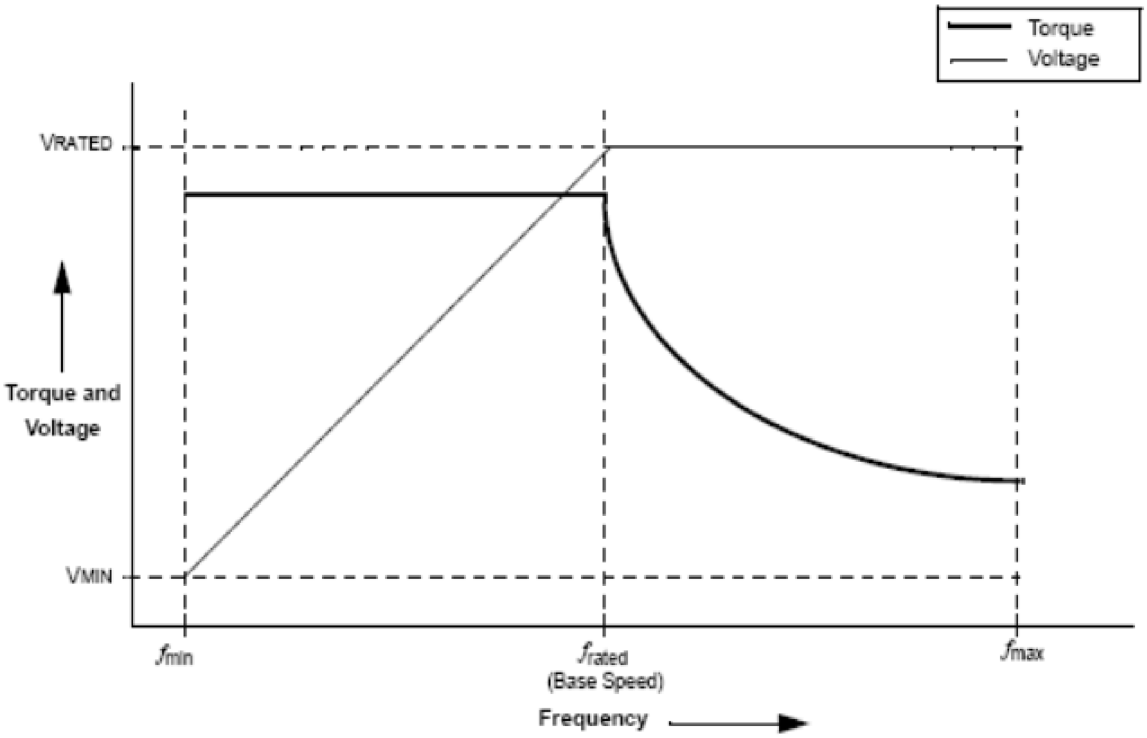

Figure 17: Torque and speed in V/F control.

The subsequent sections delve into the topic of scalar control techniques and implementation.

2.3.1.1 Volts/Hz Constant Control Open Loop:

This is the simpler version. It adjusts the voltage and frequency together while maintaining a constant V/f ratio.

The V/F control system operates by taking in the desired speed set point, which is usually given by either the operator or control system. From this speed reference, the control system calculates the necessary frequency for the motor to achieve the desired speed. At the same time, the V/F control system ensures that the voltage applied to the motor is adjusted in proportion to the frequency, then boost voltage V_0 is introduced to compensate for the voltage drop across the stator resistance and to maintain a constant voltage/frequency ratio.

$$V_0 = I_s \times R_s \tag{2-2}$$

$$V_s^* = V_0 + K_{vf} f_s \tag{2-3}$$

By integrating the desired frequency, an angle signal is created. This angle along with the desired voltage V_s^*, is then utilized to generate a three-phase voltage with specific amplitude and angle as shown in Figure 18 [10].

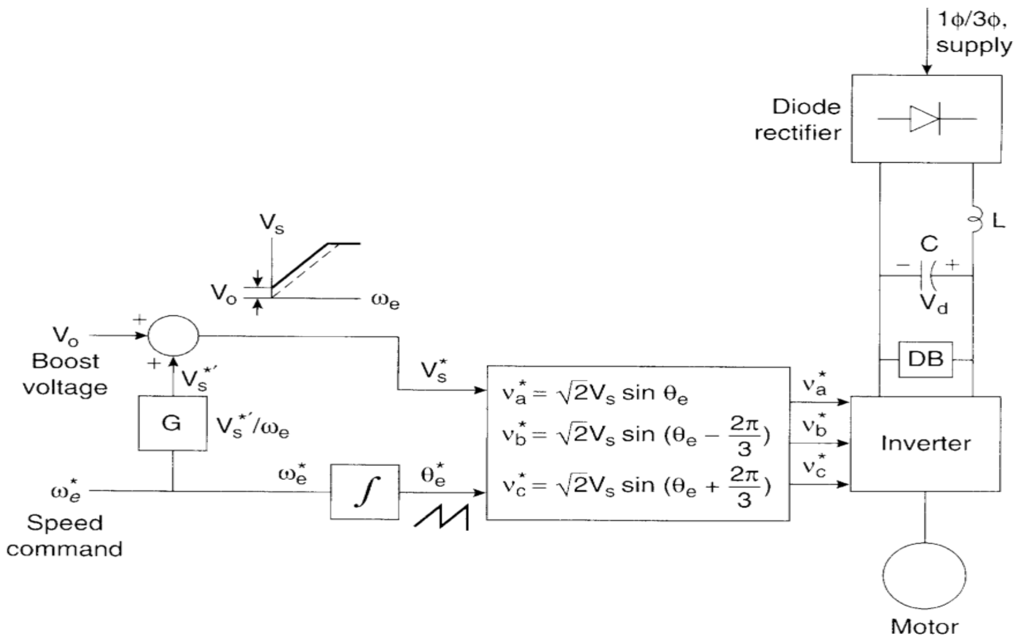

Figure 18: Block diagram of open loop V/F control

Open-loop scalar control provides a straightforward and economical method for regulating the speed of induction motors. It is particularly suitable for situations where the load remains constant and precise speed control is not a significant requirement. The drawbacks of this technique is;

The motor's speed cannot be perfectly regulated due to the rotor speed being slower than the synchronous speed. Instead, it is the stator frequency that is adjusted. Since the rotor speed is not measured, so the slip speed is not measured, as well the load torque if it’s increased beyond rated torque, this can result in unstable operation. As a consequence, there is a risk of exceeding the rated current and jeopardizing the inverter-rectifier combination [3].

2.3.1.2 Volts/Hz Constant Control Closed Loop:

The closed-loop approach presents a more accurate solution for regulating speed compared to the open-loop approach.

A feedback speed is added with slip regulation as shown in Figure 19. In this setup, the slip speed $\boldsymbol{\omega_{sl}^*}$ command is generated from the speed loop error using a proportional-integral (P-I) controller and a limiter. This slip speed is then combined with the feedback speed $\boldsymbol{\omega_r^*}$ signal to produce the synchronous speed $\boldsymbol{\omega_e^*}$ command. Additionally, the frequency command is used to generate the voltage command through a volts/Hz function generator, which compensates for the low-frequency stator drop [12].

$$\omega_e = \omega_r + \omega_{sl} \tag{2-4}$$

Electronic current limiting is a crucial feature in many AC motor drive applications. It plays a vital role in protecting both the motor and the drive itself from overcurrent. The motor drive uses current limiting to prevent the motor from drawing too much current and thus suffering damage.

PI controller is used to get good steady-state accuracy, and to attenuate noise. If we have a decrease of speed during loaded condition, PI controller quickly matched the desired speed.

Encoders speed provide essential feedback by sensing the motor's speed

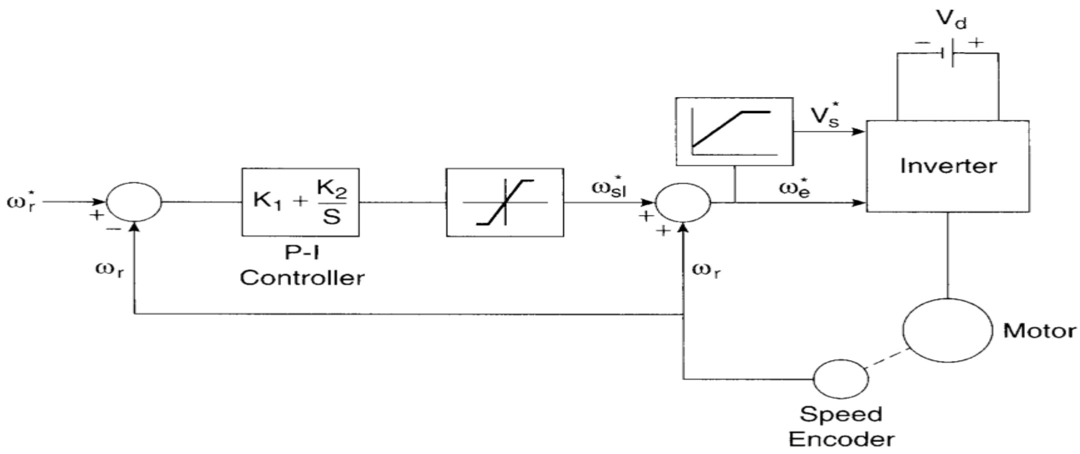

Figure 19 Block diagram of closed loop V/F control

We have seen that if the magnitude of the flux wave in an induction motor is kept constant, the torque in the normal operating region is directly proportional to the slip speed, this system can be seen as an open loop torque control within a speed control loop. When a step-up speed command is given, the machine accelerates freely until it reaches a slip limit determined by the stator current or torque limit. It then settles into a steady state with a slip value dictated by the load torque [12]. On the other hand, if the command speed (w) is decreased by a step, the drive enters regenerative or dynamic braking mode and decelerates with a constant negative slip.

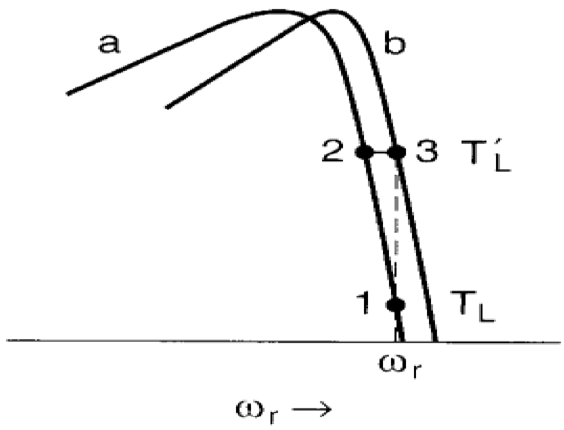

Figure 20: Changing in load torque.

Figure 20 illustrates the impact of changes in load torque and line voltage. When the load torque is increased from T_L to T_L', the speed will decrease, leading to point 2. However, the speed control loop will adjust the frequency to restore the original speed at point 3. It is important to note that without closed-loop flux control, variations in line voltage can result in flux drift [10].

To achieve variable frequency control using a voltage source inverter, it is important to consider the voltage drop across the stator leakage impedance. This voltage drop is influenced by the frequency and current of the motor, making it challenging to determine it without current feedback.

2.3.1.3 Variable Frequency Control from Current Source Inverter:

In an induction motor powered by a voltage source inverter, the voltage given to the stator is directly linked to the frequency, while also considering the voltage drop at stator resistance at lower speeds to maintain the flux constant. However, the stator voltage drop is determined by the stator current, and thus it cannot be accurately compensated by adjusting terminal voltage according to the preset voltage/frequency characteristics if the load changes and during acceleration and deceleration [13].

To keep the air gap flux constant, it is crucial to keep the magnetizing current constant. This means that the stator current of the induction motor needs to be controlled [3], in addition to its frequency.

$$\boldsymbol{I_r = \frac{E_1}{(R_r/s) + jL_{lr}\omega_s} = \frac{jL_m\omega_s}{(R_r/s) + jL_{lr}\omega_{sL}} I_m = \frac{jL_m\omega_s s}{R_r + jL_{lr}\omega_{sL}} I_m} \tag{2-5}$$

$$\boldsymbol{I_s = I_r + I_m = I_m\left(1 + \frac{jL_m\omega_s s}{R_r + jL_{lr}\omega_{sL}}\right) = I_m\left(\frac{R_r + jL_r\omega_{sL}}{R_r + jL_{lr}\omega_{sL}}\right)}$$

$$|\boldsymbol{I_s}| = \boldsymbol{I_m}\sqrt{\frac{\boldsymbol{R_r^2} + (\boldsymbol{L_{lr}} + \boldsymbol{L_m})\boldsymbol{\omega_{sL}})^2}{\boldsymbol{R_r^2} + (\boldsymbol{L_{lr}}\boldsymbol{\omega_{sL}})^2}} \quad (2\text{-}6)$$

The relation of stator current and the slip speed deduced in equation (2-6) is shown in Figure 21.

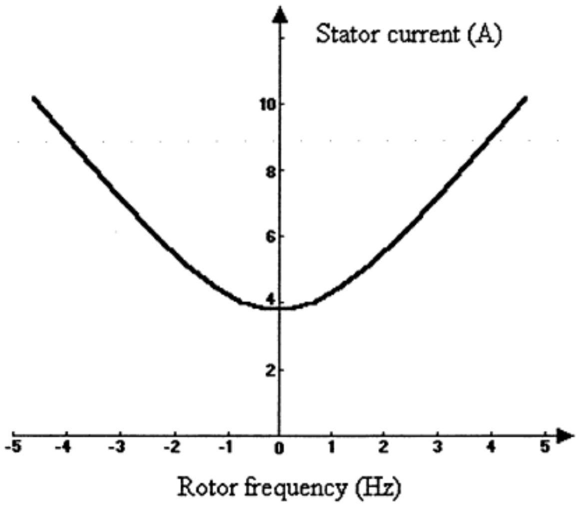

Figure 21: Relation between the stator current and rotor frequency (example).

The stator current of an induction motor operating on a variable slip frequency, $\boldsymbol{I_m}$ is held constant at the no-load operation, when the load increased the slip frequency increase then the stator current must be consequently increased then $\boldsymbol{I_m}$ can be held constant.

2.3.1.4 Constant Air Gap Flux Closed Loop Control:

The implementation of constant air gap flux control of induction motor cannot done with open loop, because the rotor speed is needed, the slip compensation used to improve the performance.

As we discussed the air gap flux can be maintained constant by controlling the stator current depend on rotor frequency, Torque control can be achieved by controlling the slip frequency as shown in the developed equation (2-7)

$$\tau = 3\mathrm{P}(\frac{V_s}{\omega_s})^2 \times \frac{R_r/\omega_{sL}}{(R_r/\omega_{sL})^2 + {L_{lr}}^2} = 3(\phi_m)^2 \times \frac{R_r/\omega_{sL}}{(R_r/\omega_{sL})^2 + {L_{lr}}^2} = K_{tm}\frac{R_r/\omega_{sL}}{(R_r/\omega_{sL})^2 + {L_{lr}}^2}$$

$$\tau = K_{tm}\frac{R_r/\omega_{sL}}{(R_r/\omega_{sL})^2 + {L_{lr}}^2} \quad (2\text{-}7)$$

K_{tm} : torque constant.

The torque is directly proportional to slip frequency with the constant airgap flux, the torque response is instantaneous because the slip speed can change instantly.

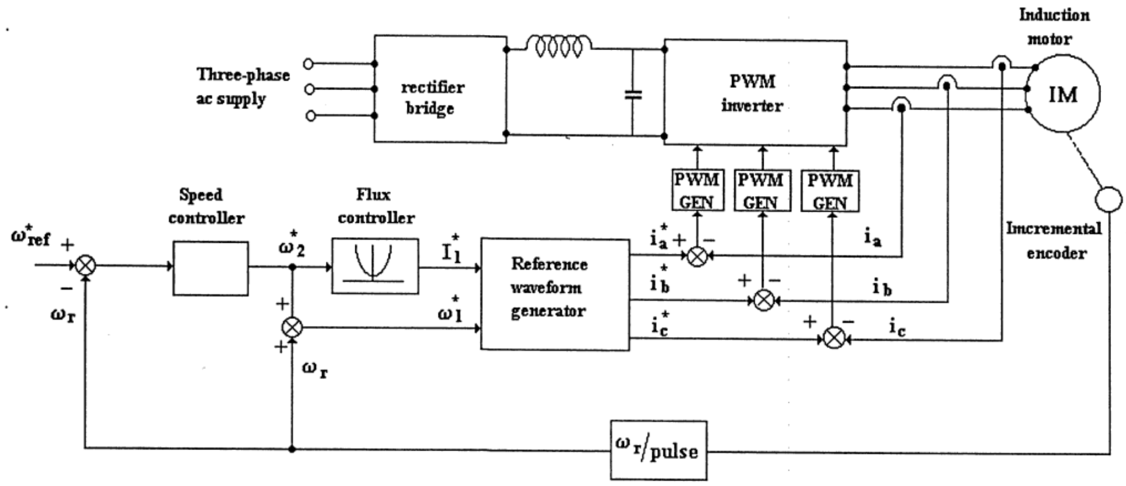

Figure 22: block diagram of closed air gap flux.

The implementation of closed loop control air gap flux constant can be done as shown in Figure 22, The speed controller utilize proportional-integral compensation. Its output is utilized as the slip frequency, which is constrained to the maximum torque value to ensure it does not surpass the breakdown threshold.

Then the flux controller generate a stator current with its corresponding rotor frequency,

The function generator creates the necessary command for current amplitude based on the connection between slip frequency and stator current. This helps maintain a constant airgap flux.

The control is operative until the rotor attains the desired speed with the required slip frequency.

2.4 Vector Control:

In systems like robotics, electrical vehicles and machine tools where precise speed and torque control is necessary, vector control is a preferred choice for high performance.

The vector control technique offers improved precision in regulating the torque and flux of AC motors, as compared to scalar control [3]. By employing mathematical transformations (D-q), advanced control strategies can be employed to separate the torque generation and magnetization functions of an AC induction motor. This section provides a brief overview of the two primary methods used in vector control.

2.4.1 Field Oriented Control:

Field Oriented Control can be implemented in three different orientations: stator, air gap, and rotor flux linkage. Rotor Flux Orientation is a technique that allows for the separation of stator currents in a squirrel-cage induction motor into two components: magnetizing current (ids*) and torque current (iqs*). This separation enables independent control of torque and flux in the motor, providing greater flexibility and efficiency.

$$\tau = \frac{3}{2}\frac{P}{2}\frac{L_m^2}{L_R} i_{qs} i_{ds} \tag{2-8}$$

The equation (2-8) was developed using (D-q) model of induction motor reference frame seeing in first chapter, and Orientation of d-axis of dq rotating frame toward the Ψ_r axis as shown

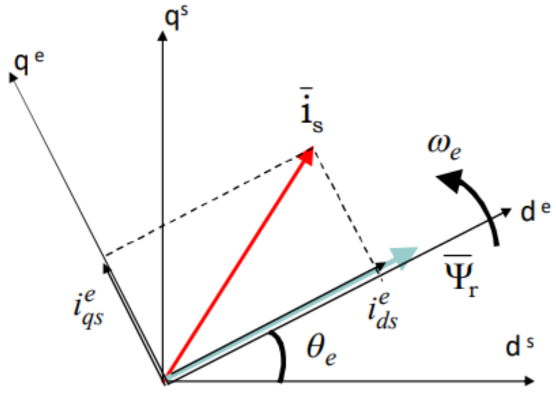

Figure 23: From ds to de.

θ_e is the angle between d^e and d^s where:

$$\theta_e = \int \omega_e dt \tag{2-9}$$

This angle must be known to convert the desired reference values set in dq^ereference frame to their corresponding values in dq^ereference frame.

There are essentially two approaches to Field Oriented control, depending on how the rotor angle is determined. The first method involves directly measuring the oriented flux components to find the rotor angle θ_e. The second method, known as Indirect Rotor Field orientation (IRFOC), calculates the rotor angle using computations and machine parameters. Rotor field orientation (RFO) is typically the preferred choice for IRFOC.

2.4.1.1 Direct rotor field-oriented control (DRFOC):

This method involves directly measuring the oriented flux components proposed by Blaschke (2-10) to find the rotor angle θ_e, to measure this, costly and unreliable flow sensors are necessary.

$$\tan\theta_e = \frac{\varphi_{\beta r}}{\varphi_{\alpha r}} \tag{2-10}$$

Where $\varphi_{\beta r}$ and $\varphi_{\alpha r}$ are the rotor flux components in the stationary reference frame?

2.4.1.2 Indirect Rotor Field-Oriented Control (IRFOC):

The indirect field oriented control involves determining the rotor flux (both amplitude and position) indirectly by utilizing the field control equations and existing estimations of speed and slip.

In summery vector control or field-oriented control, is an advanced method that allows for accurate and effective management of induction motors. It achieves this by independently controlling the motor's magnetic flux and torque elements.

2.5 Proportional Integral Derivative Control:

One of the widely used control strategy in industrial applications is PID controller, it is a simple and very stable controller that can be easily tuned. This controller is well known in the field of induction motor control as it helps in the tracking of target motor speed even when environmental conditions and disturbances change.

2.5.1 Basic concept of PID:

A PID controller modifies the control input to a system based on the difference between the intended target and the actual output. The control formula consists of three components:

Proportional (P) Component: This part generates an output that is proportional to the current error value. It provides immediate correction based on the size of the error.

Integral (I) Component: This part generates an output based on the accumulation of past errors. It helps eliminate residual steady-state errors by integrating the error over time.

Derivative (D) Component: This part generates an output based on the rate of change of the error. It anticipates future errors by considering the error's derivative, thereby enhancing system stability and response.

The combined PID control formula is as follows:

$$u(t) = K_p e(t) + K_i \int_0^t e(\tau) d\tau + K_d \frac{d}{dt} e(t) \tag{2-11}$$

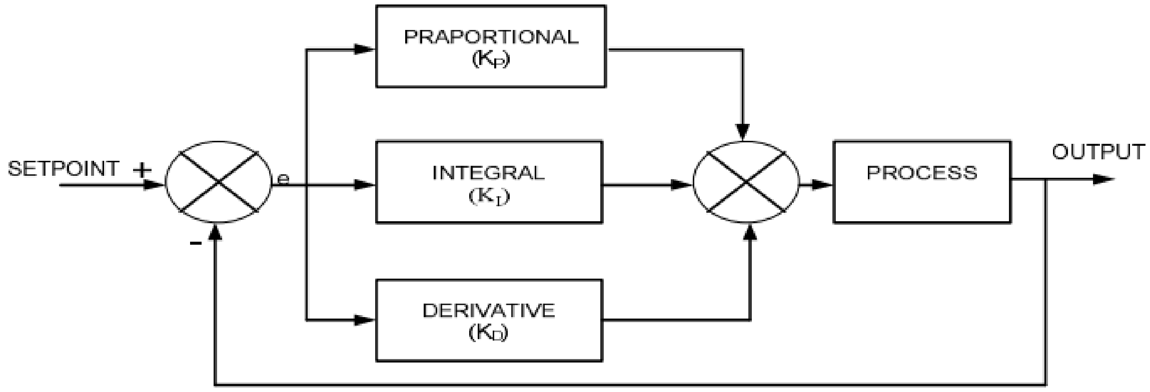

Figure 24: PID block diagram.

2.5.2 Tuning the PID Controller:

Tuning a PID controller can be performed using various methods including Simulink, automation software, and algorithm-based approaches. Here are detailed descriptions of each method:

- **Simulink-Based Tuning**: The Simulink PID Tuner app provides an interactive and visual platform for tuning the PID controller. This method allows the user to adjust the PID parameters while observing the real-time response of the system, enabling a more intuitive and hands-on approach to tuning. The app offers features such as step response analysis, disturbance rejection, and stability margin evaluation, helping the user to find the optimal PID settings for their specific application. This method is particularly useful for systems with relatively simple dynamics or when a quick, iterative tuning process is preferred [14].
- **Automation Software:** Tia Portal and LabVIEW's PID Tuning Wizard offer automated tuning capabilities, leveraging advanced algorithms and optimization techniques to determine the optimal PID parameters. These software tools can analyze the system's dynamics, identify the appropriate PID structure [14], and automatically compute the controller settings based on user-defined performance criteria, such as settling time, overshoot, and steady-state error. The automated approach is advantageous for complex systems or when a more rigorous and systematic tuning process is required. It can also be particularly useful when dealing with systems with significant nonlinearities or time-varying characteristics.
- **Algorithms-Based Tuning:** This method involves the implementation of optimization algorithms, such as Genetic Algorithms (GA) or Particle Swarm Optimization (PSO), to tune the PID controller. These algorithms are designed to search for the optimal PID parameters by iteratively evaluating a performance metric, such as the Integrated Absolute Error (IAE) or the Integral of Time-weighted Absolute Error (ITAE). The algorithm-based approach can handle systems with complex dynamics and is particularly useful when the system's response is not well-known or difficult to model. This method can provide robust and efficient tuning, but may require more computational resources and expertise in implementing the optimization algorithms.

The choice of tuning method depends on the complexity of the system, the desired accuracy of the tuning, and the available resources. Simulink-based tuning is ideal for simple systems and provides a visual and interactive experience, while automation software is better suited for more complex systems and offers a systematic approach. Algorithm-based tuning is the most robust and versatile method, but may require more computational resources and expertise. In practice, a combination of these methods or a tailored approach may be necessary to achieve the best possible PID controller performance for a specific application.

2.6 Variable Frequency Drives (VFDs):

In the preceding section, we delved into different methods of managing induction motors. These techniques employ Variable Frequency Drives (VFDs) as the technology that makes it possible. VFDs, which are electronic devices, are specifically designed to adjust the frequency and voltage of the electrical power that is provided to the motor. This adjustment enables accurate control over the motor's speed and torque.

The VFDs based on two main part power circuit and control circuit

2.6.1 Power circuit of VFDs:

The power circuit in Variable Frequency Drives (VFDs) plays a vital role in converting AC power from the utility grid into adjustable-frequency AC power that can effectively control the speed of induction motors containing:

2.6.1.1 Three phase rectifier:

The rectifier takes the sinusoidal input and transforms it into a pulsating direct current (DC) that fluctuates between the highest positive peak and zero volts. This component consists of six diodes or thyristors [15]. While the diode rectifier is utilized for uncontrolled conversion, the thyristor allows for controlled switching, adjusting the output DC power. The VFD's Rectifier section connects the input AC supply, converting the AC power into unfiltered DC through a full-wave rectifier [16].

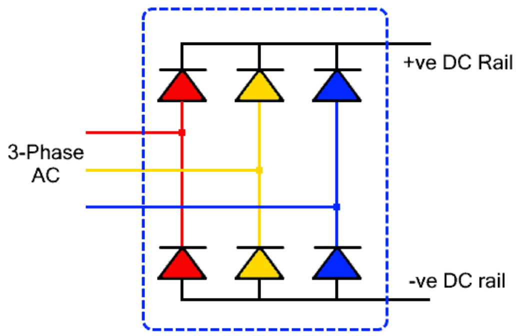

Figure 25: three phase rectifier using six diode

2.6.1.2 The DC Bus and Filter:

After being rectified, the DC power is sent to the DC bus capacitor bank, where it is made smooth and stored. Depending on the type of ripples, it might also have an inductor in case of current as shown in Figure 26.

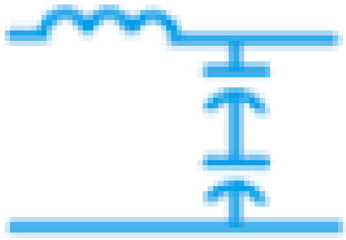

Figure 26: the dc links

2.6.1.3 The Three Phase Inverter:

This section, known as the inverter or switching component, transforms the constant DC into adjustable frequency AC. It consists of power transistors or IGBTs that swiftly toggle to generate alternating voltage at the output. The frequency of the output AC is determined by the switching frequency [15], which is regulated by the control unit for the IGBTs.

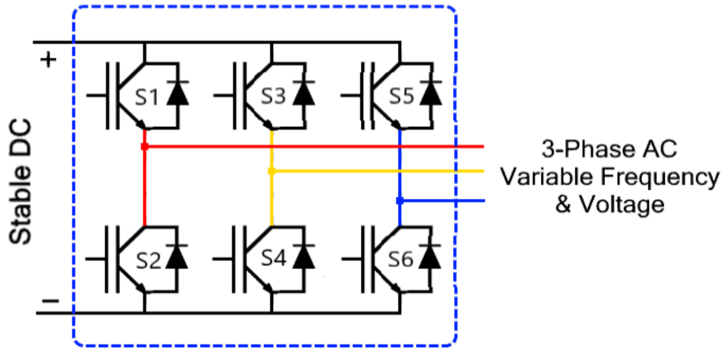

Figure 27: The Three Phase Inverter

2.6.2 Control Circuits of VFDs:

The control unit consists of an embedded microprocessor programmed for controlling the inverter section and the output of the inverter. It can react in microseconds in case of any fault conditions.

To achieve the desired output voltage or current on the inverter's line side, a suitable technique known as pulse width modulation (PWM) is utilized. There are two main categories of PWM generation methods: PWM and Space Vector based PWM (SVPWM) [17].

Space Vector Modulation (SVM), has been maintained to be the most effective method for Variable Frequency Drive (VFD) applications.

2.6.2.1 Concept of Space Vector based PWM (SVPWM)

The eight different combinations of switching patterns generate three phase voltages that can be computed and then converted into the αβ reference frame of the stator, as explained in the first chapter. This conversion leads to the creation of six voltage vectors that are not zero, along with two vectors that are zero. These non-zero vectors form the axes of a hexagon, which consists of six sectors (V1 - V6) as depicted in Figure 29. Each adjacent pair of non-zero vectors is separated by an angle of 60 electrical degrees. The zero vectors, on the other hand, are located at the origin and result in a zero voltage vector being applied to the motor. The hexagon, which is formed by the non-zero vectors, represents the outer boundary within which the maximum output voltage can be found as shown in

Voltage Vectors	Switching Vectors			Line to neutral voltage			Line to line voltage		
	S_1	S_2	S_3	U_{an}	U_{bn}	U_{cn}	U_{ab}	U_{bc}	U_{ca}
u_0	0	0	0	0	0	0	0	0	0
u_1	1	0	0	2/3	-1/3	-1/3	1	0	-1
u_2	1	1	0	1/3	1/3	-2/3	0	1	-1
u_3	0	1	0	-1/3	2/3	-1/3	-1	1	0
u_4	0	1	1	-2/3	1/3	1/3	-1	0	1
u_5	0	0	1	-1/3	-1/3	2/3	0	-1	1
u_6	1	0	1	1/3	-2/3	1/3	1	-1	0
u_7	1	1	1	0	0	0	0	0	0

Figure 28 [15].

Voltage Vectors	Switching Vectors			Line to neutral voltage			Line to line voltage		
	S_1	S_2	S_3	U_{an}	U_{bn}	U_{cn}	U_{ab}	U_{bc}	U_{ca}
u_0	0	0	0	0	0	0	0	0	0
u_1	1	0	0	2/3	-1/3	-1/3	1	0	-1
u_2	1	1	0	1/3	1/3	-2/3	0	1	-1
u_3	0	1	0	-1/3	2/3	-1/3	-1	1	0
u_4	0	1	1	-2/3	1/3	1/3	-1	0	1
u_5	0	0	1	-1/3	-1/3	2/3	0	-1	1
u_6	1	0	1	1/3	-2/3	1/3	1	-1	0
u_7	1	1	1	0	0	0	0	0	0

Figure 28: Switching patterns and output vectors.

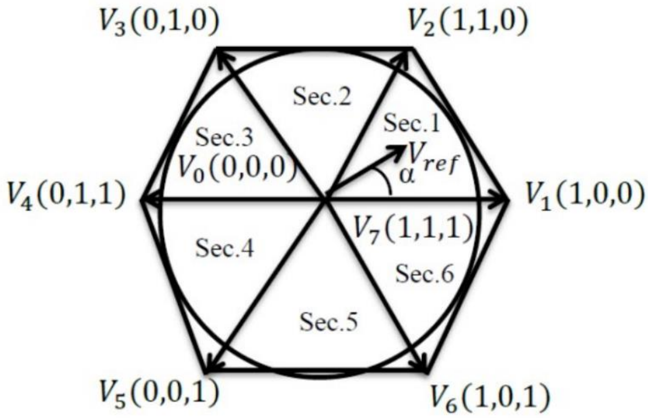

Figure 29: The space-vector representation.

Space vector PWM can be implemented by the following steps [17]:

1) Determine$V_{\alpha,\beta}$, V_{ref} and angleα.

$V_{\alpha,\beta}$ Determined using Clark transformation (1-29).

$$\begin{cases} |V_{ref}| = \sqrt{{V_\alpha}^2 + {V_\beta}^2} \\ \alpha = \tan^{-1}\dfrac{V_\alpha}{V_\beta} \end{cases} \qquad (2\text{-}12)$$

2) Determine the time durationT_1, T_2 and T_0.

The a sampling time T_s given by: $$T_s = \frac{1}{f_s} \qquad (2\text{-}13)$$

In sector 1, the space vector is formed by using non-zero vectors V_1 and V_2 during the time intervals T_1 and T_2, while the zero vector V_0 is applied during the time intervalT_0.

$$\int_0^{T_s} \overline{V_{ref}}\, dt = \int_0^{T_1} \overline{V_1}\, dt + \int_{T_1}^{T_1+T_2} \overline{V_2}\, dt + \int_{T_1+T_2}^{T_s} \overline{V_0}\, dt \qquad (2\text{-}14)$$

The equations (2-15) can be utilized to calculate the length of time it takes to switch vectors in every sector n.

$$\begin{cases} T_1 = \dfrac{\sqrt{3}T_s|V_{ref}|}{V_{dc}}\sin(\dfrac{n}{3}\pi - \alpha) \\ T_2 = \dfrac{\sqrt{3}T_s|V_{ref}|}{V_{dc}}\sin(\alpha - \dfrac{(n-1)}{3}\pi) \\ T_0 = T_s - (T_1 + T_2) \end{cases} \quad (2\text{-}15)$$

Finely determine the switching time of each transistor (S1 TO S6) in any sector as shown in **Erreur ! Source du renvoi introuvable.**.

Table 2: Switching time for each sector.

Sector	Switching Time	Upper switches (S1, S3, S5)	Lower Switches (S2, S4, S6)
1	Ta	$T_1+T_2+T_{0/2}$	$T_{0/2}$
	Tb	$T_2+T_{0/2}$	$T_1+T_{0/2}$
	Tc	$T_{0/2}$	$T_1+T_2+T_{0/2}$
2	Ta	$T_1+T_{0/2}$	$T_2+T_{0/2}$
	Tb	$T_1+T_2+T_{0/2}$	$T_{0/2}$
	Tc	$T_{0/2}$	$T_1+T_2+T_{0/2}$
3	Ta	$T_{0/2}$	$T_1+T_2+T_{0/2}$
	Tb	$T_1+T_2+T_{0/2}$	$T_{0/2}$
	Tc	$T_2+T_{0/2}$	$T_1+T_{0/2}$
4	Ta	$T_{0/2}$	$T_1+T_2+T_{0/2}$
	Tb	$T_1+T_{0/2}$	$T_2+T_{0/2}$
	Tc	$T_1+T_2+T_{0/2}$	$T_{0/2}$
5	Ta	$T_2+T_{0/2}$	$T_1+T_{0/2}$
	Tb	$T_{0/2}$	$T_1+T_2+T_{0/2}$
	Tc	$T_1+T_2+T_{0/2}$	$T_{0/2}$
6	Ta	$T_1+T_2+T_{0/2}$	$T_{0/2}$
	Tb	$T_{0/2}$	$T_1+T_2+T_{0/2}$
	Tc	$T_1+T_{0/2}$	$T_2+T_{0/2}$

In Space Vector Pulse Width Modulation (SVPWM), achieving efficient switching and minimizing harmonics involves carefully organizing the state sequence during transitions between sectors [18].

2.6.2.2 Three-Phase Sinusoidal PWM:

Pulse Width Modulation (PWM) is a technique used to control the voltage and current supplied to electrical devices, particularly in motor control applications. In three-phase systems, PWM is employed to generate three-phase AC signals from a DC source [16]. This is crucial in applications like variable frequency drives (VFDs) for induction motors, where precise control of the motor's speed and torque is required.

Crafting a three-phase inverter's six-switch PWM requires a three-step approach: First, generating three sinusoidal reference signals with distinct phases; second, creating a high-frequency triangular carrier signal; and third, precisely comparing each reference signal to the carrier signal to produce PWM signals that dictate the switching of the inverter's components

[15]. This systematic process enables the inverter to transform direct current into a three-phase alternating current output [18], adjustable in both frequency and amplitude, making it ideal for powering three-phase loads like induction motors.

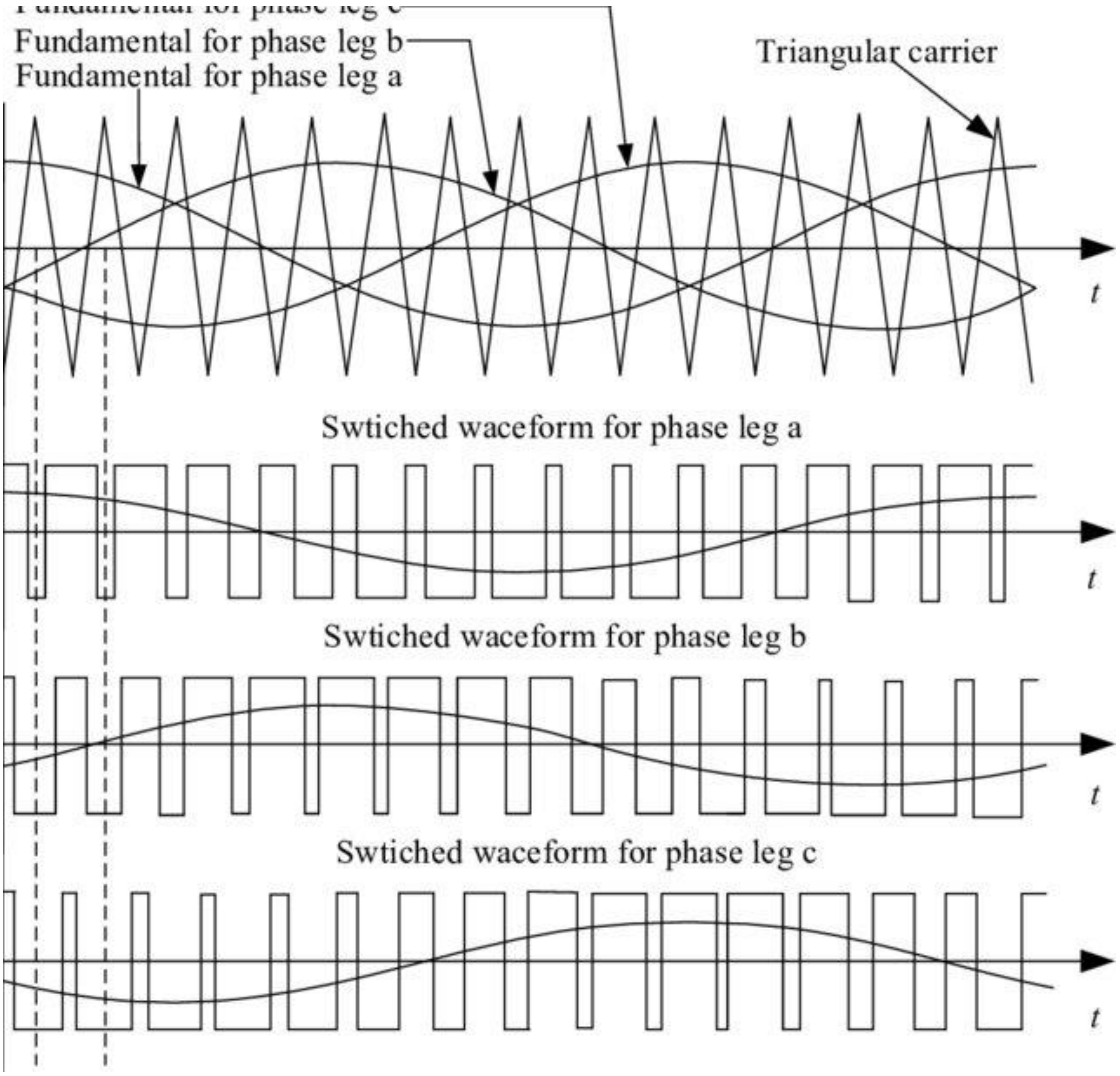

Figure 30: Working principle of SPWM in the three-phase drive system.

2.6.3 Advantages of Variable Frequency Drives:

Industrial applications have been utilizing variable frequency drives (VFDs) for over 20 years to control the rotational speed of an alternating current (AC) electric motor. It offer several advantages in motor control and energy management, including:

2.6.3.1 Starting torque and starting current:

VFDs enable smooth acceleration and deceleration of motors, the starting current can be decreased. This results in a starting current that is only 1.5 to 2 times the rated current when the motor begins running. [19].

For the starting torque, VFD might initially apply a lower voltage at the starting frequency. This reduces the magnetic flux generated in the motor, consequently reducing the starting torque compared to a DOL start where full voltage is applied immediately.

2.6.3.2 Energy saving:

By varying the pump speed, for example, energy can be saved compared to other control methods. Variable Frequency Drives (VFDs) can contribute to energy savings and operating cost reduction by reducing inrush current and utilizing dynamic voltage/frequency (v/f) methods. Additionally, employing PID controllers and a Common DC bus further enhances the efficiency and effectiveness of VFDs .

Figure 31 [20] presents a visual representation of the power curves for fixed speed and variable frequency drive (VFD) pumps. It is evident that when a VFD is used, the motor operates at 50% of its power, whereas without a VFD, it operates at 95% of its power. This implies that the use of a variable speed drive significantly reduces power consumption by half, and save the energy.

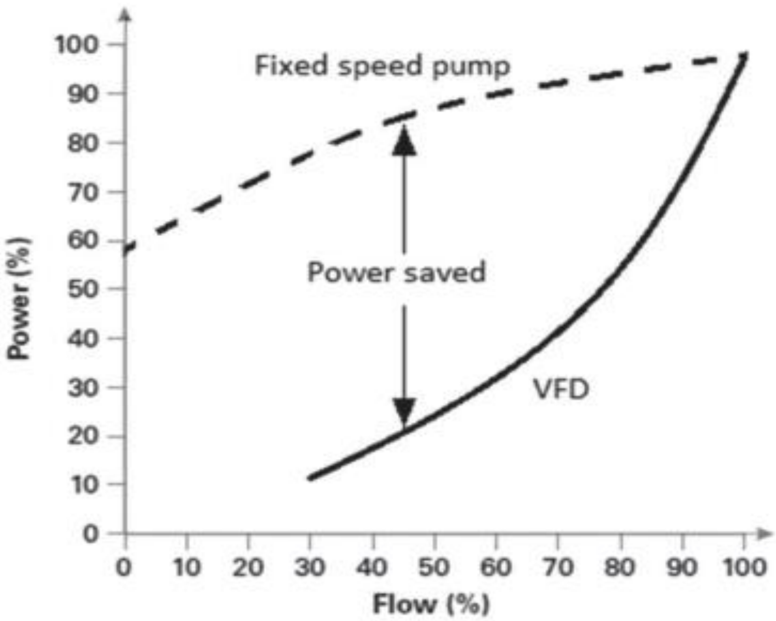

Figure 31: Comparison of fixed speed and VFD pump power

2.6.3.3 Improved Process Control:

Variable Frequency Drives (VFDs) greatly improve process control by offering precise speed control, seamlessly integrating with control systems, reducing upsets in the process, and adapting motor speed to match process requirements. With VFDs, operators can achieve precise control over motor speed, resulting in consistent and optimized process conditions. VFDs can interact with PLCs or react to sensor data, automatically modifying motor speed to maintain desired process conditions. By adjusting motor speed according to process demands, VFDs optimize production capacity, enhance product quality, and reduce waste, ultimately boosting productivity and efficiency in industrial settings [19].

2.6.3.4 Protection features:

Variable frequency drives, or VFDs, are outfitted with an array of protective mechanisms to insulate the motor and the VFD from environmental risks, malfunctions, and electrical faults. The majority of VFDs have the following essential safety features:

Protection for motor against overload, overcurrent, thermal and phase loss.

There is protection for the VFD against temperature, ground fault, overvoltage and short circuit. There is protection for the VFD against temperature, ground fault, overvoltage, and short circuit [21].

2.6.3.5 Additional Features:

A lot VFDs have a number of extra features that improve the functionality of the system as a whole. These might consist of:

Reducing the reactive power component increases the power system's efficiency through power factor correction.

Reduced Noise: VFDs can greatly reduce noise levels by controlling motor speed, particularly during startup and lower speed operation.

Increased Equipment Life: lessening the mechanical strain on the motor and its associated machinery. Longer motor, pump, fan, and other machinery lifespans result from this [19].

2.6.4 Drawbacks of Variable Frequency Drives:

Although VFDs offer numerous benefits, they also have a few drawbacks that should be taken into account:

1. Possibility of Harmonics: VFDs have the potential to introduce harmonics into the electrical supply. Harmonics are distortions in the AC waveform that can lead to problems such as overheating of other electrical equipment. It may be necessary to implement mitigation strategies like harmonic filters.

2. Electromagnetic Interference (EMI) and Radio Frequency Interference (RFI): VFDs can generate EMI and RFI, which can interfere with the operation of sensitive electronic devices nearby. It is crucial to utilize proper shielding and grounding techniques in order to minimize these issues.

3. Maintenance Considerations: While VFDs can prolong the lifespan of motors, they themselves require some level of maintenance. This may involve conducting periodic inspections, cleaning fans and heat sinks, and potentially replacing capacitors or other components over time.

2.7 Conclusion:

The chapter delves into the methods of controlling induction motors, specifically focusing on scalar and vector control techniques. Scalar control methods, which include open and closed loop constant V/f with slip speed regulation and closed loop constant air gap flux, have certain limitations in terms of accuracy and performance. On the other hand, vector control techniques such as direct and indirect rotor field-oriented control offer improved precision and efficiency, enabling optimal performance under various conditions. The chapter also explores the role of variable frequency drives (VFDs) in achieving precise speed and torque control using these techniques, introduces Space Vector Pulse Width Modulation (SVPWM) as an advanced modulation technique, and we talk about the advantage and disadvantage of using VFDs.

These methods provide valuable insights into the complexities of controlling induction motors, ensuring optimal performance and efficiency in both industrial and commercial settings.

Chapter 3 Programmable Logic Controllers (PLCs)

3.1 Introduction:

In the preceding chapter, we emphasized that one the benefit of Variable Frequency Drives (VFDs) is can be integrating with automation systems.

This chapter delves into the realm of Programmable Logic Controllers (PLCs) and Human-Machine Interfaces (HMIs). Additionally, we will explore TIA Portal, a specific software platform widely employed for programming Siemens PLCs. These intelligent elements serve as the control system's central nervous system, facilitating effective operation, monitoring, and interaction with the VFD-controlled induction motor.

3.2 Programmable Logic Controllers (PLCs):

The PLC is a digital computer that is specifically designed for controlling machines in industrial settings. It is equipped with unique input/output interfaces and a control programming language. As a result, most manufacturers refer to their programmable controller as a PLC, which stands for "programmable logic controller." While the initial purpose of the PLC was to replace relay logic, its functionality has expanded greatly over time, allowing it to be used in more complex applications. Due to its architecture being based on computer principles, the PLC can not only perform relay switching tasks, but also other functions such as timing, counting, calculating, comparing, and processing analog signals [22, 23].

3.2.1 Main Parts of a PLC:

The components that make up a Programmable Logic Controller (PLC) work together to ensure its proper functioning. These components handle the reception, processing, and transmission of data, ultimately controlling the connected machinery and processes. Let's take a look at the crucial components of a PLC:

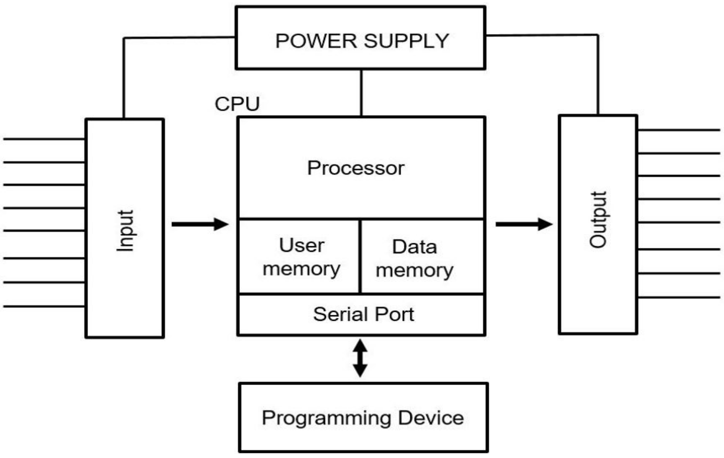

Figure 32: structure of plc

3.2.1.1 Central Processing Unit (CPU):

Serving as the PLC's brain, the CPU takes charge of all its operations. It runs the control program stored in its memory, processes incoming data from the inputs, carries out logical operations, and sends signals to control the outputs.

3.2.1.2 I/O Modules:

The I/O system acts as the link between the controller and field devices. Its role is to prepare and adjust the signals coming from or going to external devices. Input devices like pushbuttons, limit switches, and sensors are directly connected to the input terminals. Output devices like motor starters and indicator lights are directly connected to the output terminals. To ensure that the internal components are protected from the input and output terminals, PLCs often use an optical isolator, which utilizes light to connect the circuits.

3.2.1.3 Power Supply:

The Power Supply unit is another critical component. It converts the incoming power to the levels required by the PLC components. Most PLCs operate on 24V DC power, though some may require other voltage levels.

3.2.1.4 Programming Devices:

A PLC is a type of computer that uses a microprocessor to control different devices. The Programming Device is used to input the control program into the memory of the PLC. Usually, this involves using a computer with software that allows the user to program the PLC using a specific programming language, which we will talk about in more detail later on.

3.2.2 PLC Programming Languages:

PLC programming languages form an essential part of PLC operations.

The International Electrotechnical Commission (IEC) has standardized five types of PLC programming languages under IEC 61131-3. These are Ladder Diagram (LD), Structured Text

(ST), Instruction List (IL), Function Block Diagram (FBD), and Sequential Function Chart (SFC) [23].

3.2.2.1 Ladder Diagram:

Ladder Diagram (LD) is the primary programming language for PLCs, as it was specifically designed for this purpose. The language is graphical and resembles a ladder with vertical rails and horizontal rungs. Each rung represents a specific operation in the control process, making it intuitive for users familiar with electrical control circuits.

3.2.2.2 Structured Text (ST):

Structured text is a high-level textual language similar to Pascal or C. It is used for more complex PLC programs that require mathematical and logical computations. ST can be easier to read and write than graphical languages like LD, especially for those with a background in traditional computer programming.

3.2.2.3 Instruction List (IL):

Instruction list is a low-level textual language similar to assembly language. Each line of an IL program represents a single operation, which makes it highly efficient but also harder to read and write than high-level languages like ST.

3.2.2.4 Function Block Diagram (FBD):

Function Block Diagram (FBD) is a visual programming language that resembles the design of electronic circuits. It depicts programs as interconnected networks, where each network encompasses one or more logical operation pathways. The language utilizes binary and analog signals, which are linked through various boxes. These boxes employ familiar logical symbols derived from Boolean algebra to represent binary logic.

3.2.2.5 Sequential Function Chart (SFC):

Sequential Function Chart (SFC) is a graphical language that represents control processes as a series of steps with actions. Transitions between steps are triggered by specific conditions, making SFC ideal for sequential control processes.

3.2.3 Communication Protocols in PLC:

In a PLC, communication plays a key role. Beyond the standard hardware IOs, communication protocols offer greater variety and adaptability for exchanging data through different channels. Let's explore the different communication techniques implemented within a PLC :

3.2.3.1 Modbus:

Modbus is a widely used communication protocol within the industrial automation sector. It is an open standard that facilitates communication between devices made by different manufacturers with its master/slave design.

A slave is any peripheral device such as an I/O transducer, valve, network drive, or other measuring types of devices which processes information and sends its response message to the master using Modbus.

Masters can address individual slaves or initiate a broadcast message to all slaves. Slaves return a response to all message queries addressed to them individually, but do not respond to broadcast messages.

3.2.3.2 Profibus:

Profibus is a popular protocol for process automation that allows devices like PLCs, sensors, and actuators to communicate at high speeds. It is a deterministic protocol that ensures data transmission accuracy and speed.

3.2.3.3 Ethernet/IP:

Ethernet/IP is a popular open standard utilized in industrial automation that operates on the Ethernet protocol and uses the traditional TCP/IP protocol to communicate between devices [22]. It allows for instantaneous connectivity between devices, making it perfect for applications that demand rapid and precise data exchange.

Ethernet is a wired system that started with using coaxial cable and has successfully progressed to now using twisted pair copper wiring and fiber optic wiring.

3.2.4 Advantage and disadvantage of PLCs:

There are several advantages to using programmable logic controllers (PLCs) in industrial control systems:

1) Increased efficiency and productivity: PLCs play a crucial role in improving effectiveness and output in various sectors. They automate tasks to ensure consistency and minimize mistakes, while simultaneously monitoring processes in real-time. Their rapid response times minimize downtime, and they offer adaptable programming to adjust to evolving demands without interruption. When integrated with SCADA systems, they provide a comprehensive view of the process, facilitating predictive maintenance and energy optimization. Additionally, PLCs promote safety by incorporating features such as emergency stops and interlocking mechanisms, guaranteeing a secure work environment.
2) Enhanced flexibility and adaptability: Programmable Logic Controllers (PLCs) offer flexibility and adaptability in managing industrial processes. PLCs can be customized to integrate new equipment, modify processes, and meet changing production requirements without significant downtime. PLCs also excel in real-time monitoring and data acquisition, allowing for quick adjustments and optimal process conditions. Integration with other automation systems and software platforms improves data transmission and supports predictive maintenance. Leveraging PLC capabilities can improve production flexibility, reduce costs, and maintain competitiveness in today's industrial landscape.

3) Improved quality control and consistency: When it comes to manufacturing and industrial processes where precision is key, utilizing Programmable Logic Controllers (PLCs) can result in substantial enhancements in quality control and consistency. Plc provide various characteristics to improve control by giving accurate process control, automated quality checks, feedback control loop, data logging and analysis and fault detection and alarms.
4) Cost saving and resource optimization: The installation of Programmable Logic Controllers (PLCs) can bring considerable financial advantages through cost reduction and resource optimization in various industrial operations. There are several essential areas where PLC implementation can generate financial benefits such as energy efficiency, reduce down time, optimize resource utilization, predictive maintenance,
5) Enhanced safety and reliability: By utilizing Programmable Logic Controllers (PLCs), businesses can improve their operational efficiency while simultaneously increasing workplace safety and reliability. PLC systems offer a number of benefits when it comes to workplace security such as safety interlocks, emergency stop, safety monitoring, training simulation and remote monitoring and diagnostics.

Programmable Logic Controllers (PLCs) have transformed industrial automation, but they come with drawbacks and challenges such as:

1) Complexity and learning curve: PLC programming challenges require understanding complexities and overcoming learning curves. Technical complexity is high, with expertise needed in reasoning, data processing, and programming languages. System integration complexities arise from interaction needs with control systems, sensors, and networks. Safety issues add complexity, requiring knowledge of safety standards and fail-safe programming. Thorough testing, debugging, and continuous learning are crucial. Adequate instruction, access to tools, and collaboration with experienced programmers accelerate proficiency. Documentation and maintenance policies improve system longevity and scalability.
2) Maintenance costs and down time: Managing maintenance costs and minimizing downtime are critical aspects of maintaining the efficiency and reliability of PLC systems. Here are some crucial ways to properly deal with these challenges such as proactive maintenance, software updates, training and knowledge transfer and documentation and asset management.
3) Limited scalability and expansion: To maintain a high level of productivity and success, organizations must confront the distinct obstacles that arise when they attempt to enlarge their PLC-based systems. These challenges can be managed by implementing the following strategies such as hardware limitation, programming complexity, integration with new technologies, vendor and support consideration
4) Cybersecurity risks: Protecting Programmable Logic Controllers (PLCs) from cybersecurity threats is crucial for industrial processes. Upgrading firmware and software, implementing network security measures, enforcing strong authentication methods, providing cybersecurity training, and deploying intrusion detection systems and incident response plans all contribute to enhancing PLC cybersecurity and protecting industrial infrastructure.

3.2.5 Choice of PLC:

There are many considerations that should be taken into account to help narrow down the options for a particular application:

The number of I/O points required for the application.

The amount of processing power and memory necessary to run the software.

Communication protocols and interfaces with other systems.

The ease of programming and the availability of programming and debugging software tools for the PLC.

The supplier’s reputation for quality and customer service.

The PLC’s cost, which includes hardware, software, and installation.

Taking into account the points highlighted previously, we have chosen the Siemens S7-1200 PLC for this study.

3.2.6 Siemens PLC S7-1200:

The Siemens S7-1200 is a versatile and powerful programmable logic controller (PLC) designed for industrial automation. It features a compact and modular design, allowing for easy integration and scalability. The PLC offers high processing speeds, integrated Profinet connectivity, a built-in web server for remote monitoring, and data logging capabilities. It supports various integrated technology functions, such as PID control and motion control [22], and can be programmed using the intuitive TIA Portal software. The S7-1200 also incorporates robust security features to protect against unauthorized access and cyber threats [22].

Figure 33: SIMATIC S7 1200.

3.2.6.1 SIMATIC S7-1200 Modules:

Siemens S7-1200 series PLCs are a widely used family in industrial automation. They come with a broad range of modules to suit different automation requirements. These modules include Figure 34 [24]:

Figure 34: S7-1200 Modules.

Signal Modules (SM): Digital input, digital output, analog input, analog output.

Function Modules (FM): used for counting, Positioning and closed loop.

Communication Processors (CP): point to point, profibus, industrial Ethernet and profinet.

Power supply (SP): provide necessary power to the entire plc system.

3.3 The Totally Integrated Automation (TIA) Portal:

Siemens offers a complete range of software tools that allow for the programming, configuration, and monitoring of their Programmable Logic Controllers (PLCs) and Human-Machine Interfaces (HMIs).

The Siemens TIA Portal (Totally Integrated Automation) platform is the latest development in Siemens programming software. This platform combines the programming of all the devices in a plant in a single program [24]. In addition to the PLC, this software can be used to program and configure HMI devices, drives, etc.

The version used in this study is TIA Portal V15.1

Figure 35: TIA Portal V15.1 logo.

3.3.1 SIMATIC STEP 7 in TIA Portal:

STEP 7 is used for programming and engineering. It is an essential component of the Totally Integrated Automation (TIA) Portal that combines multiple automation tasks into a unified engineering environment. STEP 7 empowers users to configure hardware, program PLCs, and simulate control logic. It provides support for several programming languages such as ladder logic (LAD), function block diagram (FBD), structured text (ST), and sequential function chart (SFC).

3.3.1.1 Portal View and Project View:

In TIA Portal, there are two important views the portal view and the project view. At startup, the portal view presented in Figure 36 is displayed by default. The portal view provides an overview of the project and access to tools for developing it. It contains portal for different tasks to access to devices and component, actions for task selected and selection window for the selected action.

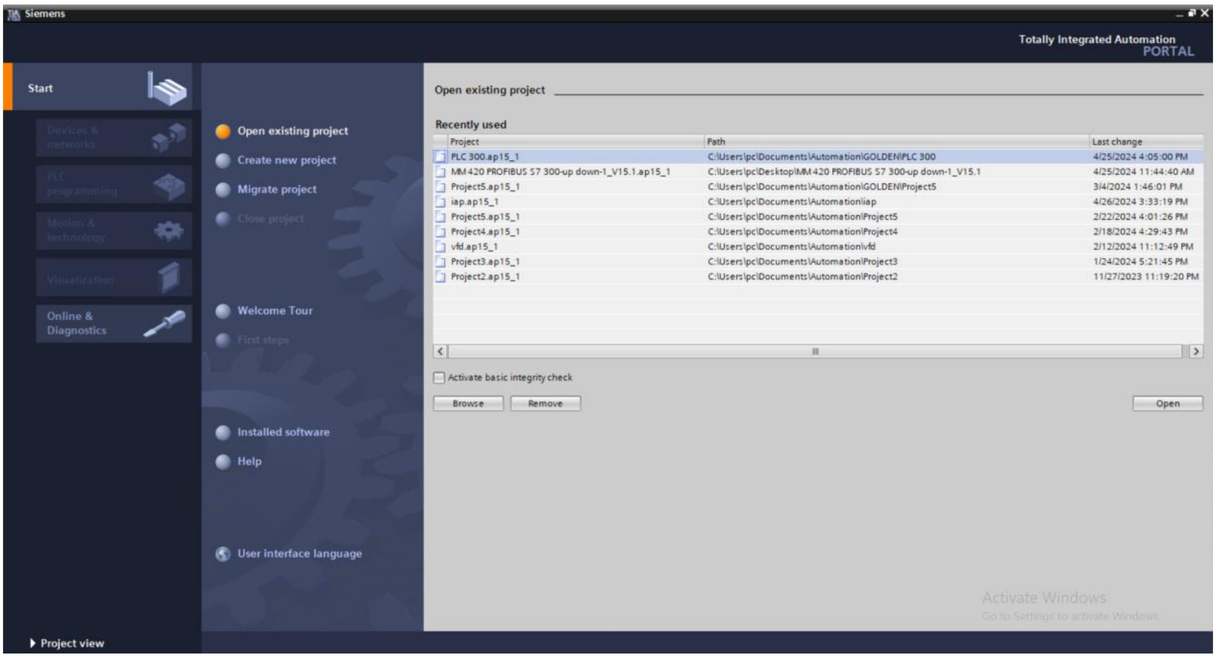

Figure 36: Portal view.

Project view presented in Figure 37 contains all components and project data of an automation solution. All components can be opened from there. It's the working area, the objects opened for editing are displayed in the working area. These objects include, hardware components, blocks, PLC tag tables, screens of HMI devices etc.

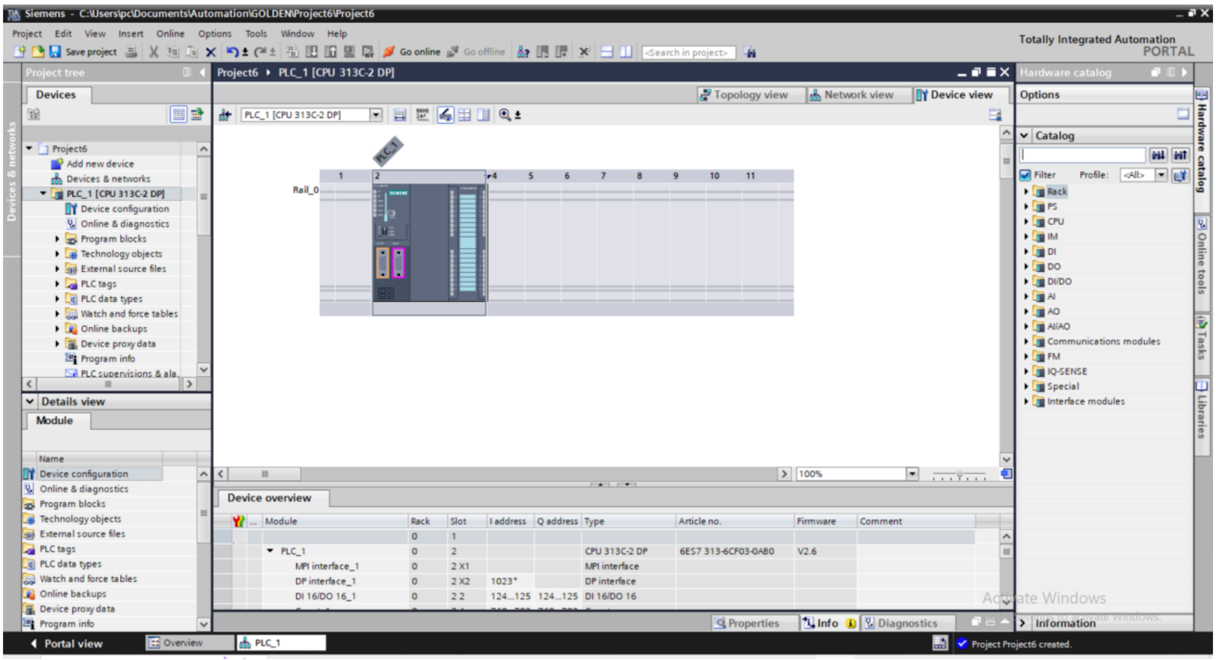

Figure 37: Project view.

3.3.1.2 Program Blocks:

The automation system provides various types of blocks in which the user program and the related data can be stored. Depending on the requirements of the process, the program can be structured in different blocks.

- Organization blocks (OB): form the interface between the operating system and the user program.
- Functions (FCs): contains a partial functionality of the program. . It is possible to program functions as parameter-assignable so that when the function is called it can be assigned parameters. As a result, functions are also suited for programming frequently recurring, complex partial functionalities such as calculations
- Function blocks (FBs): Basically, function blocks offer the same possibilities as functions. In addition, function blocks have their own memory area in the form of instance data blocks. As a result, function blocks are suited for programming frequently recurring, complex functionalities such as closed-loop control tasks.

When we add a new block as presented in Figure 38 we select the type of the block and the language of code described in section 3.2.2.

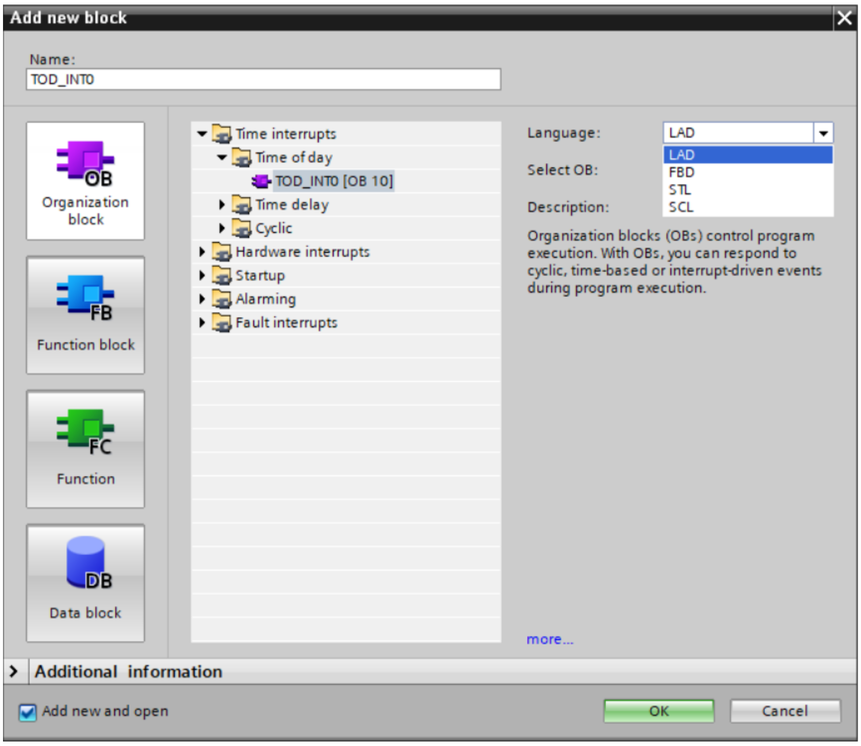

Figure 38: Program blocks.

3.3.2 SIMATIC WinCC:

Siemens TIA Portal includes WinCC, which is a software for HMI (Human-Machine Interface). It helps in the creation, setup, and operation of HMIs that manage industrial processes. WinCC includes functions like dynamic graphics, trend analysis, alarm management, and reporting. It is available in different versions that suit different levels of complexity and project sizes.

3.3.2.1 WinCC Configuration Interface:

First of all we add an HMI device in portal view then we design, configure and operate our HMI.

In the Project tree, all devices and their configuration and parameter assignments are displayed in a tree structure as presented in Figure 39. The working area is the central configuration area in which objects of the operator panel are edited with the started editor.

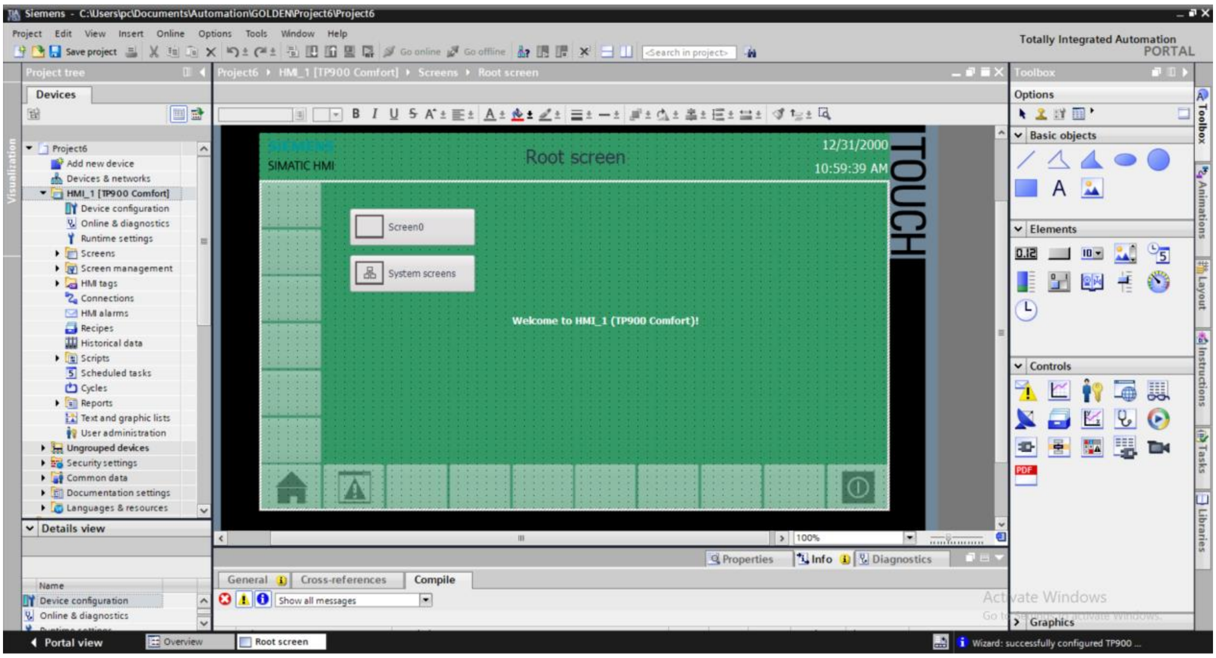

Figure 39: WinCC view.

3.4 **Conclusion:**

In conclusion, Chapter 3 delves into the realm of Programmable Logic Controllers (PLCs) and Siemens software, offering a comprehensive overview of their functionality and applications. The chapter navigates through fundamental concepts of PLC programming, encompassing ladder logic design and execution, with a specific focus on Siemens PLCs. Detailed discussions elucidate the programming environment, addressing key features and capabilities of Siemens software tools. Practical examples illustrate the implementation of various control tasks, ranging from simple to complex automation scenarios. Additionally, the chapter delves into advanced topics such as data handling, networking, and integration with Human-Machine Interfaces (HMIs). Through this exploration, readers gain a profound understanding of PLCs and Siemens software, equipping them with the knowledge necessary for proficient design and implementation of industrial automation systems.

Chapter 4 Simulation, Implementation and Discussion.

4.1 Introduction:

This chapter conducts a thorough investigation into open-loop and closed-loop V/F control strategies for induction motors, utilizing a Siemens G120 VFD and an S7-1200 PLC. Beginning with simulation in MATLAB's Simulink, the chapter describes the model's construction and execution for both control methods, including PID controller tuning for closed-loop scenarios. Transitioning to practical implementation, hardware configurations and PLC programming details are outlined, followed by an evaluation of real-world performance. Comparative analysis between simulation and implementation outcomes highlights discrepancies and insights, crucial for refining control strategies and optimizing industrial motor control systems. Through this exploration, the chapter aims to provide a comprehensive understanding of V/F control methodologies, facilitating informed decision-making in industrial settings.

4.2 Simulation:

In this section, we go in for simulation of the open loop and closed-loop scalar V/F control speed of the induction motor using Simulink. The simulation aims to verify the theoretical concepts and methodologies presented in the earlier chapters. Using the features of Simulink, it becomes possible to develop a detailed model of the control system whereby we are able to observe and analyze the dynamic behavior of the induction motor under different operating conditions.

4.2.1 Simulink model:

In the Simulink model depicted in Figure 40, we have assembled the essential building blocks for our closed-loop scalar V/F control system for an induction motor simulation. These interconnected subsystems, such as the inverter, the closed-loop V/F control unit, the 6-pulse switch generator, and the induction motor block, form the foundation of our system.

Each of these elements plays a crucial role, facilitating the conversion from DC to AC power, maintaining the voltage-to-frequency ratio, generating the gate signals, and modeling the behavior of the motor.

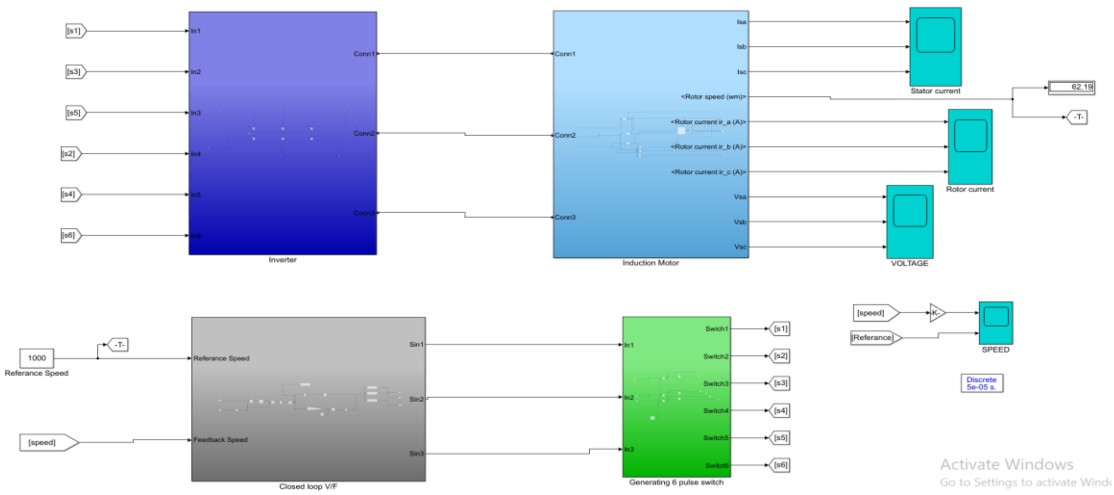

Figure 40: Simulation of Closed loop scaler control of Induction motor.

4.2.1.1 Inverter:

The inverter block is an important block in the V/F control system. The block is used for the conversion of direct current obtained from the power supply into an alternating current, which will drive the induction motor.

Contains six IGBTs with diodes and V_{dc} are connected together as bridge.

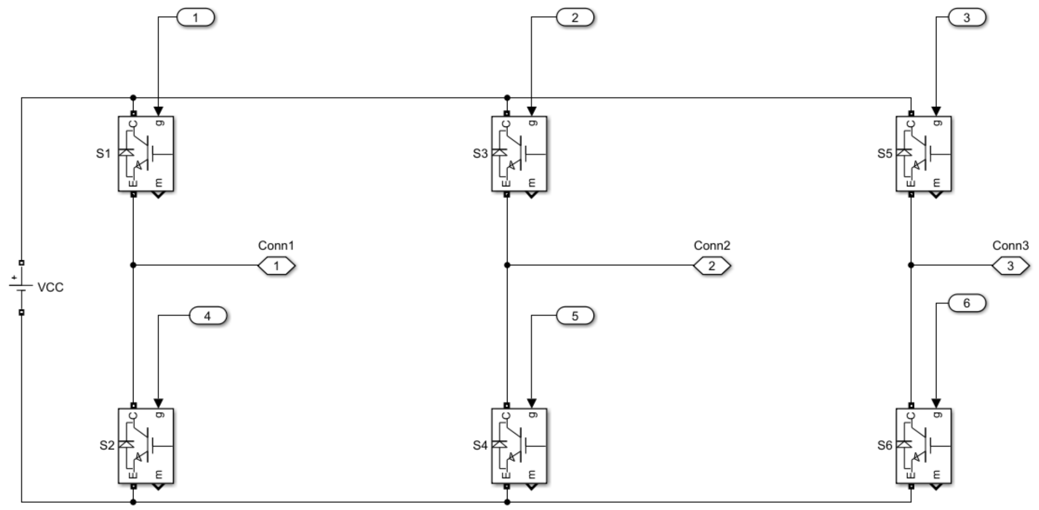

Figure 41: Three phase inverter subsystem.

1) Configuration:

Calculation of Input Voltage V_{dc} : To determine the DC bus voltage V_{dc} for an inverter powering a three-phase induction motor, connection between the inverter's input voltage V_{dc} and its output voltage V_o.

$$V_{dc} = V_{opk} \times 2\sqrt{2} \qquad 4\text{-}1)$$

We have $V_{o\,rms}$ of our motor 400V.

Then $V_{dc} = 653.19V$

The IGBT/DIODE switches:

The gate single input is connected to the control signal that governs the switching behavior of the switch.

Emitter terminal is the reference point for the switch it's connected the emitter.

Collector terminal is where the current flows through the switch.

2) Operation:

The inverter module takes the direct current (DC) input and transforms it into a three-phase alternating current (AC) output. Adjusting the control signals allows the inverter to regulate the amplitude and frequency of the output voltage, a crucial factor in maintaining the desired voltage-to-frequency (V/F) ratio and controlling the speed of the motors.

4.2.1.2 V/F block:

The subsystem of V/F is the implementation of block diagram of V/F open and closed loop control shown in Figure 18 Figure 19 described in chapter 2.

A. <u>open loop V/F:</u>

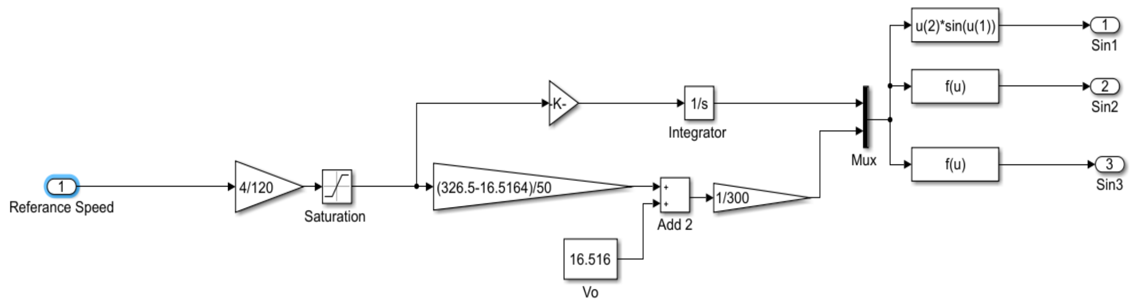

Figure 42: Open loop V/F.

The details of this blocks used will be described in the next section.

<u>Operation:</u>

When the desired speed is specified, it is multiplied by a gain to determine the desired frequency. This frequency is then multiplied by an additional gain and combined with a boost voltage to generate the desired voltage. This voltage is then divided by half of the supply voltage to calculate the modulation index. In a parallel process, the desired frequency is converted to angular velocity (omega), which is subsequently integrated to obtain the phase angle (theta). Finally, three signals are generated based on the desired speed.

B. <u>closed loop V/F:</u>

Using different Simulink blocks we get the model shown in Figure 43

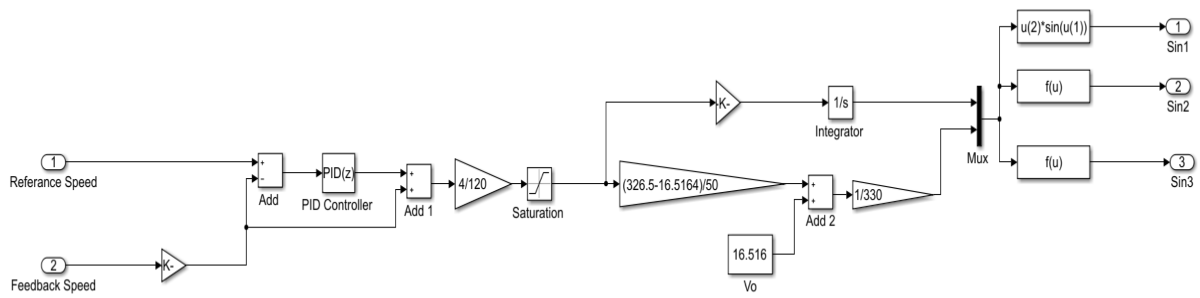

Figure 43: Closed loop V/F.

1) Configuration:

Calculating the boost voltage using (2-2):

We have $I_{s\,rms} = 3.139A$ and $R_s\ = 5.26omh$ so $V_O = 16.516V$.

The saturation block is used to limit the frequency in the range of [0 – 50Hz]

The feedback speed is the actual speed of the motor.

The function block to generate three sine wave with same amplitude and frequency shifted by 120°. The equation that generate the signal is shown below in Figure 44.

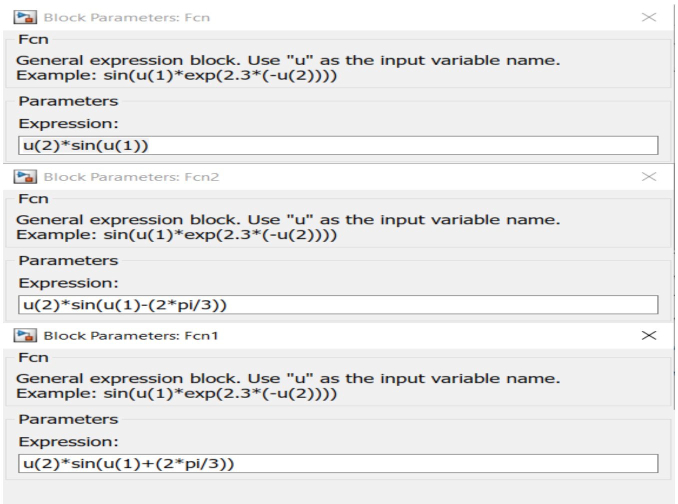

Figure 44: Functions blocks.

For the PID controller, the non-linear workings of the semiconductor's pose challenges during the tuning process.

System identification has been used to identify a plant model from simulation input-output data using system identification Toolbox. The basic idea of this method is remove the PID temporally in the model, an input signal is injected where the output of PID is used to be, the resulting signal at the point where the PID input used to be logged. This input/output data describe the response of the plant seen by the controller, then the PID tuner use this response data to estimate a linear plant model.

After generating an error signal we select the model structure based on number of poles, than I have tuned the model parameter interactively using auto estimate until i get good fit between model and simulation data finely the linear model is obtained for PID tuning

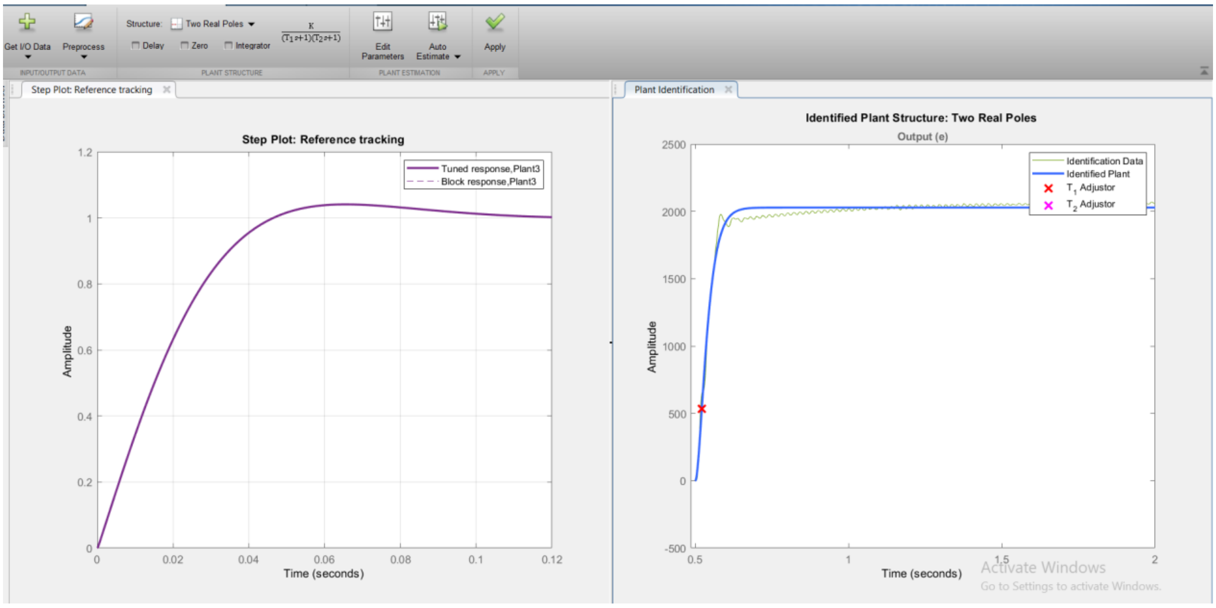

Figure 45: System identification toolbox.

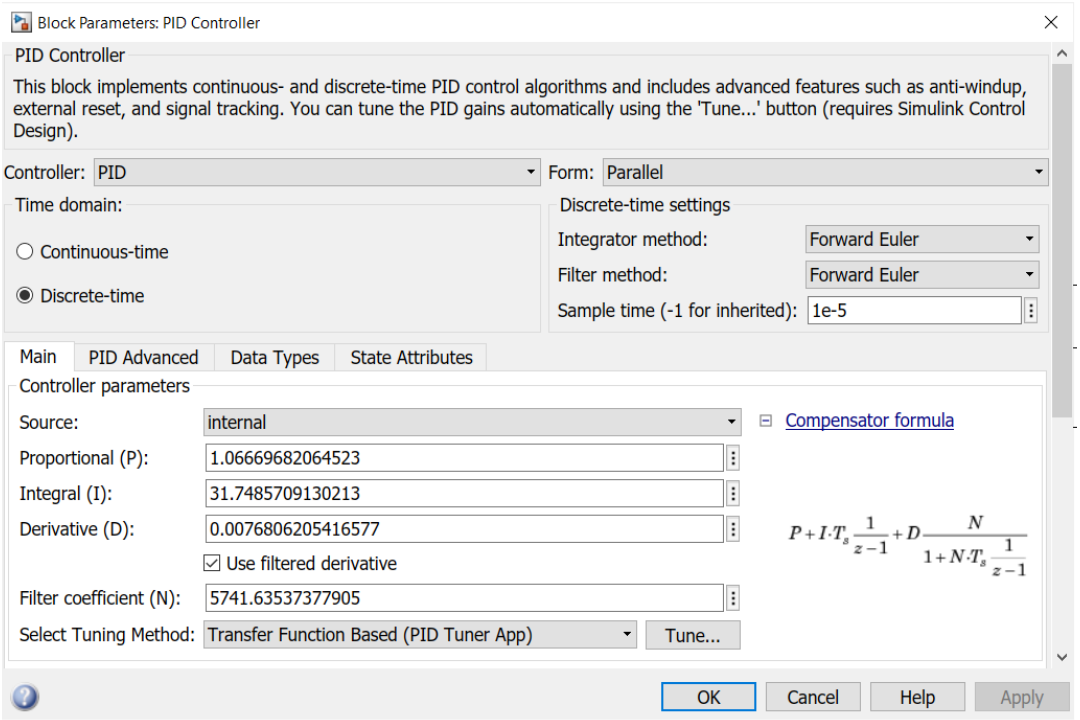

Figure 46: PID parameter using tuning.

2) Operation:

To begin, the desired speed is set, and it is compared to the actual motor speed, which has been converted to revolutions per minute (RPM) using a gain. This generates an error signal that enters the PID (Proportional-Integral-Derivative) blocks, which quickly match the desired speed and produce a slip speed. The actual speed is then added to the slip speed to calculate the synchronous speed. Next, the desired frequency is obtained by multiplying the synchronous speed by a gain.

The frequency is then multiplied by another gain and added to a boost voltage, as described in equation (2-3), to generate the desired voltage. This voltage is then divided by half the supply voltage to produce the modulation index. In a separate path, the desired frequency is converted to omega, which is then integrated to obtain theta. Finally, three signals are generated based on the desired speed.

4.2.1.3 Pulse Width Modulation:

To control the speed of the induction motor using the inverter, we generate six gate signals through a technique called PWM (Pulse Width Modulation). This technique involves comparing a reference signal, usually a sinusoidal waveform, with a high-frequency triangular waveform known as the carrier signal.

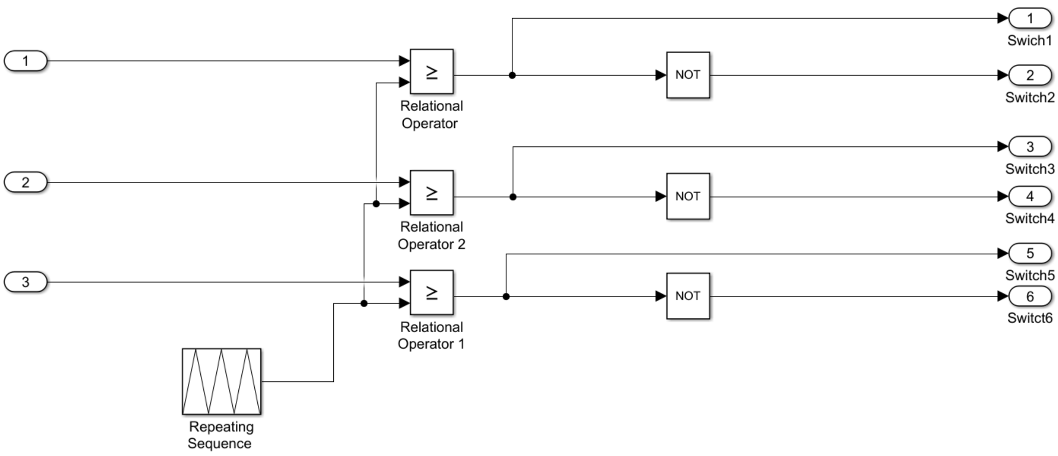

Figure 47: PWM subsystem

1) **Configuration:**

Reference signal : to generate a triangular signal with high frequency I have used the block of repeating sequence, this block generate triangular signal with amplitude of 1 and frequency of 5kHz

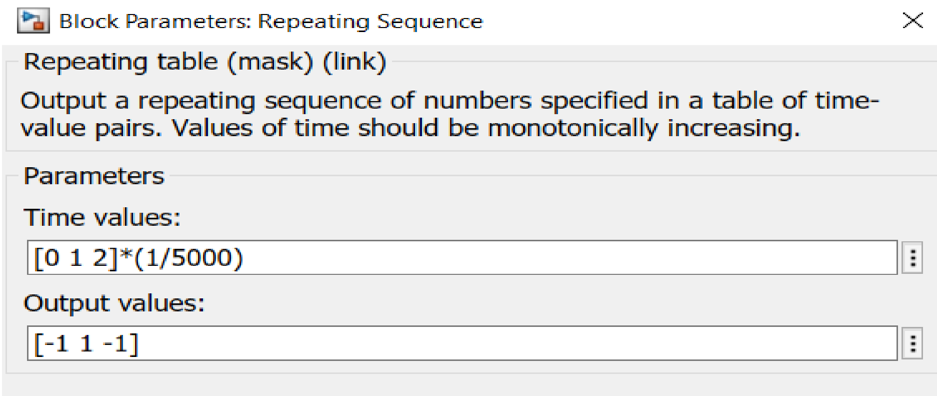

Figure 48: Configuration of repeating sequence.

Relational operator is a comparator that compere two signal and generate an output 0 or 1.

2) **Operation:**

The role of this subsystem is generating six switches signal based on desired speed. The switches are generated by comparing two signal the triangular with high frequency and the carrier signal generated by closed loop V/F subsystem as describe earlier. When the carrier signal is higher than a reference signal, the relational operator output will be 1 otherwise 0. A pulse signal will be generated based on this comparison.

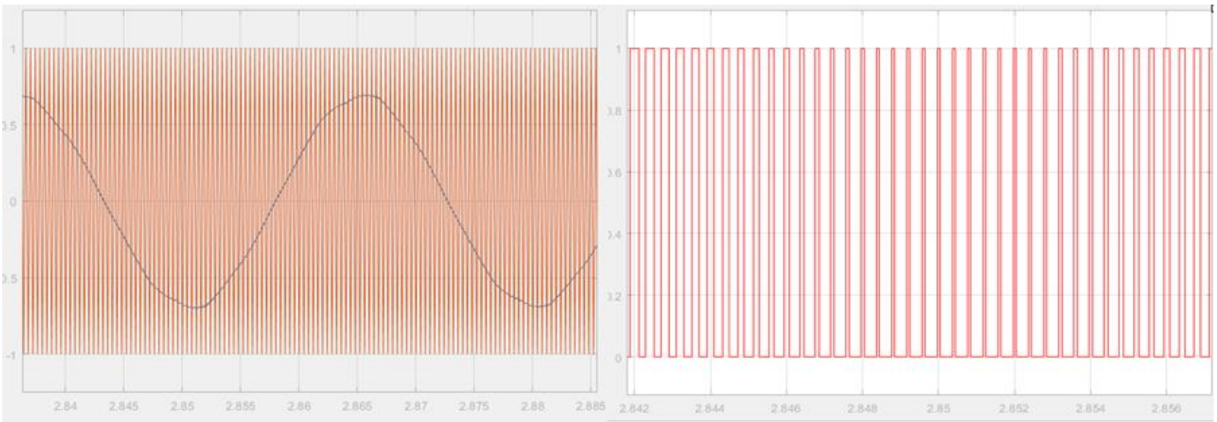

Figure 49: Input and the output of comparator.

4.2.1.4 Induction motor:

The Induction Motor block in Simulink is an essential tool for simulating and analyzing the performance of induction motors. We have integrated this block into our model to effectively study scalar control techniques and optimize motor speed control strategies. This integration provides valuable insights into the motor's dynamic behavior and significantly enhances the design of control systems.

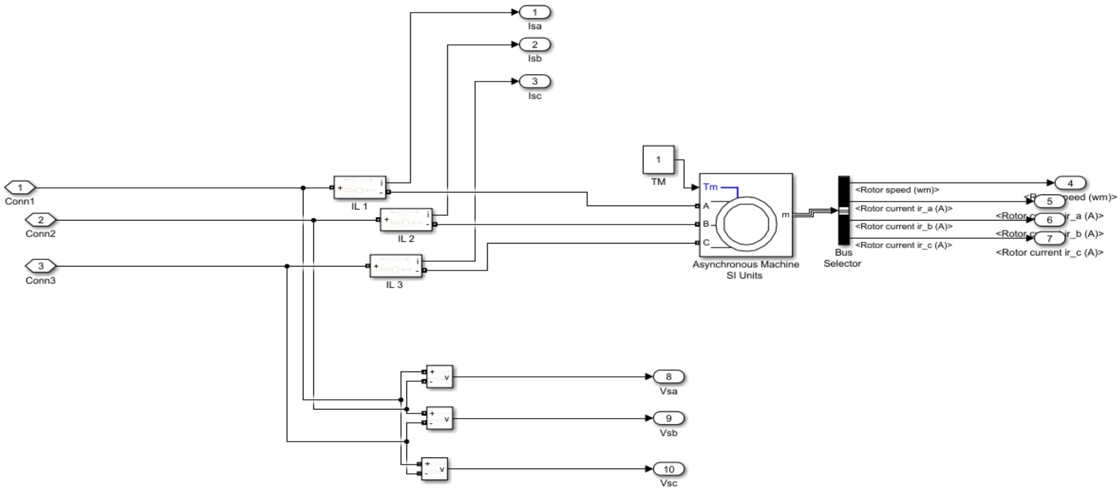

Figure 50: Induction motor subsystem.

1) Configuration:

The parameters of the Induction Motor block were configured as follows:

- Rotor Type: Set to squirrel-cage.

- Motor Parameters: The motor specifications fed into the Simulink block are real-world measurements and estimates supplied by the SINAMICS G120 variable-frequency drive. Correctly obtaining these specifications is vital for accurate simulation and control programming within the Simulink platform.

Table 3 Induction motors parameters.

Stator resistance (Ω)	**5.57**
Rotor resistance (Ω)	**3.2**
Stator inductance (mL)	**16.21**
Rotor inductance (mL)	**16.99**
Magnetizing inductance (mL)	**353.03**

2) Operation:

The induction motor is a critical component that converts electrical power from the inverter subsystem into mechanical energy to drive the motor. The inverter generates a variable-frequency, variable-voltage power source tailored to the induction motor's needs. The motor's speed is fed back to the control circuit, which continuously monitors the actual speed and adjusts the power input to maintain the desired speed. The interaction between the induction motor, inverter, and control circuit is a complex, dynamic process that requires precise coordination to achieve optimal performance, efficiency, and torque output for the application. The variable power source generated by the inverter is a key enabler for the system's speed control capabilities, allowing the control circuit to regulate the motor's speed for maximum energy efficiency.

4.2.2 Results:

The results of simulating open-loop and closed-loop V/F (Voltage/Frequency) control methods for an induction motor using Simulink. The purpose of this study is to compare the performance of these two control strategies in terms of speed regulation, stability, and response characteristics.

Table 4: Desired speeds.

Time (s)	Desired Speed (RPM)
0 – 2.24	0
2.24 – 18	500
18 – 47	1000
47 – 50	100

4.2.2.1 Open loop results:

The following results detail the performance of the induction motor under open-loop V/F control. The key parameters monitored are motor speed, supply voltage, and motor current.

1) Speed graph

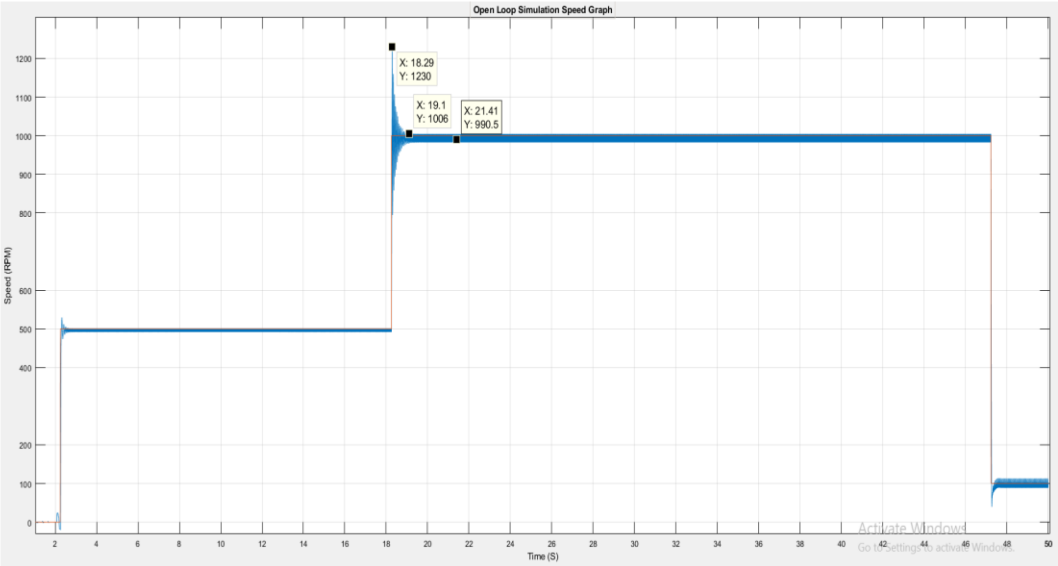

Figure 51: Open loop V/F Speed plot.

Description:

The graph shows the speed response of the induction motor under open-loop control with setpoint changes at specific intervals:

1. Initial Phase (0 to 2.24 seconds):
    - The desired speed is set to 0 RPM, and the motor remains stationary as expected.
2. First Speed Change (2.24 to 18 seconds):
    - The desired speed is set to 500 RPM. The motor reaches the setpoint with an overshoot around 520 RPM before settling at the desired speed. This indicates a transient response with overshoot and stabilization.
3. Second Speed Change (18 to 47 seconds):
    - The desired speed is increased to 1000 RPM. The motor accelerates to the setpoint, again showing an overshoot, reaching approximately 1230 RPM before settling at around 1005 RPM. There is a notable transient response with overshoot and minor steady-state error.
4. Final Speed Change (47 to 50 seconds):
    - The desired speed drops to 100 RPM. The motor decelerates rapidly with a slight overshoot and stabilizes at around 100 RPM.

2) Current graph:

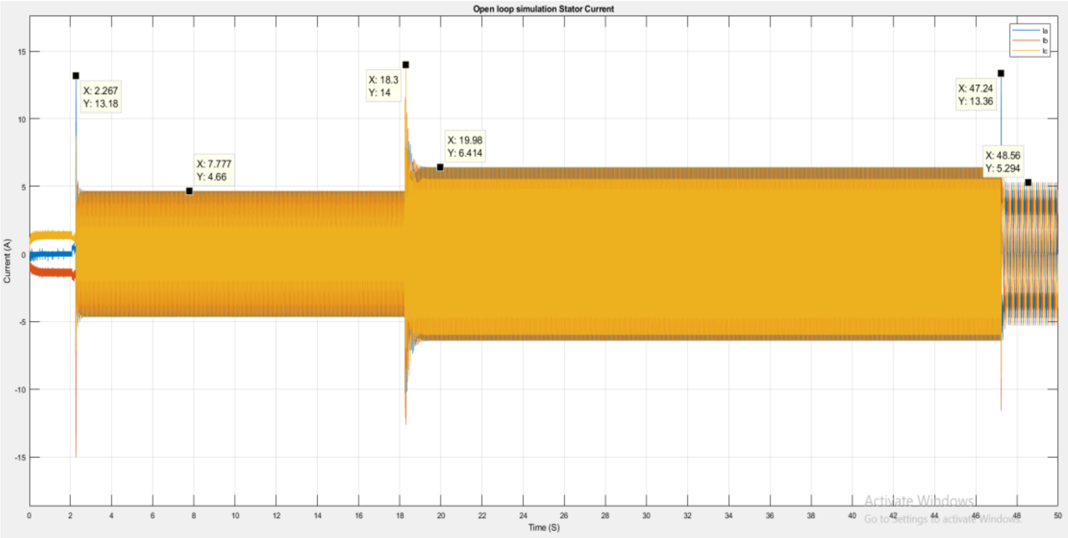

Figure 52: Open loop three phase stator current plot.

The open loop simulation current graph shows the stator current characteristics under the same setpoints. The waveform is not a pure sine wave, indicating that the power conversion is not entirely efficient. Fluctuations and harmonics are present, which is typical in an open loop control system due to the lack of feedback for precise current regulation.

4.2.2.2 Closed loop results:

The following results detail the performance of the induction motor under closed-loop V/F control. The key parameters monitored are motor speed, supply voltage, and motor current.

1) Speed graph:

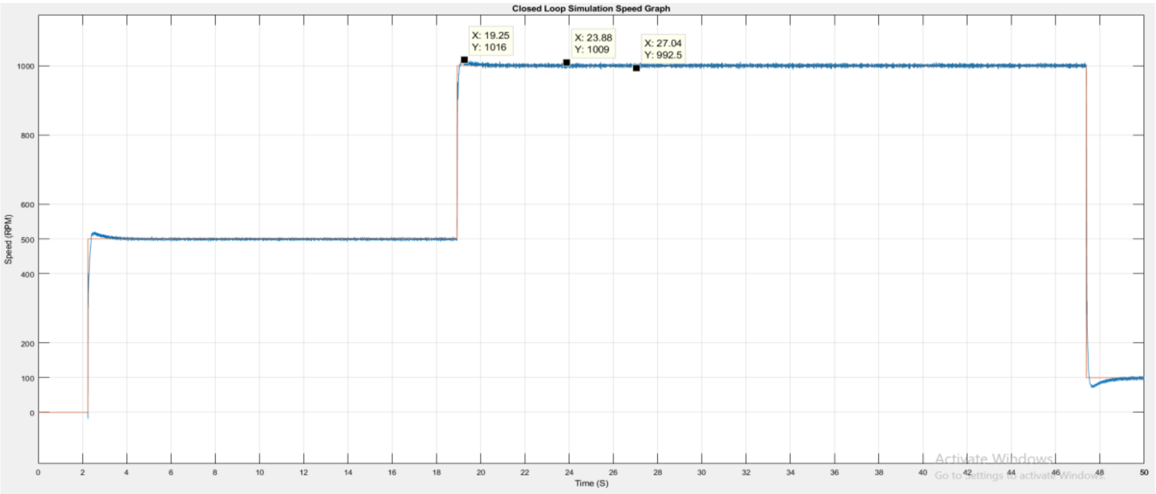

Figure 53: Closed loop speed graph.

Description:

- **Initial Response**: At the beginning (0 to ~0.3 seconds), the motor speed rapidly increases from 0 RPM to around 1200 RPM. This indicates a quick acceleration phase.
- **Steady-State Operation**: From ~0.3 seconds to ~2.8 seconds, the motor speed stabilizes around 1000 RPM. This suggests that the control system successfully maintains a steady speed, which aligns with the desired set speed.
- **Set Point Change**: At around 2.8 seconds, there is a sudden drop in the speed set point from 1000 RPM to approximately 500 RPM. This could represent a change in the desired operating speed.
- **Response to Set Point Change**: Following the set point change, the actual speed quickly decreases to match the new set point of 500 RPM. After the initial drop, the speed stabilizes around the new set point, although there appears to be some small oscillations or noise in the speed signal, indicating minor fluctuations around the set speed.

2) ***Current graph:***

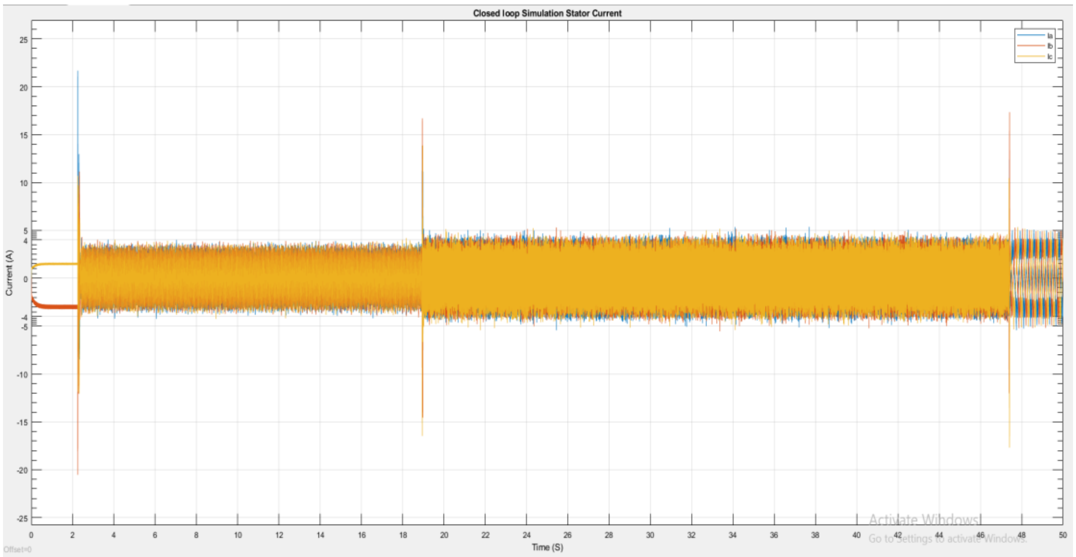

Figure 54: Closed loop three phase stator current.

In the closed loop simulation current graph, the stator current still shows fluctuations but is better regulated compared to the open loop. Although it is not a pure sine wave, the current waveform is more stable and consistent, reflecting the benefits of feedback control in managing the motor's electrical parameters.

Open-Loop vs. Closed-Loop: The open-loop control lacks feedback, which makes it more susceptible to overshoot and oscillations, particularly in response to setpoint changes. This results in moderate stability and precision. The closed-loop control, on the other hand, uses feedback to continuously correct errors, leading to higher stability, minimal overshoot, and greater precision in maintaining the desired speed.

4.2.2.3 Comparison and discussion:

Open-loop control exhibits a steady-state error due to the lack of feedback, leading to deviations from the desired speed. In contrast, closed-loop control continuously monitors the actual speed and adjusts the frequency and voltage to minimize the error, resulting in more accurate speed regulation and compensation for disturbances.

In terms of dynamic response, open-loop control shows significant overshoot or undershoot when the set point changes, with a slower settling time. Closed-loop control, on the other hand, exhibits a more responsive and stable transition with minimal fluctuations.

Regarding current performance, open-loop systems lack control over acceleration, leading to high starting currents that can stress the motor and drive components. Closed-loop control can manage the starting current more effectively, contributing to the overall efficiency and longevity of the system.

Finely, the closed-loop V/F control system offers significant advantages over the open-loop system, including improved speed accuracy, dynamic response, and overall stability. The closed-loop system effectively handles the inductive motor's non-linear characteristics, ensuring precise speed regulation and robust performance under varying loads. While open-loop control is simpler and less costly, its limitations in speed accuracy and disturbance response make it less suitable for applications requiring high precision and stability. The closed-loop system's sophisticated feedback mechanism and optimized tuning make it the superior choice for such demanding applications, despite its higher complexity and implementation cost.

4.3 Implementation:

In this section, we focus on the practical implementation of the speed control system. Initially, the system is simulated using MATLAB/Simulink to validate the control strategy and ensure robust performance. Following the simulation, the system is implemented using a Siemens S7-1200 PLC for real-time control, and the SIMANTIC G120 to send the appropriate frequency and voltage commands to the motor based on the command speed.

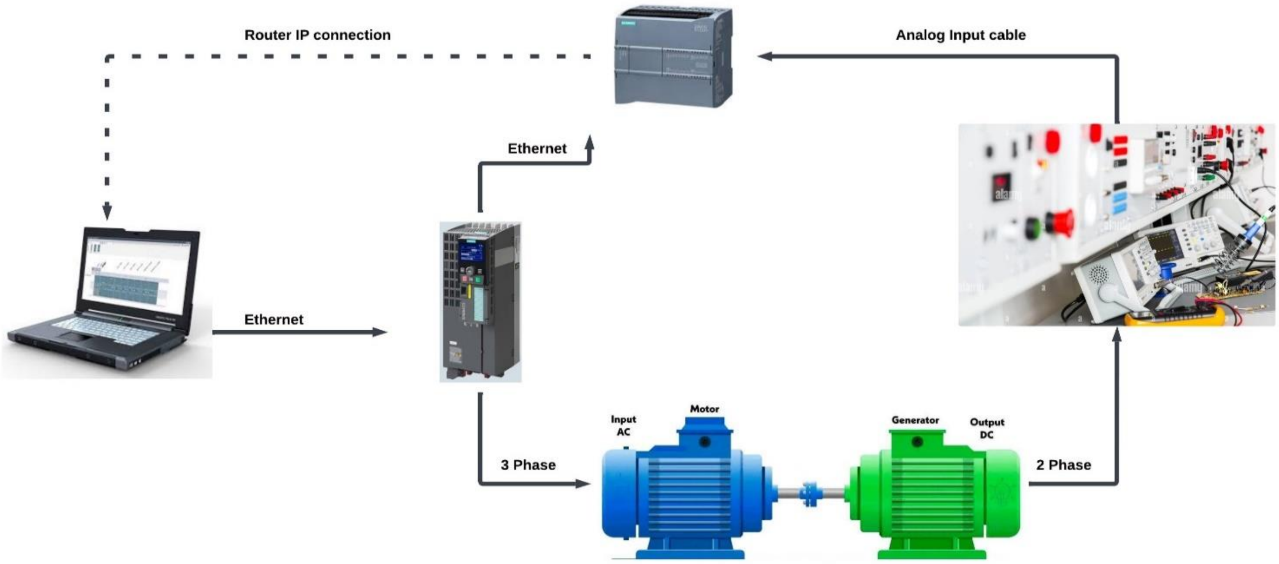

Figure 55: Implementation block diagram.

4.3.1 Materials and software:

Here's a description of materials and software typically used in a setup involving an induction motor, VFD G120, PLC S7-1200, instrumentation for measurement, and TIA Portal with STARTDRIVE:

4.3.1.1 Materials:

Induction Motor: From ECODIME Company, with a power rating of 1.5 kW, rated speed of 1410 rpm, and a power factor of 0.83.

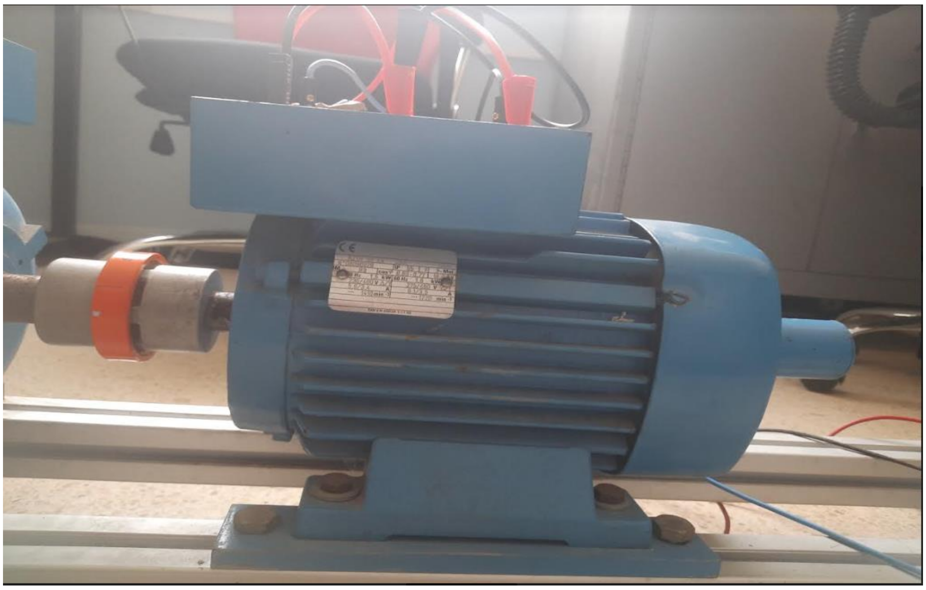

Figure 56: Employed Induction Motor.

<u>PLC S7-1200 with CPU 1212C AC/DC/Rly</u>: is a versatile and powerful industrial automation controller. It features a compact design with a 75 KB work memory, enabling efficient processing of control logic and data manipulation. The controller offers extensive I/O capabilities, integrating seamlessly with sensors, actuators, and peripherals. With support for communication modules, it easily integrates into existing automation networks, facilitating data exchange and interoperability. Its rapid processing time of 0.04 ms/1000 instructions ensures quick response and precise control, optimizing production efficiency. The PROFINET interface allows for effortless programming, monitoring, and diagnostics via the TIA Portal software, providing a unified engineering environment. Suitable for standalone or comprehensive automation systems, the PLC S7-1200 with CPU 1212C AC/DC/Rly delivers reliability, scalability, and performance for industrial automation applications.

Figure 57: CPU 1212C AC/DC/RLY.

<u>SINMATIC G120 Control Unit CU240E-2 PN:</u> The G120 Control Unit CU240E-2 PN is a high-performance industrial motor control technology designed for precision and efficiency in automation systems. It features PROFINET compatibility for seamless integration and rapid data exchange. The unit offers a diverse range of connectivity options, including analog and digital inputs/outputs, and relay outputs, enabling integration with various sensors, actuators, and peripherals. It incorporates safety functions like Safe Torque Off (STO) to prioritize performance and compliance with industry standards. Housed in a robust IP20-rated enclosure, the G120 Control Unit CU240E-2 PN delivers reliable and long-lasting operation in harsh industrial environments, whether used independently or with a programmable logic controller (PLC).

Figure 58: G120 CU 240E-2 PN.

Tachogenerator:

In this tachogenerator, the relation of speed and voltage is that at1500RPM speed, the voltage is 92V.

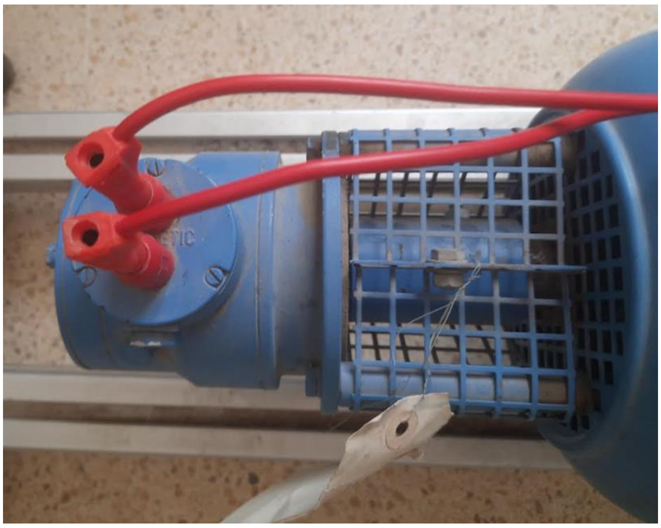

Figure 59: Employed Tachogenerator Speed Sensor.

3-Phase Power supply:

Figure 60: Employed 3-Phase power supply.

4.3.1.2 Software:

Tia Portal V15.1 (Totally Integrated Automation Portal): is a comprehensive software suite developed by Siemens that provides a unified engineering environment for industrial automation projects. It integrates various components, such as Programmable Logic Controllers (PLCs), Human-Machine Interfaces (HMIs), and drive systems.

Stardrives V15.1: A component of TIA Portal used specifically for commissioning and parameterizing drive systems, including VFDs like G120.

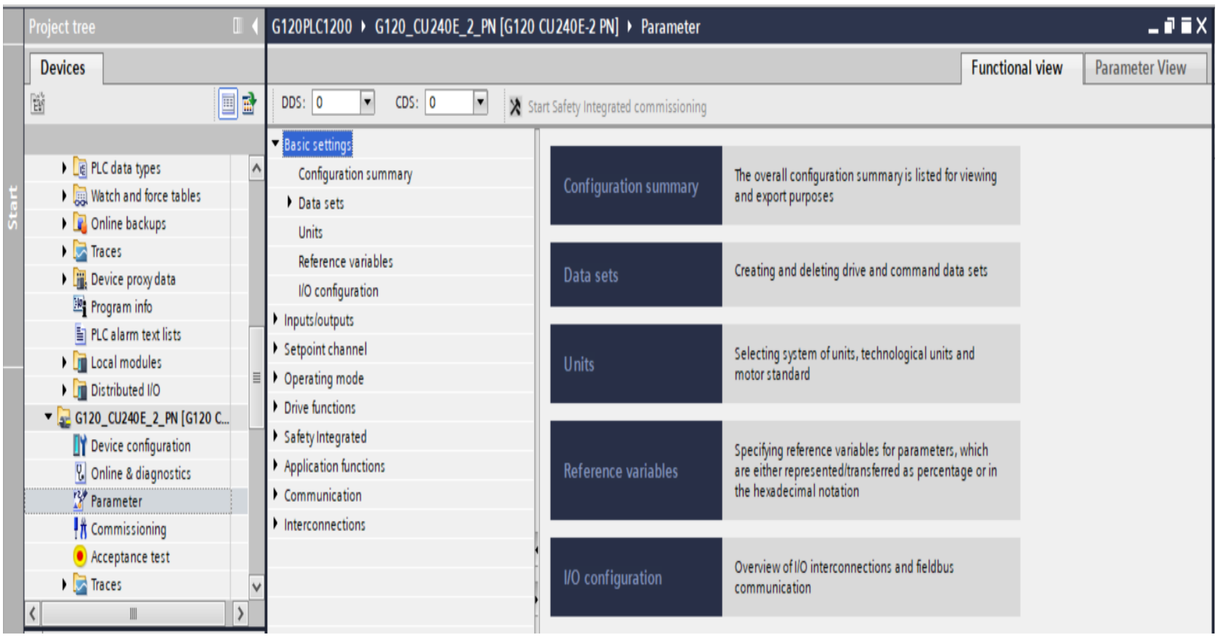

Figure 61: Startdrive in TiaPortal.

The combination of TIA Portal and Startdrive allows for a comprehensive and integrated approach to configuring the material used in the implementation.

4.3.2 Configuration and Program:

For the complete implementation involving the induction motor, VFD G120, PLC S7-1200 with CPU 1212C AC/DC/Rly, and associated software configuration, the process typically involves several steps. Here's an overview of the implementation and software configuration:

4.3.2.1 Software configuration:

Create a new project for the automation system in Tia portal, and add PLC S7-1200 and VFD G120 with corresponding version and ID number.

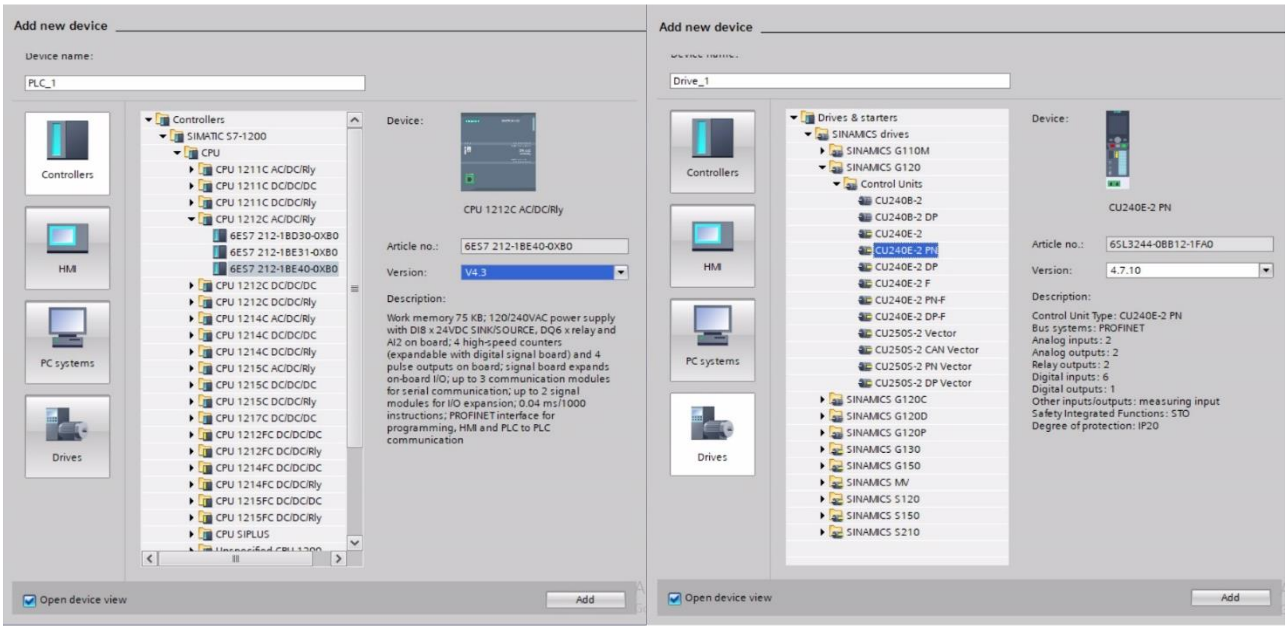

Figure 62: Add devices in Tia Portal.

To configure the communication settings for the PLC S7-1200 and the G120 VFD, including setting up the PROFINET interface for programming, follow these steps. The CPU 1212C AC/DC/RLY has only one Ethernet port, but it must communicate with both the VFD and the computer. The G120 VFD has two Ethernet ports, allowing it to act as a bridge. By configuring one of the VFD's Ethernet ports as a router for the PLC and setting the VFD's PROFINE address, ensure that all devices are connected without needing an external switch.

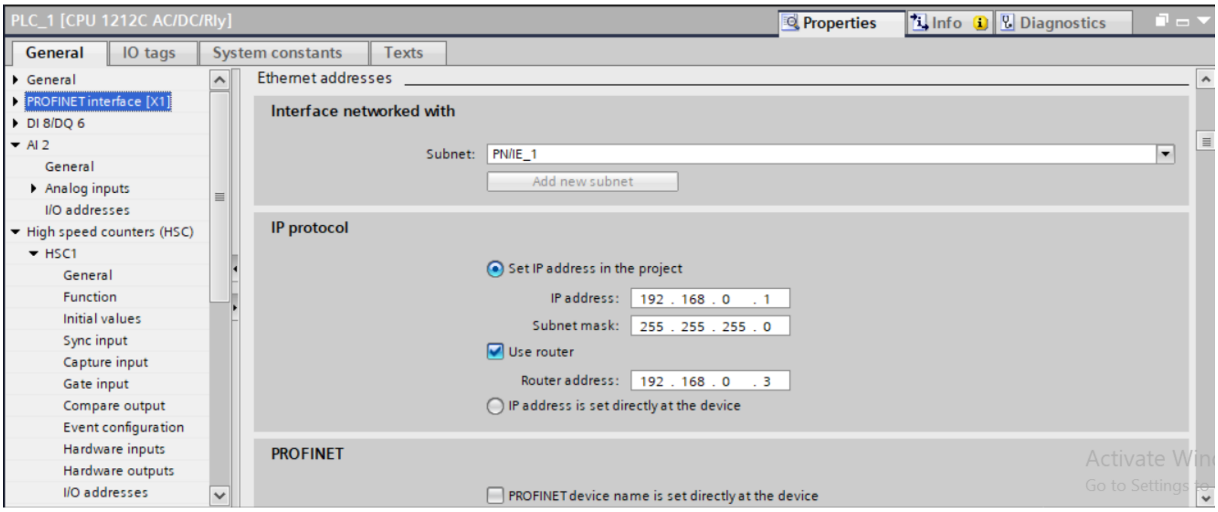

Figure 63: Ethernet address configuration.

Then connect the PLC and the VFD as shown. Process data are exchanged between SIMATIC controller and SINAMICS drive is specified by the frame type (in the example: standard telegram 1).

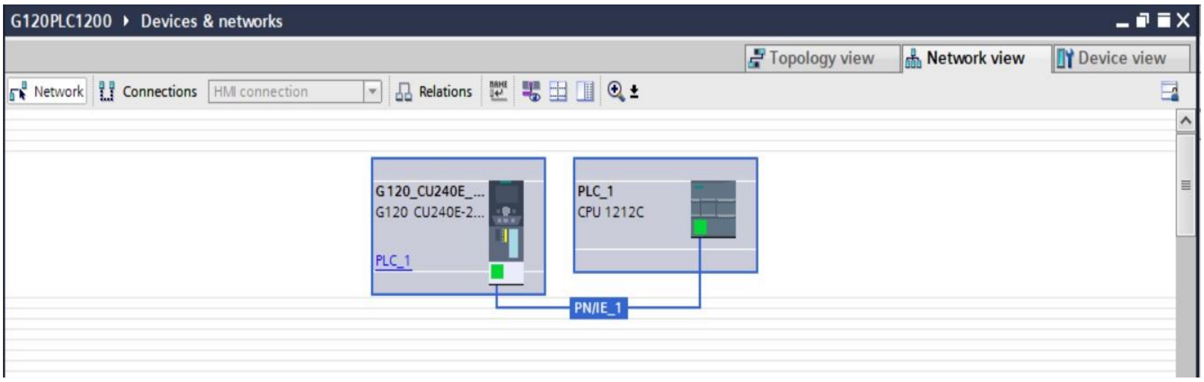

Figure 64: Connections devices.

Startdrive can be used to establish an online connection to the drive for performing the commissioning of the drive Figure 66. To do so, select the drive in the project navigation and click “Go online” in the toolbar Figure 65.

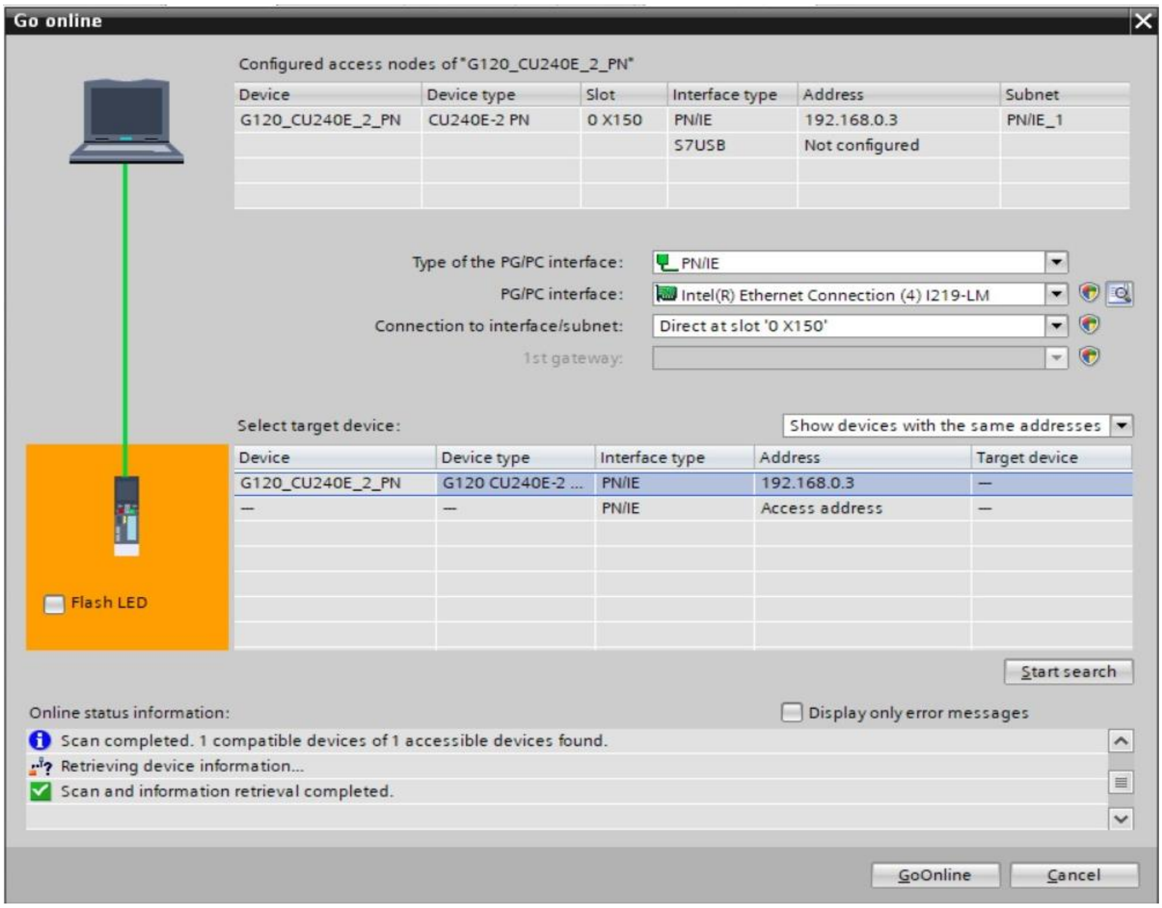

Figure 65: GO-ONLINE (G120)

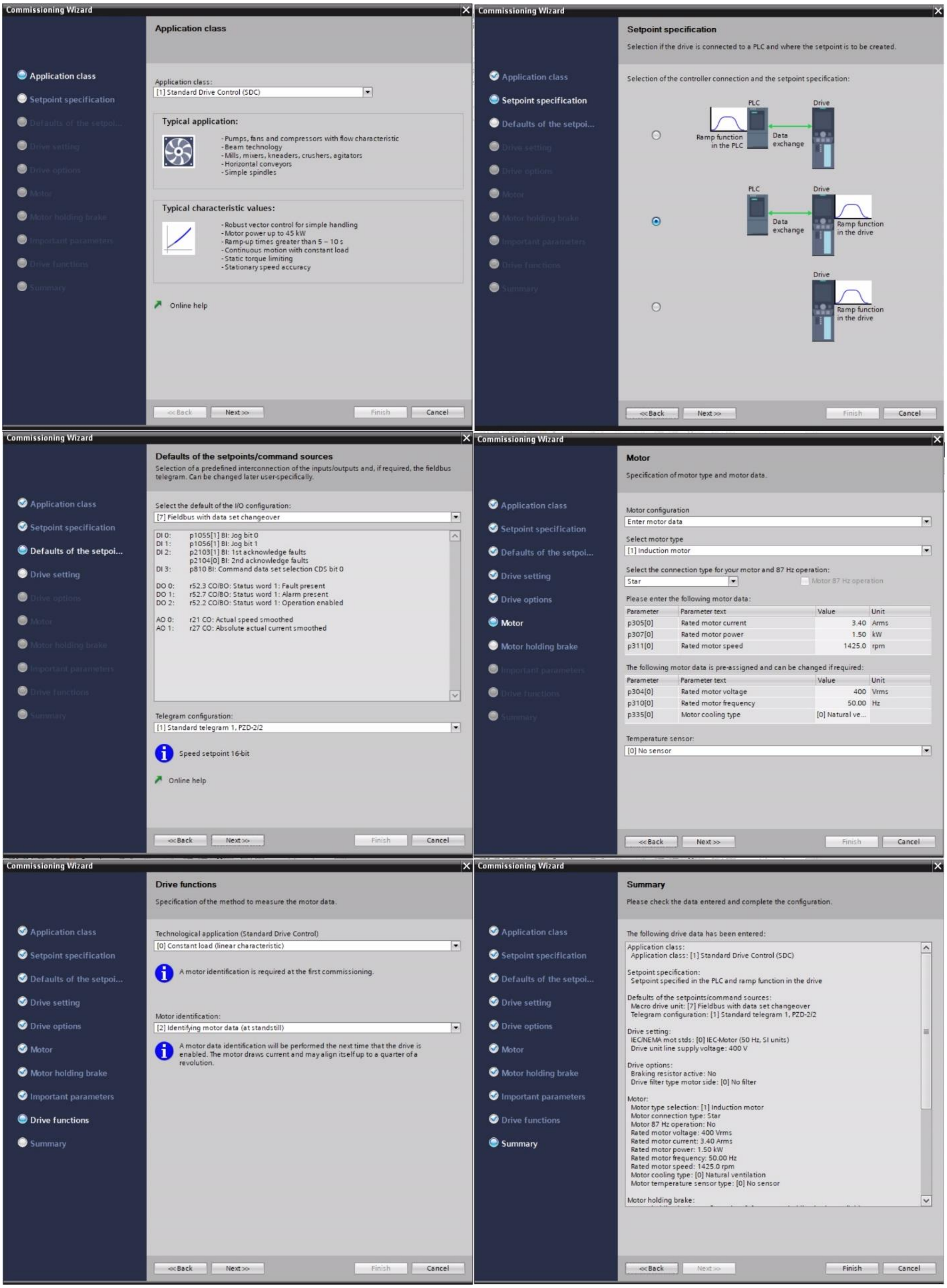

Figure 66: Commissioning the drive.

Finnally downloading the program of the SIMATIC controller, by selecting the S7 controller in the project tree then loading the project into the controller.

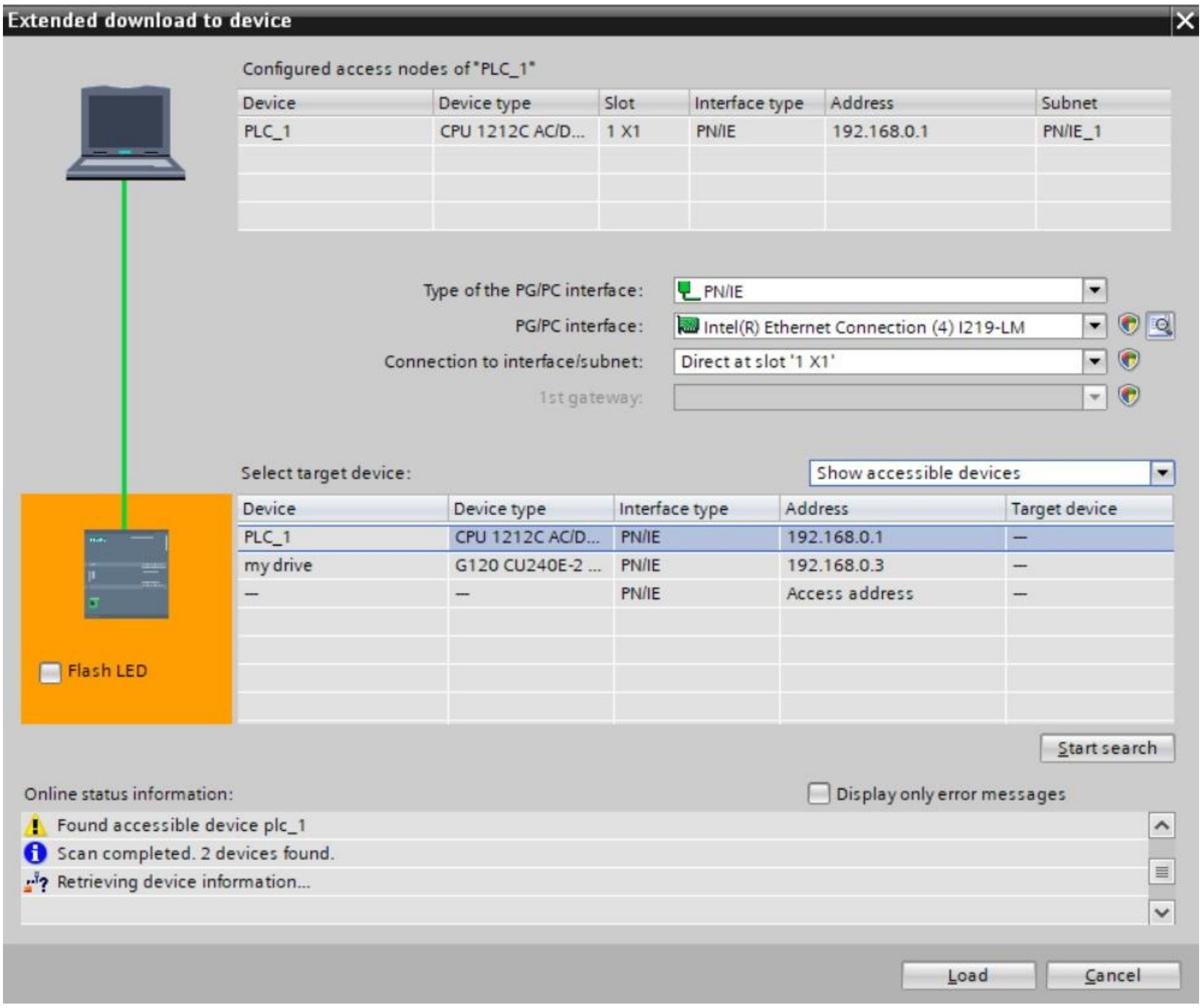

Figure 67: Downloading the program to controller.

4.3.2.2 Program Overview:

Communication between the SINAMICS G120 and SIMATIC S7-1200 is handled through the "SINA_SPEED" block in the process data range. The S7-1200 transmits the control word and the desired speed value to the drive, while the drive sends the status word and the actual speed value back to the S7-1200. This data exchange occurs cyclically, meaning it happens during each bus cycle, ensuring the information is transferred as rapidly as possible. The use of the standard block "SINA_SPEED" offers a quick and simple option to control the SINAMICS drive.

For identifying the feedback speed from the voltage sensor I have used some instructions to measure the analog input voltage.

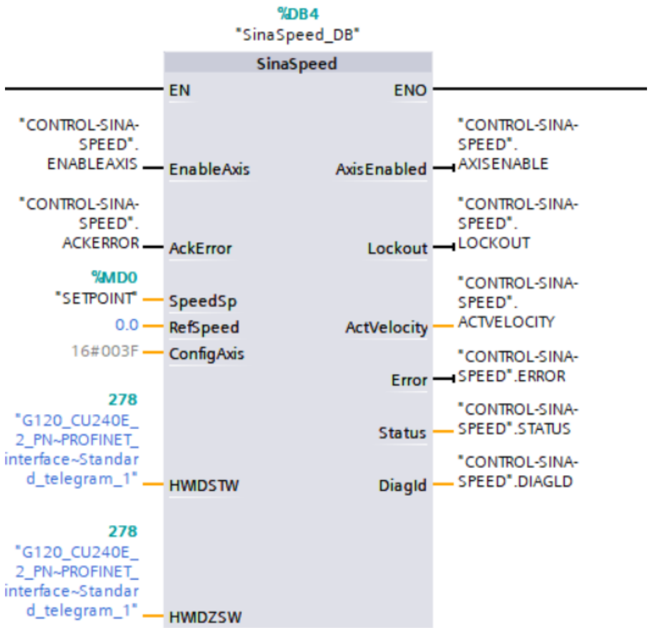

Figure 68: Sina Speed block data.

This data block contain input and output parameters, start the VFD, insert set point speed, and rest the error. Also give us the feedback speed and the state of the VFD.

The data block contain both input and output parameters. It enables initiating the Variable Frequency Drive (VFD), set the desired speed, and reset any errors. Additionally, the data block provides with the actual feedback speed and the current status of the VFD.

This tags are declared in data block.

CONTROL-SINA-SPEED

	Name	Data type	Start value	Retain	Accessible f...	Writa...	Visible in ...	Setpoint
1	▼ Static			☐	☐	☐	☐	☐
2	ENABLEAXIS	Bool	false	☐	☑	☑	☑	☐
3	ACKERROR	Bool	false	☐	☑	☑	☑	☐
4	SPEEDSP	Real	0.0	☐	☑	☑	☑	☐
5	AXISENABLE	Bool	false	☐	☑	☑	☑	☐
6	LOCKOUT	Bool	false	☐	☑	☑	☑	☐
7	ACTVELOCITY	Real	0.0	☐	☑	☑	☑	☐
8	ERROR	Bool	false	☐	☑	☑	☑	☐
9	STATUS	Word	16#0	☐	☑	☑	☑	☐
10	DIAGLD	Word	16#0	☐	☑	☑	☑	☐

Figure 69: "SinaSpeed" instance data blocks.

For identification of feedback speed we use scaler and normalize instruction, first we create function then insert the two instruction as shown

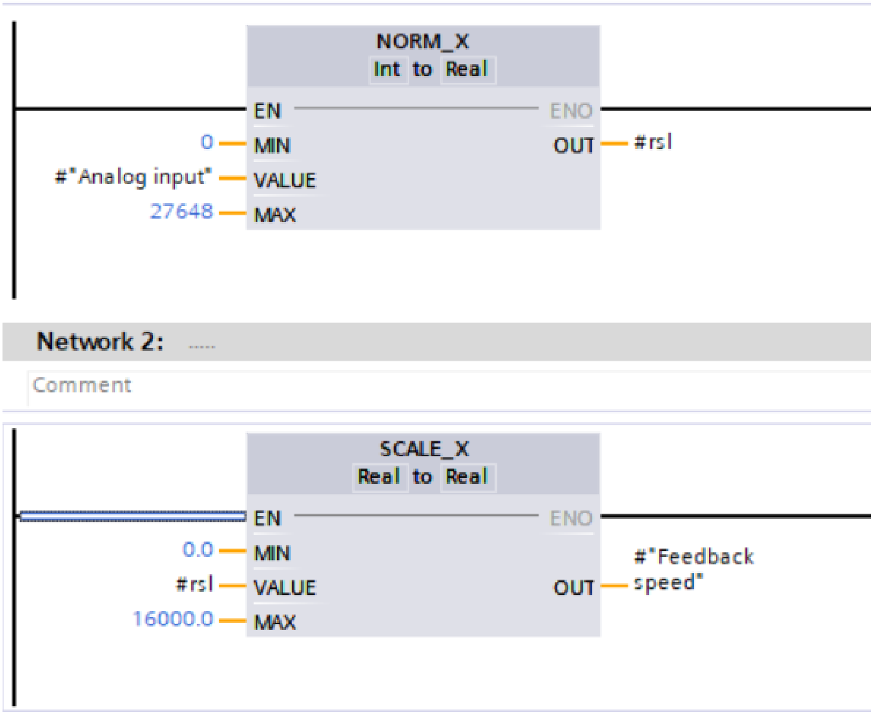

Figure 70: NormX and ScaleX instructions.

Then we call this function in the main OB

4.3.2.3 Hardwar Configuration:

- First we supply the drive G120 by three phase 380-V, and the output is connected to the motor in Y connection.
- Second the Ethernets connections, PLC is connected to first port of G120 and the second is connected to computer.
- Thirdly connect the output signal to voltage sensor and graph for displaying result.
- Finally we connect output of voltage sensor to analog input of plc to perform the closed loop operation and the tuning of PID.

4.3.2.4 Open Loop and Closed Loop Configurations:

After configuring the devices and completing the hardware connections and coding, we downloaded the program into both the PLC and VFD.

Open loop:

The open loop is the direct connection between our materials,

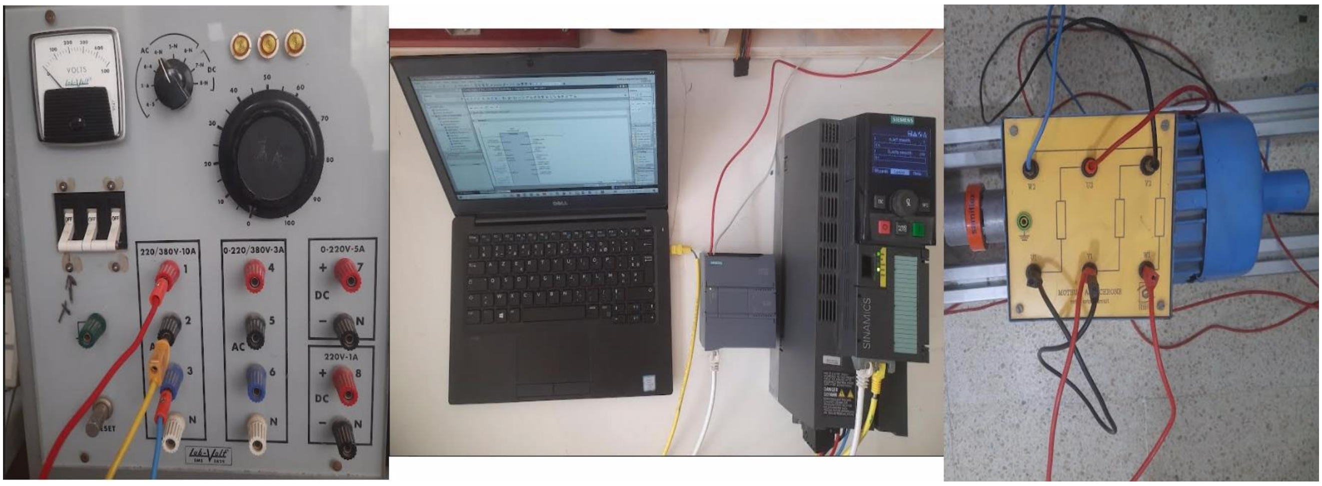

Figure 71: Open loop implementation.

1. **<u>Operation:</u>**

After following the steps of configuration and running the program, we inserted two desired speeds for testing:

500 RPM and 1000 RPM from PLC in online mode.

Figure 72: a) 500 RPM, b) 1000 RPM.

The control panel of the drive give us some measurement in the corresponding selected speed.

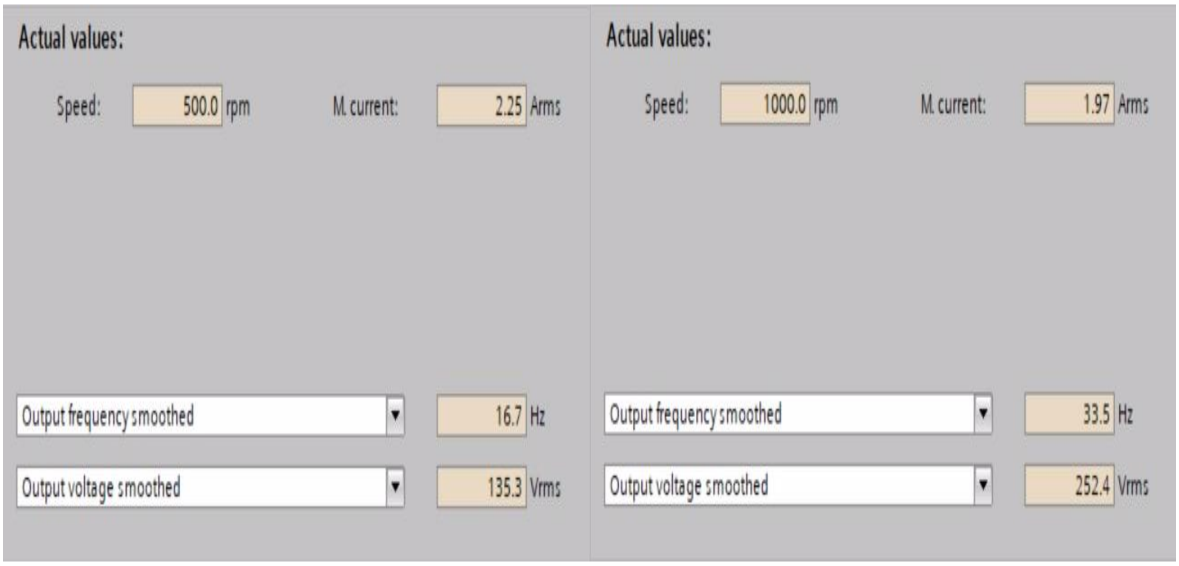

Figure 73: Control Panel Measurement.

4.3.2.5 Closed loop:

In the context of motor speed control, implementing closed-loop control typically involves using feedback to adjust the motor's speed to match the desired setpoints accurately. This is often achieved using a PID controller, which relies on real-time feedback from sensors such as incremental encoders.

The project is limited to open-loop control due to the absence of an incremental encoder, the theoretical framework and simulations demonstrate the potential benefits of closed-loop control with optimized PID. Future work will focus on integrating the necessary feedback components to implement and fine-tune the closed-loop control system, achieving precise and stable motor performance.

By clearly outlining the practical constraints and the impact of these limitations, this section provides a comprehensive explanation for the lack of closed-loop implementation and sets the stage for future enhancements.

4.3.3 Result:

The result it displayed in Matlab using Real Time Unit

1) Speed graph

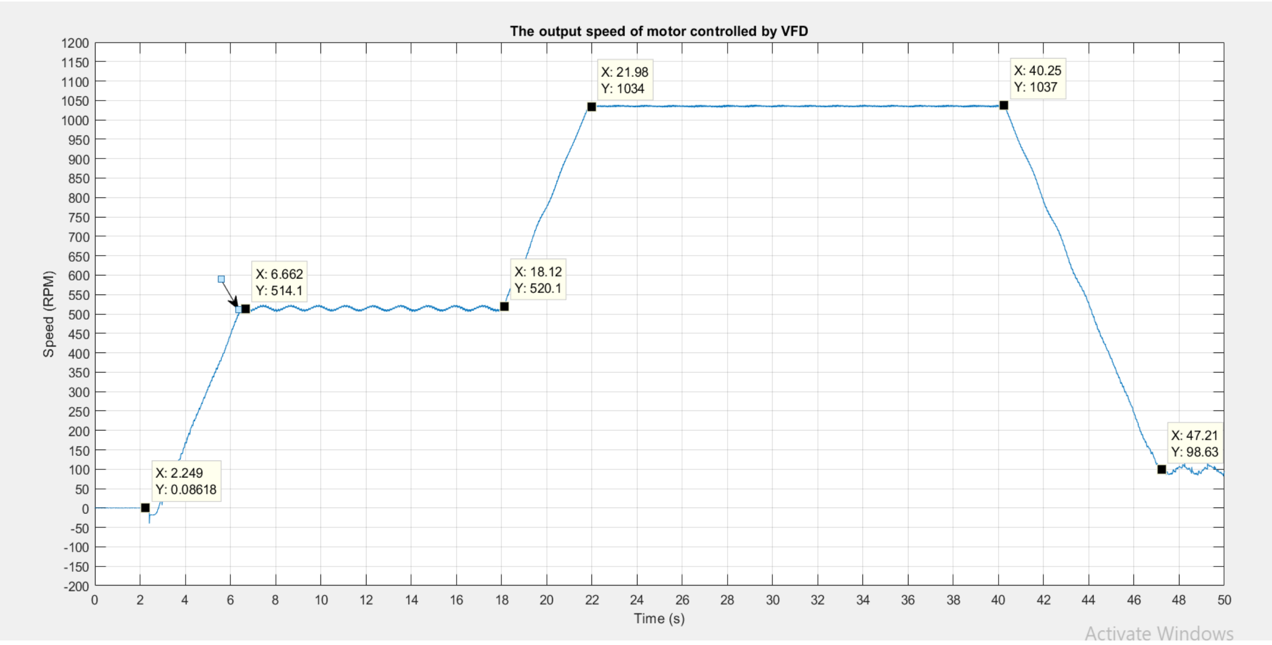

Figure 74: The output speed of motor controlled by VFD

Description:

The desired speed is initially set to 500 RPM at around 2 seconds, where the motor speed overshoots slightly, reaching about 514 RPM in 6.662 seconds. The speed then fluctuates around 514 RPM, displaying instability and an inability to precisely maintain the desired speed due to the open-loop control.

At 18 seconds, the desired speed is increased to 1000 RPM. The motor speed ramps up, reaching approximately 1034 RPM after 21.98 seconds, again showing an overshoot above the desired speed. The speed then stabilizes around 1034 RPM, indicating a consistent overshoot in the open-loop response.

Finally, at 40 seconds, the desired speed is reduced to 100 RPM. The motor speed decreases and reaches approximately -98 RPM after 47.21 seconds, indicating an undershoot below the desired speed and even a reversal in direction.

2) Current graph:

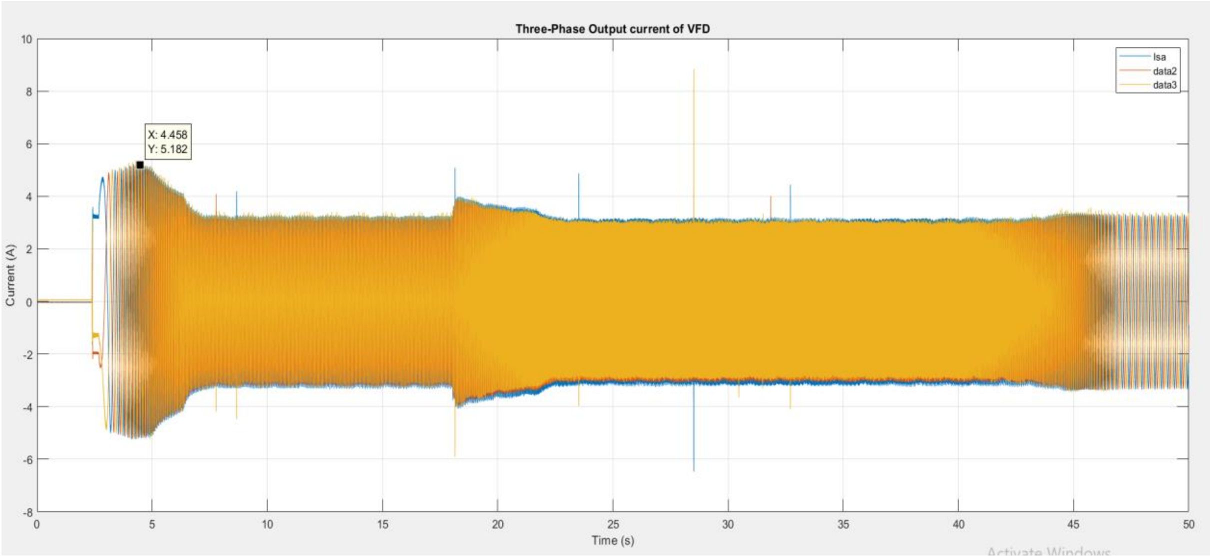

Figure 75: Three-Phase stator current

Description:

In the initial behavior phase, from 0 to approximately 2.5 seconds, the current starts at around 0 A and ramps up quickly. By 4.458 seconds, the current reaches approximately 5.182 A (Isa), with significant oscillations observed during this ramp-up phase. Following this, during the steady-state behavior phase from about 4.5 to 40 seconds, the currents stabilize, fluctuating around a mean value for all three phases, indicating a steady-state operation. The periodic oscillations visible in the waveform are typical of the Pulse Width Modulation (PWM) control used in VFDs. A second ramp-up occurs between 40 and 45 seconds, where a noticeable change in current magnitude suggests a change in the operating condition or load. In the final phase, from approximately 45 to 50 seconds, the currents begin to decrease and oscillate significantly, likely corresponding to the deceleration or stopping phase of the motor.

Analyses:

- **Initial Ramp-Up**: The initial increase in both speed and current indicates the motor overcoming initial inertia and stabilizing.
- **Steady-State Operation**: The stability in both current and speed graphs during the steady-state phases indicates normal operation under a constant load.
- **Ramp-Up and Load Change**: The correlation between speed increases and current changes indicates the VFD adjusting to new setpoints or loads.
- **Deceleration**: The rapid changes and oscillations in both graphs during deceleration highlight the motor slowing down or stopping, with the VFD managing this transition.

4.4 Discussion:

Open-Loop Simulation:

The open-loop simulation results showed notable overshoots during speed changes, indicating the system's inability to quickly settle at the desired speed. This behavior is typical in open-loop control systems, as there is no feedback mechanism to correct deviations. The steady-state error was significant, reflecting the challenge of maintaining precise speed without feedback.

Closed-Loop Simulation:

In contrast, the closed-loop simulation demonstrated significantly improved performance. The system quickly settled at the desired speed with minimal overshoot, showcasing the effectiveness of the PID controller in reducing speed oscillations and errors. The closed-loop control maintained stability and accuracy, highlighting the importance of feedback in dynamic environments.

Open-Loop Implementation:

The practical implementation of the open-loop control reflected the challenges observed in the simulation. The speed graph showed overshoots and a slower response to speed changes, similar to the simulation. However, the steady-state error was influenced by real-world factors such as measurement inaccuracies, system inertia, and load variations. The VFD's internal filters, safe acceleration, and ramp-up time also affected the results, contributing to a smoother transition but introducing additional delays.

Current Waveform Analysis:

The simulation and implementation of the current waveform revealed a key difference: the simulated current waveform was not a pure sine wave, showing the effects of PWM control and harmonic distortion. In contrast, the practical implementation achieved a more sinusoidal current waveform, benefiting from the VFD's internal filtering and advanced modulation techniques. This improvement in the actual system highlights the effectiveness of hardware enhancements in reducing current distortion.

Explanation of Table Comparison:

The open-loop simulation exhibited significant overshoots and high steady-state errors, reflecting the limitations of open-loop control in handling speed changes and maintaining accuracy. The closed-loop simulation, with the inclusion of a PID controller, showed minimal overshoot and low steady-state errors, demonstrating the benefits of feedback in achieving precise control and stability.

The open-loop implementation results were influenced by real-world factors such as measurement inaccuracies, system inertia, and load variations. These factors contributed to moderate overshoot and steady-state errors, indicating the challenges of practical implementation. Additionally, the VFD's internal filtering and ramp-up time of 10 seconds helped achieve smoother transitions but introduced some delays.

The current waveform analysis highlighted the differences between simulation and implementation. The simulation showed distorted sine waves due to PWM control, while the implementation achieved a more sinusoidal waveform thanks to the VFD's filtering and advanced modulation techniques.

Overall, these results underscore the importance of closed-loop control and hardware enhancements in achieving precise and stable motor speed control in industrial applications.

Table 5: Result summery

Criteria	Open loop simulation	Open loop implementation	Closed loop simulation
Desired speed (RPM)	0, 500, 1000, 100	0, 500, 1000, 100	0, 500, 1000, 100
Actual Speede (RPM)	0, 514.1, 1037, 98.63	0, 520.1, 1034, 88.6	0, 506, 1009, 992.5
Overshoot	High	Medium	Low
Steady state error	High	Medium	Low
Response time	Moderate	Longer	Fast
Stability	Moderate stability with notable oscillations	Greater stability with fewer oscillations	High stability with minimal oscillations
Precision	Moderate precision, notable deviations from setpoints	Higher precision, closely follows setpoints	High precision, closely follows setpoints
Current waveform	Not pure sine wave	Pure sine wave	Not pure sine wave

4.5 **Conclusion:**

This chapter examined the simulation and practical implementation of open-loop V/F control for an induction motor using a Siemens G120 VFD and an S7-1200 PLC. The simulation provided an idealized response, with rapid speed stabilization and minor oscillations. In contrast, the practical implementation exhibited more gradual transitions and significant oscillations due to real-world factors like system inertia and load variations. The closed-loop control was simulated but not practically implemented due to the unavailability of an incremental encoder, which hindered precise feedback and PID optimization. Future work should secure all necessary components to fully leverage the benefits of both open-loop and closed-loop control systems. The comparative analysis underscored the need for robust control strategies to manage transitions smoothly and maintain stable operation, with the VFD's ramp-up time and current limiting features playing crucial role

General Conclusion

This work examined the implementation and simulation of speed control methods for a three-phase induction motor in an industrial automation system. The integration of a Siemens G120 VFD and an S7-1200 PLC highlights the crucial role of automation in enhancing industrial processes. Automation systems that leverage advanced control technologies, such as VFDs and PLCs, offer significant improvements in efficiency, accuracy, and reliability of motor-driven operations.

The study focused on both open-loop and closed-loop control methods. In the open-loop control implementation, practical experiments revealed distinct differences from the simulated model, particularly in response to speed changes and current behavior due to real-world factors like system inertia and load variations. Despite these differences, the practical implementation demonstrated precise speed control with minimal errors, showcasing the VFD's capability in managing smooth transitions and stable operation.

For the closed-loop control, simulation with PID tuning using both PLC and Simulink MATLAB indicated enhanced performance and stability. However, practical implementation was limited by the unavailability of an incremental encoder, which is essential for precise feedback and PID optimization.

This project emphasizes the significance of integrating VFDs and PLCs in industrial automation systems, highlighting their potential to enhance efficiency, precision, and reliability in motor-driven operations.

Enhanced motor efficiency, reduced power needs, and improved process management. By applying cutting-edge control methods and automation, industries can boost productivity, minimize operating expenses, and increase dependability in motor-driven operations.

This research offers a thorough examination of V/F control approaches, underscoring the necessity for resilient control techniques and precise PID calibration to optimize motor performance in real-world industrial settings. Upcoming efforts should address hardware limitations to fully harness the advantages of closed-loop control in practical deployments.

Future Work:

Upcoming efforts should focus on resolving hardware limitations to fully unlock the advantages of closed-loop control in real-world applications. Integrating cutting-edge industrial advancements like Industry 4.0, the Industrial Internet of Things (IIoT), and advanced machine learning algorithms could also further improve motor control systems. Establishing connections between variable frequency drives (VFDs), programmable logic controllers (PLCs), an OPC server, and a SCADA system will be essential in this evolution, enabling enhanced connectivity, data analytics, and autonomous decision-making. These advancements hold the potential to deliver greater efficiency, precision, and adaptability to motor control and broader industrial domains.

Bibliography

[1] A. E. Fitzgerald, C. K., Electric Machinery, McGraw-Hill,, 2003, pp. 306-350.

[2] T. GÖNEN, Electical machines with MATLAB, 2nd ed., CRC press, 2012, pp. 207-273.

[3] K. Aissa, *EE533 - Machine and Drives*, 2023.

[4] S. J. Chapman, Electric Machinery Fundamentals, 5th éd., McGraw-Hill, 2002, pp. 307-400.

[5] F. M. Bruce, R. J. Graefe, A. Lutz and M. D. Panlener, «Reduced-Voltage Starting of Squirrel-Cage Induction Motors,» *IEEE Transactions on Industry Applications,* Vols. %1 sur %2IA-20, n° %11, pp. 46 - 55, 1984.

[6] D. Kumar, «Performance analysis of three-phase induction motor with AC direct and VFD.,» chez *Materials Science and Engineering*, 2018.

[7] R. Krishan, Electric Motor Drives Modeling, Analysis, and control, Prentice Hall, 2001, pp. 174-411.

[8] A. Belbali, S. Makhloufi, A. Kadri, L. Abdallah, and Z. Seddik, «Mathematical Modeling of a Three-Phase Induction Motor,» chez *Induction Motors - Recent Advances, New Perspectives and Applications.*, 2023.

[9] E. S. Oluwasogo, «DQ Modeling and Dynamic Characteristics of Three Phase Induction Machine,» *American Journal of Engineering Research (AJER),* vol. 6, n° %1P, pp. 207-215, 2017.

[10] B. K. Bose, Modern Power Electronics and AC Drives., Prentice Hall, 2002.

[11] S. Alagur, «Speed Control of Induction Motor by V/F Method using Fuzzy Technique,» *International Journal of Sciance and Research (IJSR)* , vol. 6, n° %19, pp. 832-837, 2016.

[12] A. Hughes, Electric motors and drives: fundamentals. Elsevier Science & Technology., 2005, pp. 286-289.

[13] L. Zhong, «Dynamics of current source inverter fed high-performance induction motor drives,» 1994.

[14] D. Saputra, E. Sartika, «Prediction of PID control model on PLC,» in *TELKOMNIKA (Telecommunication Computing Electronics and Control)*, 2019.

[15] M. H. Rashid, Power Electronics Handbook : Devices, Circuits, and Applications., 2nd éd., Burlington, 2007.

[16] T. H. Blair, «Variable Frequency Drive Systems,» chez *Energy Production Systems Engineering*, IEEE, 2017, pp. 441-466.

[17] K. Vinoth, P. Angle, &. S. Kumar, «Simulation and comparison of SPWM and SVPWM control for three phase inverter.,» *ARPN journal of engineering and applied sciences.*, vol. 5, n° %17, pp. 61-74, 2010.

[18] Y. Huang, Y. Xu, Y. Li, G. Yang and J. Zou, «PWM Frequency Voltage Noise Cancelation in Three-Phase VSI Using the Novel SVPWM Strategy.,» *IEEE Transactions on Power Electronics*, vol. 33, pp. 8596-8606, 2018.

[19] M.Deepa, «Design of VFD Drive for a 3-Phase InductionMotor,» *International Journal of Innovative Research in Science, Engineering and Technology*, vol. 4, 2015.

[20] Ö. B. İnal and G. Koçak, "A Case Study on the Variable Frequency Drive for Ship Engine Room Ventilation", Mar. Sci. Tech. Bull., vol. 12, no. 3, pp. 252–258, 2023, doi: 10.33714/masteb.1299692., 43-51.

[21] SIEMENS, *Operating Instructions of SINAMICS G120 Converter with CU250S-2 Control Unit,*, 2023.

[22] SIEMENS, «S7-1200 Programmable controller,» chez *System Manual*, 2012.

[23] SIEMENS , «Learn-/Training Document,» chez *TIA Portal Module, Basics of FB Programming with SIMATIC S7-1200.*, R&D institutions, 2018.

[24] SIEMENS , «SITRAIN: Training for Industry,» chez *SIMATIC TIA Portal Programming*, 2014.